2015

GSK3 regulation of suprachiasmatic neuronal excitability and light entrainment

Jodi Paul
University of Alabama at Birmingham

GSK3 REGULATION OF SUPRACHIASMATIC NEURONAL EXCITABILITY AND LIGHT ENTRAINMENT

by

JODI R. PAUL

KAREN L. GAMBLE, COMMITTEE CHAIR
FRANK AMTHOR
BUREL GOODIN
JOHN HABLITZ
ROBERT SORGE

A DISSERTATION

Submitted to the graduate faculty of The University of Alabama at Birmingham,
in partial fulfillment of the requirements for the degree of
Doctor of Philosophy

BIRMINGHAM, ALABAMA

2015

GSK3 REGULATION OF SUPRACHIASMATIC NEURONAL EXCITABILITY AND LIGHT ENTRAINMENT

JODI R. PAUL

PROGRAM NAME

ABSTRACT

Circadian rhythms are approximately 24-hour cycles in behavioral and physiological processes, such as sleep/wake cycles and cognition. In mammals, these rhythms are endogenously generated and entrained to the external light cycle by the primary circadian pacemaker, the suprachiasmatic nucleus (SCN). A hallmark characteristic of SCN neurons is the daily rhythm in the spontaneous action potential frequency, with high activity during the day and low activity at night. These SCN firing rate patterns are critical for maintaining robust, consolidated behavioral rhythms, and persistent changes in SCN neuronal activity are involved light-induced behavioral shifts. Many of the ionic components underlying daily and light-responsive changes in SCN physiology have been described; however, the mechanism controlling expression of these currents is not known. Glycogen synthase kinase 3 (GSK3) is a serine-threonine kinase that is an emerging regulator of mammalian circadian rhythms and has been implicated in a variety of neurological, neurodegenerative, and psychiatric disorders. In the SCN, GSK3 exhibits daily rhythms in activity. This dissertation examines the role of GSK3 activity in regulating SCN neuronal excitability and photic (light) entrainment of the circadian system, using circadian behavioral analysis, immunohistochemistry, real-time bioluminescence, and whole-cell electrophysiology in the presence of chronic GSK3 activation and following pharmacological inhibition of GSK3. In the main chapters we show that: 1) loss of rhythmic GSK3 inactivation disrupts behavioral and

neurophysiological rhythms in the SCN, 2) GSK3 mediates light-induced SCN excitability and phase-resetting, and 3) GSK3 activity regulates SCN neurophysiological excitability through modulation of the persistent sodium current. The results presented here expand upon the current understanding of GSK3's involvement in the circadian system, and provide novel insight into the mechanism controlling SCN membrane physiology. Because GSK3 has been implicated in numerous clinical disorders which also exhibit circadian disruption, a better understanding of the role of GSK3 in circadian regulation could lead to new treatment strategies for these disorders in the future.

TABLE OF CONTENTS

LIST OF TABLES

Table *Page*

CHAPTER 2

LIST OF FIGURES

Figure *Page*

CHAPTER 1

CHAPTER 2

CHAPTER 3

CHAPTER 4

LIST OF ABBREVIATIONS

5-HT	serotonin
AD	Alzheimer's disease
AHP	after-hyperpolarization
AP	action potential
AVP	arginine-vasopressin
Aβ	amyloid β
BK	large-conductance Ca^{2+}-activated potassium
BMAL1	brain and muscle arnt-like
C57	C57BL/6J
Ca^{2+}	calcium
CaMKII	Ca^{2+}/calmodulin-dependent protein kinase II
CHIR	CHIR-99021
CK1	casein kinase 1
CLOCK	circadian locomotor output cycles kaput
CNS	central nervous system
CREB	Ca^{2+}/cAMP response element binding protein
CRY	cryptochrome
CT	Circadian Time
DD	constant dark

DKI	$GSK3\alpha^{S21A/S21A}/\beta^{S9A/S9A}$
DLAMO	depolarized low amplitude membrane oscillations
ERG	electroretinogram
ERK1/2	extracellular signal-related kinase 1/2
FDR	fast-delayed recifier potassium current
g_{NaP}	conductance of I_{NaP}
GSK3	glycogen synthase kinase 3
GSK3-KI	$GSK3\alpha^{S21A/S21A}/\beta^{S9A/S9A}$
IHC	immunohistochemistry
I_{NaP}	persistent sodium current
I_{NaT}	transient sodium current
LD	12:12 light/dark cycle
LGN	lateral geniculate nucleus
LP	acute light-pulse
LUC	luciferase
MAPK	mitogen-activated protein kinase
mTOR	mammalian target of rapamycin
MUA	multi-unit activity
NMDA	N-methyl-D-aspartate
NPY	neuropeptide Y
ODN	oligodeoxynucleotide
PER	period
PNR	photopic negative response

RACK1	Receptor for Activated C-Kinase 1
RHT	retinohypothalamic tract
R_{input}	input resistance
RMP	resting membrane potential
SCN	suprachiasmatic nulceus
SCNX	SCN lesion
SFR	spontaneous firing rate
TTFL	transcriptional/translational feedback loop
TTX	tetrodotoxin
VIP	vasoactive intestinal polypeptide
WT	wild-type
ZT	Zetigeber Time
α	alpha, active period
α-KI	$GSK3\alpha^{S21A/S21A}$
β-KI	$GSK3\beta^{S9A/S9A}$
ΔΦ	phase-shift
τ	tau, free running period
X^2	chi-squared

CHAPTER 1

INTRODUCTION

Overview of Circadian Rhythms

Circadian rhythms are approximately 24 hour cycle in various biological (e.g., metabolism, blood pressure) and behavioral processes (e.g., sleep/wake and cognition). These daily rhythms, found in nearly all organisms ranging from bacteria to mammals, allow for the anticipation of environmental changes associated with the Earth's rotation. Evidence of the advantage provided by this anticipation can be seen even at the single cellular level. In cyanobacteria strains with molecular rhythms of varying lengths (such as less than, greater than or equal to 24 hours), the strain oscillating at a frequency that most closely matched the environmental temperature cycle had the highest survival rate (Ouyang et al., 1998). Moreover, the importance of proper circadian functioning in humans is highlighted by the far-reaching negative health outcomes associated with circadian disruption, including negative impacts on obesity, cancer, and cardiometabolic function (Takahashi et al., 2008). Even though circadian rhythms developed as a response to environmental cycles, they are endogenously driven and persist under constant conditions, thus providing the means of anticipation of regularly-occurring daily events.

Perhaps the most obvious, and therefore most commonly studied circadian rhythm that exists in animals is the daily cycle in activity levels or sleep/wake (Figure 1). When placed into constant dark (DD), mammals exhibit a free-running period length (tau) that

is usually slightly less than or greater than 24 hours (Figure 1 (Pittendrigh and Daan, 1976)). Because these rhythms are not perfectly 24 hours in length, the animal must continuously resynchronize its internal clock with the environment through a process known as entrainment. Specific environmental stimuli, known as "zeitgebers" (time givers), provide time-of-day information used to align endogenous rhythms with the external cycle. To effectively synchronize the internal clock to the environment, these cues elicit different phase-shifting effects depending on the time of day at which it is presented (Daan and Pittendrigh, 1976). By exposing an animal to stimuli such as an acute pulse of light or novel running wheel at various points throughout the circadian cycle and measuring the direction (i.e., advance or delay) and magnitude of the behavioral phase-shift ($\Delta\Phi$), it is possible to construct a phase-response curve for the stimuli (Daan and Pittendrigh, 1976).

In mammals, multiple cues can act as an entraining signal, including nonphotic stimuli such as arousal or novel-wheel induced exercise, but light is the strongest zeitgeber (Czeisler, 1995, Golombek and Rosenstein, 2010). Given that the purpose of entrainment is to rectify differences between internal and external time, light is maximally effective at shifting the clock when presented during the night, when light levels would typically be low (Figure 1 (Daan and Pittendrigh, 1976)). Specifically, light exposure during the early-night results in a phase-delay (Figure 1- "B"), while light exposure in the late-night causes a phase-advance (Figure 1- "C" (Daan and Pittendrigh, 1976)). In fact, the effect of photic stimuli in the early- and late-night are so robust that mice are capable of entraining to a skeleton photoperiod consisting of two short light pulses that are separated by long periods of dark (e.g., 1:10:1:12 LDLD, (Pittendrigh and

Daan, 1976)). Conversely, exposure to light during the day has little to no phase-shifting effects, even when the animal is housed in DD (Figure 1- "A" (Daan and Pittendrigh, 1976)).

At the molecular level, proper circadian timing is controlled by a transcriptional/translational feedback loop (TTFL) of well-established core "clock" components (Figure 2): the positive regulators, CLOCK (circadian locomotor output cycles kaput) and BMAL1 (brain and muscle arnt-like), and the negative regulators, PER (period 1-3) and CRY (cryptochrome 1-2) (for review see (Takahashi et al., 2008)). The TTFL cycle begins with the complex of CLOCK and BMAL1, which acts as a basic helix-loop-helix transcription factor by binding to E-box elements within the promoter regions for *Per* and *Cry* genes and driving their expression (Ueda et al., 2005). As time passes, the proteins products accumulating in the cytoplasm of the cell heterodimerize in various combinations of PER1-3 and CRY1-2. These PER/CRY heterodimers then translocate back into the nucleus of the cell and interact with the CLOCK/BMAL1 complex to inhibit their own transcription. Eventually, the PER and CRY proteins are degraded, relieving the inhibition on CLOCK and BMAL1, and the cycle starts over.

Under normal conditions, the cycle takes approximately 24 hours to complete; however, the exact timing of this process is subject to fine-tuning by posttranslational modification (such as phosphorylation) of each component by kinases like casein kinase 1 (CK1 δ and ε) and glycogen synthase kinase 3 (GSK3; (Gallego and Virshup, 2007)). Phosphorylation of PER and CRY proteins can act to speed up or slow down the TTFL cycle by promoting nuclear translocation or protein degradation, respectively. In a second feedback loop, the BMAL1/CLOCK complex drives *Rev-Erbα* transcription, and the

REV-ERBα protein, in turn, inhibits the expression of *Bmal1* (Preitner et al., 2002, Ueda et al., 2005). Although this auxiliary loop is not necessary for the rhythmicity of the primary TTFL (Liu et al., 2008), it contributes to the robustness of the circadian clock (Preitner et al., 2002).

All of the core TTFL components, with the exception of CLOCK, exhibit daily rhythms in expression (Reppert and Weaver, 2002). Development of numerous reporter models has enabled researchers to examine the real-time expression of individual clock components across multiple circadian cycles. One commonly used model is the PER2::LUC transgenic mouse line, which express a fusion protein of PER2 and firefly luciferase (LUC, (Yoo et al., 2004)). Due to the wide variety of biological processes exhibiting daily rhythms, it is not surprising that the presence of clock gene/protein oscillations is not limited to one organ system. In fact, groups of rhythmic cells can be found in nearly every tissue type, including liver, lung, pancreas and fibroblasts; however, when these peripheral oscillators are cultured *in vitro*, their rhythms gradually dampen, until they are lost entirely (Yamazaki et al., 2000). This loss of rhythmicity is not a result of a loss of TTFL rhythms at the single cell level but is due to the individual rhythms drifting out of phase with one another as a result of the weak coupling between cells within the population. For this reason, peripheral tissues require input from a central, master oscillator to synchronize and regulate circadian rhythms throughout the entire body (Welsh et al., 2010).

The Suprachiasmatic Nucleus

In mammals, the central pacemaker is located in the suprachiasmatic nucleus of the hypothalamus (SCN). Lying dorsal to the optic chiasm and surrounding the third ventricle, the SCN consists of two nuclei that each contain approximately 10,000 densely packed, small GABAergic granule cells (Abrahamson and Moore, 2001). The nuclei are divided into two distinct subdivisions based on structure and neurochemical expression: the arginine-vasopressin (AVP) expressing, dorsomedial "shell" and the vasoactive polypeptide expressing, ventrolateral "core." Entraining signals are transmitted to the SCN through three main afferent pathways. Light information is projected from the retina directly to the SCN through the retinohypothalamic tract (RHT), while nonphotic information is communicated to the SCN through the release of neuropeptide Y (NPY) and GABA from the lateral geniculate nucleus (LGN) and serotonin from the dorsal raphe nucleus (Dibner et al., 2010). Afferent projections from the RHT synapse on neurons within the SCN core which project mainly to the AVP expressing cells (Leak et al., 1999).

As the primary circadian pacemaker, the SCN is responsible for the generating endogenous circadian rhythms. Evidence for this comes from two separate lines of research: SCN lesion and SCN transplant studies. First demonstrated in rats (Stephan and Zucker, 1972), electrolytic lesioning of the SCN renders wheel-running and drinking behavior arrhythmic in constant conditions (Figure 1- "SCNX"). This effect has since been replicated in a range of other rodent models and extended to other physiological rhythms such as core body temperature (Eastman et al., 1984), hormonal secretion (Wollnik and Turek, 1989), cognition (Phan et al., 2011), and more. The behavioral

arrhythmicity caused by an SCN lesion can be rescued through transplantation of SCN tissue from a fetal donor into the third ventricle (Ralph et al., 1990). Furthermore, the tau of the restored behavioral rhythm is dependent on the tau of the donor, not the host animal (Ralph et al., 1990). Taken together, these studies illustrate that the endogenous rhythms generated within the SCN drive circadian rhythms throughout the entire organism.

Electrophysiological properties of SCN neurons

Like many other populations of pacemaker neurons found in the central nervous system (CNS; (Llinas, 1988)), SCN neurons are spontaneously active, generating action potentials (APs) through endogenous mechanisms at a steady rate. Time-of-day information is communicated by the SCN to the rest of the body through characteristic rhythms in spontaneous AP firing, with high frequency activity during the day and low activity at night (Inouye and Kawamura, 1979). These SCN firing patterns are critical for maintaining robust and consolidated behavioral rhythms (Schwartz et al., 1987, Meredith et al., 2006); furthermore, disruption of SCN neuronal activity has been seen in animal models of neurodegeneration and aging (Kudo et al., 2011b, Kudo et al., 2011c, Nakamura et al., 2011, Farajnia et al., 2012). Additionally, SCN cells exhibit daily changes in membrane properties such as input resistance (R_{input}), resting membrane potential (RMP) and AP waveform properties (Kuhlman and McMahon, 2004, Itri et al., 2005). Numerous ionic components underlying SCN neuronal activity have been identified, and many express day/night differences in mRNA expression, protein levels and/or current density (for review see (Colwell, 2011)).

In the SCN, the excitatory drive towards threshold is responsible for spontaneous AP firing and is provided by two mechanisms. The first is the slow-inactivating, or persistent, sodium current (I_{NaP}; Figure 3- "1"; (Pennartz et al., 1997, Jackson et al., 2004, Kononenko et al., 2004)). Compared to the transient sodium current (I_{NaT}) that is more traditionally associated with voltage-gated sodium channels, I_{NaP} activates at more hyperpolarized potentials, inactivates at a slower rate and is much smaller in magnitude (approximately 1%; (Stafstrom, 2007)). Although both I_{NaT} and I_{NaP} are tetrodotoxin (TTX) -sensitive and likely originate from alternate gating mechanisms of the same ion channels (Stafstrom, 2007), I_{NaP} can be isolated using the pharmacological blocker, riluzole. The importance of I_{NaP} in generating spontaneous action potentials in the SCN has been demonstrated using riluzole in dispersed neurons and intact, fresh brain slices (Kononenko et al., 2004). In both SCN preparations, blocking I_{NaP} with riluzole dramatically suppresses SCN neuronal activity, often to the point of silencing the neurons entirely.

The second source of excitatory drive in the SCN is driven by L-type calcium (Ca^{2+}) channels (Figure 3- "2"), which cause high frequency fluctuations in the membrane potential of SCN neurons. These subthreshold oscillations can be seen in some SCN neurons during the day (but not the night), when sodium-dependent AP firing is blocked with TTX (Pennartz et al., 2002). Notably, the frequency of the subthreshold oscillations positively correlates with the AP frequency of the neuron prior to TTX-treatment, suggesting a role for L-type Ca^{2+} channels in determining the spontaneous firing rate (SFR), to a certain extent.

Also increased during the day, fast delayed rectifier (FDR) potassium currents, promote rapid repolarization and decrease AP spike width, enabling SCN neurons to fire at a higher frequency (Figure 3-"3"; (Itri et al., 2005, Kudo et al., 2011a)).

At night, when the cells are typically quiescent or spiking at a low frequency, increased potassium leak conductance results in a more hyperpolarized membrane potential, driving the cell further from AP threshold (Kuhlman and McMahon, 2004). Expression of KCNMA1, the pore forming subunit of large-conductance Ca^{2+}-activated potassium (BK) channels, is also elevated at night in the SCN (Meredith et al., 2006). Activation of BK-channels during an AP increases the amplitude and duration of the AP after-hyperpolarization phase (Figure 3- "4"; (Montgomery et al., 2013)), thus prolonging the inter-spike interval.

Clock control of membrane excitability

The daily rhythm of SCN neuronal activity has been replicated in a variety of preparations, including *in vivo* multiunit recordings in freely moving hamsters (Yamazaki et al., 1998) and in single cell recordings from SCN-containing fresh brain slices in which the retinal input has been severed (Green and Gillette, 1982). Additionally, firing patterns persist in dispersed SCN neurons (Herzog et al., 1998), as well as in animals housed under constant conditions (Kuhlman and McMahon, 2004, Nakamura et al., 2011). Taken together, these results show that daily rhythms in AP frequency in the SCN are not dependent on environmental, retinal or other neuronal input and point to an endogenous mechanism driving physiological rhythms at a single-cellular level – likely, the molecular clock. Evidence that the TTFL drives SCN neurophysiology comes from changes in SCN

firing patterns seen in "clock" mutant animals, where changes in molecular rhythms – either period length or arrhythmicity – are reflected in SCN activity (Liu et al., 1997, Albus et al., 2002). Despite the clear association between molecular and neurophysiological rhythms in the SCN, the mechanism by which ion currents are controlled by the key 24-h timing mechanism is still largely unknown.

Molecular and physiological response to light in the SCN

Mirroring the phase-shifting effects of light seen behaviorally, brief exposures to light at specific times of the night reset the phase of the molecular clock in the SCN (Golombek and Rosenstein, 2010). The molecular mechanisms involved in light-induced phase-resetting within the SCN have been extensively studied, but there are still many aspects that are not yet known. In both the early- and late-night exposure to an acute light-pulse (LP) stimulates glutamate release from the RHT onto retinorecipient SCN neurons (Hannibal, 2002). Glutamate activation of NMDA (N-methyl-D-aspartate) receptors causes an influx of Ca^{2+} and subsequent activation of multiple signal cascades including activation of mitogen-activated protein kinases (MAPK; (Pizzio et al., 2003)) and Ca^{2+}/calmodulin-dependent protein kinases (CaMKII; (Golombek and Ralph, 1995)). These cascades converge on Ca^{2+}/cAMP response element binding protein (CREB), increasing its activation through phosphorylation (p-CREB; (von Gall et al., 1998)). Increased p-CREB leads to a rapid induction of gene expression, including *Per1* (Travnickova-Bendova et al., 2002, Tischkau et al., 2003), followed by a persistent increase in SCN neuronal excitability 3-5 hours later (Kuhlman et al., 2003). Furthermore, blocking CRE-driven *Per1* expression with an antisense

oligodeoxynucleotide (ODN) decoy for CRE, completely blocks light- or glutamate-induced phase-advances in wheel-running behavior and SCN neuronal activity (Tischkau et al., 2003). However, the mechanism by which the acute molecular response to light can lead to changes in neuronal excitability has not yet been discovered.

GSK3: a potential link between the clock and SCN output

GSK3 is a serine-threonine kinase, with two isoforms (α and β), both of which are ubiquitously expressed throughout the body, with especially high levels in the brain (Woodgett, 1990). GSK3 is by default active and, unlike many kinases, is inactivated by phosphorylation at serine-21 and serine-9, for α and β isoforms, respectively. Daily rhythms in GSK3 activity (measured as pGSK3) occur in many different tissues, including the SCN (Iwahana et al., 2004, Iitaka et al., 2005, Iwahana et al., 2007, Kinoshita et al., 2012). Importantly, pGSK3 rhythms in the SCN persist in animals housed in DD (Besing et al., 2015), demonstrating that the regulation of GSK3 is endogenously driven and not an artifact of an external stimulus (i.e., light). Furthermore, the daily regulation of pGSK3 appears to be clock dependent, as evidenced by loss of pGSK3β rhythms in cardiomyocytes from cardiomyocyte-specific CLOCK mutant mice (Durgan et al., 2010). Though the exact mechanism controlling pGSK3 rhythms is still unknown, one likely mechanism is through rhythmic expression of *akt* (Panda et al., 2002), a known regulator of GSK3 (Hur and Zhou, 2010). Dysregulation or overactivity of GSK3 has been implicated in conditions that involve disrupted circadian behavior, such as psychiatric and neurodegenerative disorders (Meijer et al., 2004, Barnard and Nolan, 2008), as well as the typical circadian decline associated with age (Iwahana et al.,

2007). Therefore, a better understanding of GSK3's functions within the mammalian circadian system could lead to new treatment strategies for many of these disorders.

Inhibition or over-expression of GSK3 differentially affects the phase of the molecular clock *in vitro*. Previous studies in NIH3T3 cells have shown that inhibition of GSK3 with lithium delays the peak of *Per2* and *Bmal1* expression following synchronizing stimulus (i.e., serum-shock), while over-expression of GSK3β advances the peak of both genes (Iitaka et al., 2005). However, due to the nature of these experiments (i.e., chronic manipulations and short duration of the time-course), the possibility that these effects were due to changes in the period length cannot be ruled out. In fact, this interpretation is supported by experiments in Drosophila, which have shown that inhibition or over-expression of GSK3 ortholog *shaggy* respectively lengthens or shortens the tau of locomotor activity (Martinek et al., 2001). Additionally, in mice, GSK3β haploinsufficiency lengthens the tau of wheel-running behavior in DD (Lavoie et al., 2013). However, the phase-shifting effects of acute changes in GSK3 activity remain unclear, and more importantly, the potential role of GSK3 in resetting the phase of circadian rhythms has largely been ignored.

GSK3 regulates ion channel function and influences neuronal excitability, through direct and indirect mechanisms, in various brain areas (Wildburger and Laezza, 2012). For example, in hippocampal neurons, activation of GSK3 by exposure to amyloid β ($A\beta_{42}$) increases phosphorylation of Kv4.2 channels and AP firing, and both effects are blocked with pharmacological inhibition of GSK3 (Scala et al., 2015). Indirectly, GSK3 can influence neuronal excitability by regulating localization of voltage-gated sodium channels to the axon initial segment (Tapia et al., 2013). In the SCN, acute application of

lithium, a non-specific inhibitor of GSK3, reduces AP firing frequency in a majority of SCN neurons (Mason and Biello, 1992), suggesting a role for GSK3 in regulation of SCN neurophysiological rhythms. However, further research is needed to determine the effect of GSK3 activation on SCN excitability and to identify which ionic component(s) is under GSK3 control in the SCN.

Hypothesis

What links the molecular clock to SCN neurophysiology is one of the most pressing questions in current circadian research (Colwell, 2011). As a kinase that is regulated in a circadian manner and capable of controlling expression and function of multiple ion channels, GSK3 is perfectly positioned to provide that link. Thus, further research into GSK3's role in the circadian system could begin to close the gap between molecular and physiological rhythms. The overall goal of this dissertation is to test the hypothesis that GSK3 activity regulates circadian behavior and photic entrainment through promotion of SCN neuronal excitability and to examine the underlying ionic component through which GSK3 influences SCN physiology. This hypothesis will be tested using a combination of circadian behavioral assessments, immunohistochemistry, and targeted loose-patch and whole-cell electrophysiology in the presence of chronic GSK3 activation and following pharmacological inhibition of GSK3.

This dissertation will be broken up into three primary chapters followed by a general discussion. Chapter 2 determines whether GSK3 activity rhythms are necessary for robust circadian behavior and daily changes in SCN neuronal activity. Chapter 3 examines the role of GSK3 in mediating light-induced SCN excitability and photic

entrainment. Finally, Chapter 4 will test the hypothesis that GSK3 activity promotes SCN neuronal excitability through enhancement of the persistent sodium current (I_{NaP}).

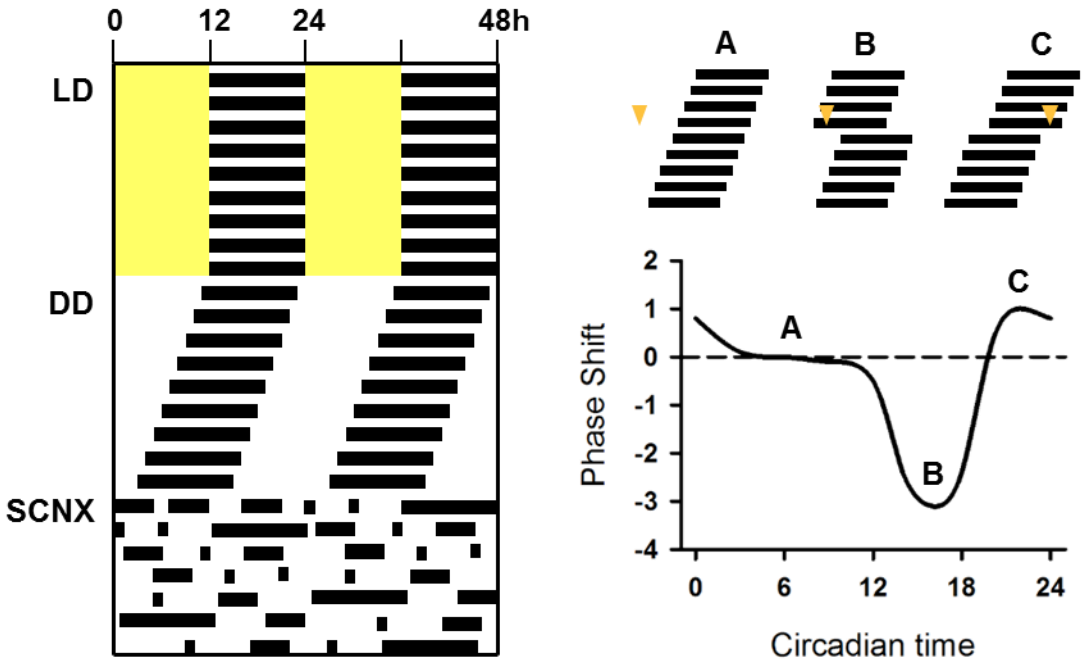

Figure 1. Behavioral analysis in rodents. *Left*, Schematic of typical double-plotted actogram where each line represents two days (second day on one line is the first day on the next line) and black marks represent the measured behavior. Initially, animal is entrained to a 12:12 light/dark cycle (LD; yellow bar indicates lights on) with activity restricted to the dark phase. In contant dark (DD), the animal exhibits free-running behavior with period greater than 24 hours which is shifted by light and after SCN lesion (SCNX). *Right*, Model of typical behavioral shifts in mouse following 15 min light pulse (yellow triangle) and a phase-response curve constructed from those results (Daan and Pittendrigh, 1976).

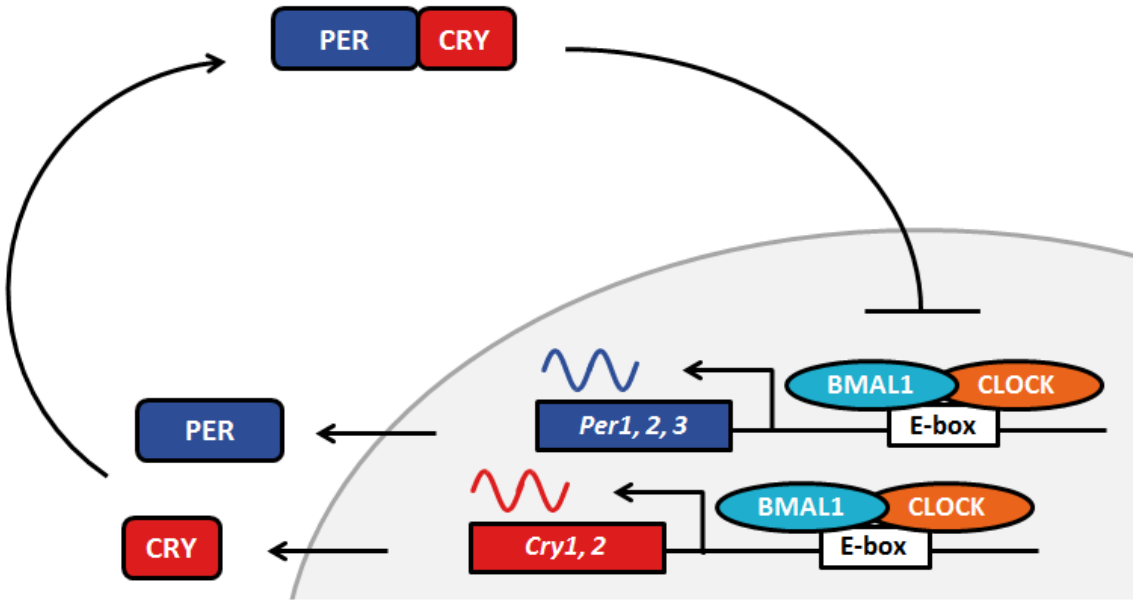

Figure 2. Model of the core molecular clock. At the start of the day, the complex of transcription factors, CLOCK and BMAL1, drive expression of the *Per* and *Cry* genes. In time, accumulating PER and CRY proteins dimerize and translocate to the nucleus where the complex inhibits its own transcription. Eventually, the PER-CRY complex is degraded, and the cycle can begin again. The entire process takes approximately 24 hours to complete.

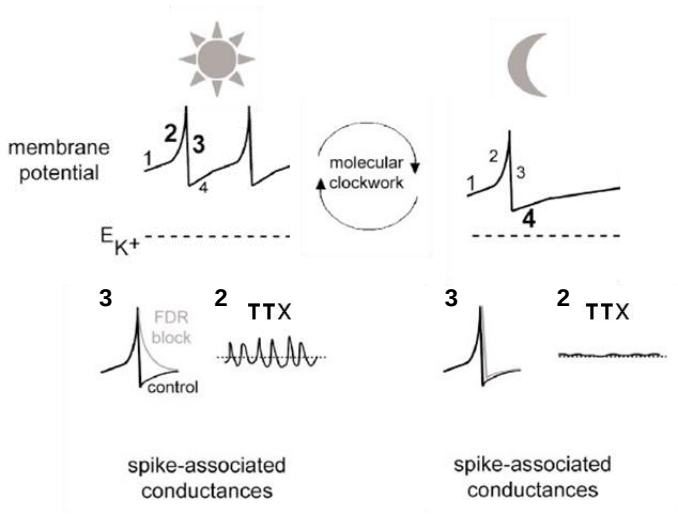

Figure 3. Schematic diagram of day/night differences in SCN neurophysiological properties. For explanation see text. Image modified with permission from (Kuhlman and McMahon, 2006).

CHAPTER 2

DISRUPTION OF CIRCADIAN RHYTHMICITY AND SUPRACHIASMATIC ACTION POTENTIAL FREQUENCY IN A MOUSE MODEL WITH CONSTITUTIVE ACTIVATION OF GLYCOGEN SYNTHASE KINASE-3

by

JODI R. PAUL, RUSSELL L. JOHNSON, RICHARD S. JOPE, AND KAREN L. GAMBLE

Neuroscience 226: 1-9

Abstract

Glycogen synthase kinase 3 (GSK3) is a serine/threonine kinase that has been implicated in psychiatric diseases, neurodevelopment, and circadian regulation. Both GSK3 isoforms, α and β, exhibit a 24-hour variation of inhibitory phosphorylation within the suprachiasmatic nucleus (SCN), the primary circadian pacemaker. We examined the hypothesis that rhythmic GSK3 activity is critical for robust circadian rhythmicity using GSK3$\alpha^{21A/21A}/\beta^{9A/9A}$ knock-in mice with serine-alanine substitutions at the inhibitory phosphorylation sites, making both forms constitutively active. We monitored wheel-running locomotor activity of GSK3 knock-in mice and used loose-patch electrophysiology to examine the effect of chronic GSK3 activity on circadian behavior and SCN neuronal activity. Double transgenic GSK3α/β knock-in mice exhibit disrupted behavioral rhythmicity, including significantly decreased rhythmic amplitude, lengthened active period, and increased activity bouts per day. This behavioral disruption was dependent on chronic activation of both GSK3 isoforms and was not seen in single transgenic GSK3α or GSK3β knock-in mice. Underlying the behavioral changes, SCN neurons from double transgenic GSK3α/β knock-in mice exhibited significantly higher spike rates during the subjective night compared to those from WT controls, with no differences detected during the subjective day. These results suggest that constitutive activation of GSK3 results in loss of the typical day/night variation of SCN neuronal activity. Together, these results implicate GSK3 activity as a critical regulator of circadian behavior and neurophysiological rhythms. Because GSK3 has been implicated in numerous pathologies, understanding how GSK3 modulates circadian rhythms and

neurophysiological activity may lead to novel therapeutics for pathological disorders and circadian rhythm dysfunction.

Introduction

Circadian rhythms are endogenous 24-hour physiological and behavioral rhythms that are present in nearly all living organisms, ranging from bacteria to mammals (Bell-Pedersen et al., 2005). Circadian disturbance in humans has been implicated in a number of pathologies including psychiatric disorders, cardiometabolic disease, inflammatory disease and cancer (Takahashi et al., 2008). In all mammals, daily physiological and behavioral rhythms are orchestrated by a primary circadian pacemaker, the suprachiasmatic nucleus (SCN) of the hypothalamus (Welsh et al., 2010). SCN neurons generate characteristic, daily rhythms in electrical activity, exhibiting high activity during the day and low activity during the night (Inouye and Kawamura, 1979). The daily rhythm in the spontaneous firing rate (SFR) of SCN cells is important for synchronous output of the central pacemaker and is necessary for normal circadian behavior (Schwartz et al., 1987). At the molecular level, 24-hour timing is driven by transcriptional/translational feedback loops of primary "clock" genes which are present in almost all cell types throughout the body (Takahashi et al., 2008). Post-translational modifications, such as phosphorylation, of the core clock components contribute to the precise timing and robustness of the primary feedback loop (Gallego and Virshup, 2007), but the roles of some kinases, such as glycogen synthase kinase 3 (GSK3), remain unclear.

GSK3 is a serine/threonine kinase that is able to phosphorylate nearly all of the circadian molecular clock components such as PER2, CLOCK, BMAL1, and REVERVBα (Iitaka et al., 2005, Wang et al., 2006, Spengler et al., 2009, Kurabayashi et al., 2010, Sahar et al., 2010). In addition, GSK3 is a therapeutic target of the mood-stabilizing agent, lithium (Klein and Melton, 1996), which can lengthen the period of behavioral and molecular rhythms of multiple organisms (LeSauter and Silver, 1993, Iwahana et al., 2004, Dokucu et al., 2005, Li et al., 2012). GSK3 has two isoforms, α and β, both of which are ubiquitously expressed throughout the brain (Woodgett, 1990). Unlike most kinases, GSK3 is by default active and can be inactivated by phosphorylation at serine-21 and serine-9 sites for α and β, respectively (Woodgett, 1990). Recent work has shown that GSK3 exhibits a daily rhythm in inhibitory phosphorylation within the SCN (Iwahana et al., 2004, Iitaka et al., 2005), yet little is known about what role this activity plays in overall circadian rhythmicity. In this study, we examine the function of rhythmic GSK3α/β phosphorylation using GSK3$\alpha^{21A/21A}/\beta^{9A/9A}$ (double knock-in, DKI) mice with serine-alanine substitutions at both inhibitory phosphorylation sites (McManus et al., 2005). With this model, we tested the hypothesis that rhythmic GSK3 activity is critical for generating robust circadian rhythms. Specifically, we measured the effect of chronic GSK3 activity on circadian wheel-running behavior in two different backgrounds of mice. We also examined the role of each GSK3 isoform individually using single transgenic animals (α-KI and β-KI). Finally, we examined whether chronic GSK3 activity disrupts day/night differences in SCN neuronal output (i.e., action potential frequency) using loose-patch recordings of

SCN neurons from DKI and wild-type (WT) mice during the subjective day and subjective night.

Materials/Methods

Animals and Housing

Male, homozygous double transgenic GSK3$\alpha^{21A/21A}$/$\beta^{9A/9A}$ (McManus et al., 2005) mice (5-7 months old) on a mixed (C57BL/6 X Balb/c) background (kindly provided by Dario R. Alessi, Dundee, Scotland) or back-crossed at least 10 generations to C57BL/6J were compared to WT mice that were strain- and age-matched (generated within the colony or purchased from Jackson Laboratories, Bar Harbor, ME). For single knock-in experiments, male, homozygous single transgenic, GSK3$\alpha^{21A/21A}$ (α-KI, 8-11 months old) or GSK3$\beta^{9A/9A}$ (β-KI, 3-6 months old) on a C57BL/6J background were compared to WT mice that were strain- and age-matched. These serine-alanine substitutions resulted in loss of phosphorylation of GSK3α and/or GSK3β within the SCN of the transgenic mice (Fig. 1). In addition, these mice develop normally and do not display any obvious behavioral or physiological phenotype. Mice were genotyped for GSK3α using the forward primer TTGAAGTGGCTGGTACTGGCTCTG and the reverse primer GTGTGCTCCAGAGTAGTACCTAGC and for GSK3β using the forward primer TCACTGGTCTAGGGGTGGTGGAAG and the reverse primer GGAGTCAGTGACAACACTTAACTT according to the specifications in (McManus et al., 2005). Mice were housed in individual wheel cages (Coulbourn Instruments, Whitehall, PA) with standard rodent chow (#7917, Harlan Laboratories, Madison, WI) and water provided ad libitum. All mice were maintained in a 12:12 light-dark (LD) cycle

for at least 9 days before being placed into constant dark (DD). All handling of animals was done in accordance with the University of Alabama at Birmingham (UAB) Institutional Animal Care and Use Committee (IACUC) and National Institutes of Health (NIH) guidelines.

Immunoblotting

In order to confirm the loss of phosphorylation of GSK3 in the SCN from the three transgenic models, the SCN was isolated from α-KI, β-KI, DKI and WT mice (2-3 months old) housed in a 12:12 LD cycle. Protein lysates were prepared and visualized using immunoblotting with an antibody to p-GSK3α S21 (1:750, Cell Signaling, Danvers, MA) or p-GSK3β S9 only (1:500, Cell Signaling, Danvers, MA). Total GSK3α/β (1:750, Cell Signal, Danvers, MA) staining was used on the same blot as a loading control.

Behavioral Analysis

Wheel-running activity was recorded and analyzed using ClockLab software (Actimetrics, Wilmette, IL). Actograms were generated using 6-min bins of activity and double plotted for ease of examination. Behavior was analyzed across 7-10 days for LD analysis, and 10 days of activity for DD analysis after the mice had been in constant conditions for 6-12 days. The activity levels were calculated using the batch analysis in ClockLab software. The free-running period (τ) and amplitude were determined by chi-squared (χ^2) periodogram analysis. Activity bout analyses were exported using the "bout" function in ClockLab, with a bout defined as a period where the activity level never fell below 3 count/min for longer than 30 minutes. Due to the low levels of activity seen in

DKI mice on the mixed background, the threshold was reduced to 1 count/min for the bout analyses in those experiments. The length of the active period (α) was measured as the time between onset and offset of activity. Activity onset was fit by eye, and activity offset was defined as the last point at which the activity in three of the previous six bins exceeded the mean activity level (Gorman and Yellon, 2010). In 2 of 16 DKI mice, activity levels were too low to reliably detect activity onset/offset, and these animals were excluded from the statistical analysis of α. Because there were no significant differences in the behavior of the WT groups age-matched to the either the α-KI or β-KI mice, the two WT groups were combined into one control group for analysis of the single KI behavior.

Slice preparation and electrophysiological recording

Mice were individually housed in constant darkness for three weeks on running wheels and sacrificed at Circadian Time (CT) 4 and 16 (where CT 12 is conventionally defined as the onset of activity) by cervical dislocation and then enucleated with the aid of night-vision goggles. Brains were harvested, sectioned on a vibroslicer (Campden 7000SMZ, World Precision Instruments, Lafayette, IN) in cold, oxygenated sucrose saline (in mM: 250 sucrose, 26 $NaHCO_3$, 1.25 Na_2HPO_4-$7H_2O$, 1.2 $MgSO_4$-$7H_2O$, 10 glucose, 2.5 $MgCl_2$, 3.5 KCl). Slices were transferred to a beaker containing 50% sucrose saline and 50% normal saline (in mM: 130 NaCl, 20 $NaHCO_3$, 1 Na_2HPO_4-$7H_2O$, 1.3 $MgSO_4$-$7H_2O$, 10 Glucose, 3.5 KCl, 2.5 $CaCl_2$) at room temperature for 20 min and then transferred to an open recording chamber (Warner Instruments, Hambden, CT) that was continuously perfused at a rate of 2.0 ml/min with normal saline, bubbled with 5% CO_2 /

95% O_2 and heated to 34 ± 0.5 ºC. Neurons were visualized with an Axio Examiner microscope (Carl Zeiss Inc., Thornwood, NY) equipped for near-IR-DIC. Loose patch recordings were made from CT 6-8 or from CT 18-20 in the medial (dorsal and ventral) SCN. Electrodes with a pipette resistance of ~3-5 MΩ were filled with filtered intracellular solution (in mM: 135 K-gluconate, 10 KCl, 10 HEPES, 0.5 EGTA; pH 7.4) (Kuhlman et al., 2003). Firing frequency was measured as the average of a 120-sec record. Electrophysiological signals were processed and controlled by a Multiclamp 700B amplifier, and pClamp 10.02 software (Axon Instruments, Union City, CA) in gap-free mode. Recordings were sampled at 20 kHz and filtered at 10 kHz (Besing et al., 2012).

Statistical Analysis

Data were analyzed using independent samples t-tests or one-way ANOVA with Tukey HSD post hoc analysis. For variables in which there were outliers and/or assumptions of normality and equal variances were violated and could not be corrected with logarithmic transformations of the data, we analyzed the data with a Mann-Whitney U test or an independent samples Kruskal-Wallis test with two-sided asymptotic significance post hoc analysis. Outliers were not excluded from the analysis. Data are presented as mean ± SEM. Significance was ascribed at $p < 0.05$.

Results

Chronic GSK3 activity disrupts circadian wheel-running behavior

To determine the importance of rhythmic GSK3 phosphorylation on mammalian circadian rhythms we measured wheel running activity of DKI mice in which GSK3α and GSK3β have been mutated at the S21 and S9 inhibitory phosphorylation sites, respectively, rendering both forms constitutively active (McManus et al., 2005). First, we examined wheel-running behavior of DKI and WT mice on a mixed (C57BL/6 X Balb/c) background. In a 12:12h light-dark cycle (LD), both DKI and WT mice were capable of entraining to the light cycle, with the majority of activity occurring in the dark phase (Fig. 2A,B). This was reflected in the percentage of lights-on activity, which did not differ between the two genotypes (Table 1, $U = 103$, $p > 0.05$). The average activity in DKI mice (2.4 ± 0.7 rev/min) was significantly reduced from that of WT mice (12.0 ± 0.9 rev/min; $U = 243$; $p < 0.001$). This decrease in activity was seen in both the light and dark phases of the light cycle (Table 1).

Under constant darkness (DD), several differences in the behavioral rhythms emerged (Fig. 2C). Periodogram analysis revealed that the free-running period (τ) of DKI mice was ~23 minutes longer than WT mice (Table 1; $U = 30$; $p < 0.001$). After only a short time in DD, 1 out of 20 DKI mice did not show a detectable rhythm and was classified as arrhythmic. The remaining DKI mice exhibited a significantly lower amplitude in circadian behavior than WT mice, as seen in the power of the χ^2-periodogram (Table 1; $U = 240$; $p < 0.001$; Fig. 2D). In addition, DKI mice showed significant fragmentation in their wheel-running rhythms, as indicated by an average of 6 activity bouts per day, compared to only 4 bouts per day in WT mice (Table 1; $U = 55.5$;

$p < 0.005$). DKI mice also had significantly longer α or activity period (14.44 ± 0.48 h) than WT controls (12.38 ± 0.73 h; $U = 52$; $p < 0.01$), suggesting a lack of consolidation of activity.

To ensure that the observed phenotype was not an effect of the mouse strain (Pendergast et al., 2010), we next examined the wheel-running behavior of DKI mice backcrossed to C57BL/6J (C57) for at least ten generations. When housed in LD, both groups successfully synchronized to the light cycle (Fig. 3A,B), and there was no difference in the percentage of lights-on activity observed between groups Fig. 4A, $t_9 = -3.46$, $p > 0.05$). As in the mixed background, overall wheel-running activity levels of back-crossed DKI mice (mean ± SEM: 8.1 ± 2.2 rev/min) were significantly reduced compared to WT mice (14.4 ± 1.0 rev/min; $t_{6.7} = -2.6$; $p < 0.05$; Fig. 3B); however, this difference was lost in DD (mean ± SEM; DKI, 7.2 ± 2.4 rev/min; WT, 10.5 ± 1.0 rev/min; $t_{6.6} = -1.3$; $p > 0.05$; Fig. 3C). Additionally, back-crossed DKI mice no longer exhibited a lengthened τ in DD (Fig. 4B; $t_9 = -0.96$; $p > 0.05$). However, the DKI mice showed noticeably dampened activity rhythms, as seen in the significantly reduced amplitude of the χ^2-periodogram (Figs. 3D and 4C; $t_9 = -3.26$; $p < 0.05$). Even though C57 DKI mice exhibited normal levels of activity in DD, the backcrossed mutants continued to show the same fragmented phenotype seen on the mixed background (Fig. 3C). Specifically, the mean α length of C57 DKI mice was nearly 2 hours longer than that of WT mice (Fig. 4D; $t_{4.6} = 4.28$; $p < 0.01$). Also, activity bouts of DKI mice were significantly greater in number per day (Fig 4E; $t_9 = 2.59$; $p < 0.05$) and shorter in mean duration (Fig 4F; $t_9 = -2.29$; $p < 0.05$).

Circadian behavior is unaltered in single transgenic, α-KI and β-KI, mice

To determine the role of rhythmic activity of each GSK3 isoform, we measured wheel-running behavior of homozygous single transgenic, GSK3$\alpha^{21A/21A}$ (α-KI) or GSK3$\beta^{9A/9A}$ (β-KI) mice and WT controls in the same manner as above. Both α-KI and β-KI mice exhibited typical entrainment to the light cycle (Fig. 5A) and similar levels of activity (rev/min) to WT mice in LD (mean ± SEM; α-KI, 12.0 ± 1.4; β-KI, 9.9 ± 1.7; WT, 12.4 ± 2.2; Kruskal-Wallis, $H_2 = 0.72$; $p > 0.05$). In DD, χ^2-periodogram analysis revealed no significant differences in τ ($F_{2,18} = 0.94$; $p > 0.05$) or amplitude ($F_{2,18} = 1.03$; $p > 0.05$) among all three groups (Fig. 5B-D). The mean α lengths for α-KI and β- KI mice were essentially identical to the WT controls ($F_{2,18} = 0.02$; $p > 0.05$; Fig. 5E). Finally, single KI and WT mice had similarly consolidated behavior, with no significant differences in the number of activity bouts per day ($F_{2,18} = 0.25$; $p > 0.05$; Fig. 5F).

Chronic GSK3 activity alters SFR rhythms in SCN neurons

In order to determine whether DKI mice have a disruption in normal pacemaker function at the level of the SCN, we next examined neurophysiological activity of SCN neurons from these mice. SCN neurons exhibit a circadian variation in the frequency of spontaneous action potential generation, with high activity during the day and low activity during the night (Inouye and Kawamura, 1979). These rhythms are a major output signal of the SCN and are important in the regulation of circadian behavior (Schwartz et al., 1987). To test the effect of chronic GSK3 activation on SFR rhythms in the SCN, we used loose-patch electrophysiological recordings of SCN neurons from WT and DKI mice during the subjective day and night. After behavioral analysis in DD, the

same C57BL/6J WT and DKI animals were sacrificed, and extracellular recordings were made from SCN neurons at CT 6-8 or CT 18-20 for day or night recordings, respectively. During the subjective day, SCN neurons exhibited similarly elevated firing in both WT and DKI mice (Fig. 6; WT, 3.9 ± 0.6 Hz, n = 23; DKI, 4.3 ± 0.5 Hz, n = 27). As expected, WT neurons had a significantly lower SFR at night (0.8 ± 0.3 Hz, n = 30; H_3 = 40.7; $p < 0.001$; Kruskal-Wallis test). Unlike WT neurons, DKI SCN cells did not exhibit a significant day/night difference in neuronal activity (DKI-night, 2.7 ± 0.4 Hz; n = 30; $p > 0.05$). The loss of rhythmic activity in the SCN of DKI mice was driven by the hyperactivity of DKI neurons at night, which were firing at a rate over three times faster than WT cells ($p < 0.05$; two-sided asymptotic significance post hoc analysis). This same pattern of high excitability at night and normal activity during the day was also replicated in SCN neurons from DKI mice on the mixed background (mean ± SEM; DKI- night, 4.1 ± 0.8 Hz, n = 20; WT- night, 1.0 ± 0.4 Hz, n = 11; DKI-day, 5.8 ± 1.0 Hz, n = 11; WT-day, 4.8 ± 1.0 Hz, n = 17; 1-2 slices per genotype per timepoint).

Discussion

The role of GSK3 as a critical regulator of the molecular clock is supported by reports showing that GSK3 phosphorylates nearly all of the core clock components in vitro (Iitaka et al., 2005, Wang et al., 2006, Spengler et al., 2009, Kurabayashi et al., 2010, Sahar et al., 2010). In addition to regulating the molecular clock, GSK3 exhibits a 24-hour variation of inhibitory phosphorylation within the SCN from mice held in an LD cycle (Iitaka et al., 2005). However, the role that this inactivation rhythm plays in the mammalian circadian system is not yet known. The present study shows, for the first

time, that rhythmic GSK3 activity is critical for robust circadian rhythmicity. Specifically, our results indicate that: (1) chronic activation of GSK3 disrupts circadian behavior by decreasing circadian amplitude and increasing fragmentation; (2) chronic activation of either GSK3 isoform alone does not alter behavioral rhythms; and (3) chronic activation of GSK3α/β eliminates rhythms in SCN neuronal activity.

Our first finding that chronic GSK3 disrupts behavioral rhythms is supported by our results that DKI mice exhibit dampened and fragmented wheel-running activity. Previous work on GSK3 and circadian behavior has predominantly focused on changes in the free-running period. For example, lithium, a known inhibitor of GSK3, lengthens the free-running period of a variety of organisms (LeSauter and Silver, 1993, Iwahana et al., 2004, Dokucu et al., 2005). Conversely, Drosophila that over-express GSK3β have a shortened τ (Martinek et al., 2001). Surprisingly, our results show that GSK3 that is chronically active (but expressed at physiological levels) causes only a slight increase in τ in mutant mice on a mixed background. In rodents, the act of running on a wheel is known to influence τ, with wheel-access being associated with a shorter period (Yamada et al., 1988). Thus, it is possible that the lengthened τ in mixed DKI mice was a result of the severely reduced activity levels seen in these animals. This explanation is supported by the lack of period change in DKI mice on the C57 background, which also did not differ from WT mice in DD activity levels. Instead, our results revealed the importance of GSK3 phosphorylation rhythms in the generation of robust circadian behavior. On both backgrounds of mice, chronic GSK3 activity reduced the amplitude of behavioral rhythms and expanded the active phase (α). This reduced amplitude was coupled with significant behavioral fragmentation, as seen in the quantification of activity bouts, which

were shorter in length and greater in number. These results are consistent with recent *in vitro* data that GSK3 inhibition increases the molecular clock amplitude (Li et al., 2012). Taken together, these findings suggest a critical role for GSK3 phosphorylation state balance in driving circadian clock amplitude.

Although the two GSK3 isoforms express 98% homology in amino acid sequence (Kaidanovich and Eldar-Finkelman, 2002), differences in α and β isoforms function has been noted in muscle metabolism (McManus et al., 2005), ischemic injury (Lal et al., 2012), and anti-depressant response (Polter and Li, 2011). Different functions of the isoforms have also been implicated within the circadian system. For example, GSK3α, but not β, interacts *in vitro* with Receptor for Activated C-Kinase 1 (RACK1) (Zeidner et al., 2011), a known regulator of the circadian clock (Robles et al., 2010). In spite of this, the differential roles of GSK3α and β in regulating circadian rhythms *in vivo* remain unclear; furthermore, the distinct function of each isoforms' rhythmic activity has been largely unexplored. In the present study, we examined the role of inhibitory phosphorylation of GSK3α and GSK3β separately by using transgenic mouse models. Interestingly, the single transgenic α-KI and β-KI mice did not exhibit any of the same behavioral disruptions that were characteristic of the DKI mice. These results suggest that, in terms of circadian rhythm function, there may be compensation for the loss of phosphorylation of one isoform. However, peak levels of p-GSK3 in these mice do not suggest that this compensation occurs at the level of GSK3 S21/S9 phosphorylation, consistent with findings of McManus et al. (2005).

In addition to disrupting circadian behavior, we found that chronic GSK3 activity altered SFR rhythms in the SCN. Our results show that loss of GSK3 inactivation, as in

the DKI mice, eliminated the day/night difference in SCN neuronal activity. This loss was due to the elevated "day"-like activity of DKI neurons during the subjective night. Importantly, the activity of SCN DKI neurons did not differ from that of WT neurons during the day, suggesting that the effects of constitutive GSK3 activation are phase-specific. These results suggest that the phosphorylation rhythm may be necessary for normal rhythmicity of spike rate in SCN neurons. Our results are consistent with a model in which active GSK3 enhances excitability while inactivation or inhibition decreases excitability. This idea is supported by previous work examining the effect of lithium on SCN activity. In hamsters, application of lithium to acute brain slices suppressed day-phase SCN neuronal firing (Mason and Biello, 1992), but this suppression may have occurred through a non-GSK3 related action of the drug. In the future, it will be important to replicate this effect with specific, small-molecule inhibitors of GSK3.

The mechanism by which GSK3 activity controls neurophysiological rhythms in the SCN remains unclear. One possible explanation for the disrupted SCN activity seen in DKI mice is an indirect consequence of disruption in the core molecular clock. However, further study *in vivo* is needed to determine how the molecular clock is affected by chronic GSK3 activity. Another possibility is that, downstream of the core clock, GSK3 activity directly influences membrane properties through an unknown mechanism. Interestingly, the effects of lithium on SCN activity are seen within 5-10 min of treatment (Mason and Biello, 1992). The rapid onset of this effect supports the notion that GSK3 is able to exert control over SCN neurophysiology without acting through the core clock. The ionic mechanisms underlying the daily rhythms in SCN activity have been extensively studied, and many of these currents have been shown to be rhythmic

themselves (Pennartz et al., 2002, Itri et al., 2005, Pitts et al., 2006, Itri et al., 2010). One of the biggest questions left unanswered is how ion channels are being regulated to produce these rhythms (Colwell, 2011). In cortical and hippocampal cell culture, GSK3 has been shown to regulate expression and function of multiple receptors including, NMDAR, AMPAR, and $GABA_AR$, through mechanisms like trafficking, clustering, and phosphorylation (Chen et al., 2007, Wei et al., 2010, Tyagarajan et al., 2011). Future research should examine the possibility that rhythmic GSK3 regulates ion channels in the SCN in a similar manner.

One notable candidate target of GSK3 is large-conductance Ca^{2+} activated K^+ (BK) channels which contribute to the nightly silencing of SCN neurons (Meredith et al., 2006). In other cell types, GSK3 can directly associate with the BKα sub-unit and regulate membrane expression of BK channels *in vitro* (Bian et al., 2011, Sokolowski et al., 2011). Furthermore, *kcnma1*$^{-/-}$ mice, which lack the pore-forming α subunit of BK channels, show strikingly similar circadian phenotypes to DKI mice, in both behavior and SCN activity (Meredith et al., 2006). Determining the role of rhythmic GSK3 activity in regulating membrane properties of the SCN could provide a missing link between the molecular clock and the circadian output signal (i.e., spike rate). With the growing number of reports showing disrupted circadian behavior together with altered neuronal rhythms (Meredith et al., 2006, Kudo et al., 2011a, Kudo et al., 2011b, Nakamura et al., 2011, Farajnia et al., 2012), understanding the link between the core clock and membrane excitability is an important direction for future circadian research.

Dysregulation of GSK3 has been implicated in many of the same pathological conditions that are linked with circadian rhythm disturbance, such as psychiatric and

aging-related disorders (Gomez-Sintes et al., 2011, Jope, 2011). Previously, DKI mice have been used as a model for bipolar disorder, with the mice displaying increased susceptibility to both manic- and depressive-like behaviors (Polter et al., 2010). In human bipolar patients, phosphorylation levels of GSK3 are decreased in peripheral blood mononuclear cells and fibroblasts (Yang et al., 2009, Polter et al., 2010). Circadian disruption is commonly seen in aging (Kondratova and Kondratov, 2012), and loss of p-GSK3 rhythms has been demonstrated in the SCN of aged hamsters (Iwahana et al., 2007). Because of its involvement in these and other pathologies, understanding how GSK3 modulates circadian rhythms and neurophysiological activity may lead to novel therapeutics for pathological disorders and circadian rhythm dysfunction.

Acknowledgements

This work was supported by National Institutes of Health, Grants R00 GM086683 (KLG) and R01 MH038752 (RSJ). We thank Xiaohua Li for backcrossing the mice, Lauren Hablitz for technical assistance, and Rachel Besing for advice on the manuscript.

References

Bell-Pedersen D, Cassone VM, Earnest DJ, Golden SS, Hardin PE, Thomas TL, Zoran MJ (Circadian rhythms from multiple oscillators: lessons from diverse organisms. Nat Rev Genet 6:544-556.2005).

Besing RC, Hablitz LM, Paul JR, Johnson RL, Prosser RA, Gamble KL (Neuropeptide Y-induced phase shifts of PER2::LUC rhythms are mediated by long-term

suppression of neuronal excitability in a phase-specific manner. Chronobiol Int 29:91-102.2012).

Bian S, Bai JP, Chapin H, Le Moellic C, Dong H, Caplan M, Sigworth FJ, Navaratnam DS (Interactions between beta-catenin and the HSlo potassium channel regulates HSlo surface expression. PLoS One 6:e28264.2011).

Chen P, Gu Z, Liu W, Yan Z (Glycogen synthase kinase 3 regulates N-methyl-D-aspartate receptor channel trafficking and function in cortical neurons. Mol Pharmacol 72:40-51.2007).

Colwell CS (Linking neural activity and molecular oscillations in the SCN. Nat Rev Neurosci 12:553-569.2011).

Dokucu ME, Yu L, Taghert PH (Lithium- and valproate-induced alterations in circadian locomotor behavior in Drosophila. Neuropsychopharmacology 30:2216-2224.2005).

Farajnia S, Michel S, Deboer T, vanderLeest HT, Houben T, Rohling JH, Ramkisoensing A, Yasenkov R, Meijer JH (Evidence for neuronal desynchrony in the aged suprachiasmatic nucleus clock. J Neurosci 32:5891-5899.2012).

Gallego M, Virshup DM (Post-translational modifications regulate the ticking of the circadian clock. Nat Rev Mol Cell Biol 8:139-148.2007).

Gomez-Sintes R, Hernandez F, Lucas JJ, Avila J (GSK-3 Mouse Models to Study Neuronal Apoptosis and Neurodegeneration. Front Mol Neurosci 4:45.2011).

Gorman MR, Yellon S (Lifespan daily locomotor activity rhythms in a mouse model of amyloid-induced neuropathology. Chronobiol Int 27:1159-1177.2010).

Iitaka C, Miyazaki K, Akaike T, Ishida N (A role for glycogen synthase kinase-3beta in the mammalian circadian clock. J Biol Chem 280:29397-29402.2005).

Inouye ST, Kawamura H (Persistence of circadian rhythmicity in a mammalian hypothalamic "island" containing the suprachiasmatic nucleus. Proc Natl Acad Sci U S A 76:5962-5966.1979).

Itri JN, Michel S, Vansteensel MJ, Meijer JH, Colwell CS (Fast delayed rectifier potassium current is required for circadian neural activity. Nat Neurosci 8:650-656.2005).

Itri JN, Vosko AM, Schroeder A, Dragich JM, Michel S, Colwell CS (Circadian regulation of a-type potassium currents in the suprachiasmatic nucleus. J Neurophysiol 103:632-640.2010).

Iwahana E, Akiyama M, Miyakawa K, Uchida A, Kasahara J, Fukunaga K, Hamada T, Shibata S (Effect of lithium on the circadian rhythms of locomotor activity and glycogen synthase kinase-3 protein expression in the mouse suprachiasmatic nuclei. Eur J Neurosci 19:2281-2287.2004).

Iwahana E, Hamada T, Uchida A, Shibata S (Differential effect of lithium on the circadian oscillator in young and old hamsters. Biochem Biophys Res Commun 354:752-756.2007).

Jope RS (Glycogen synthase kinase-3 in the etiology and treatment of mood disorders. Front Mol Neurosci 4:16.2011).

Kaidanovich O, Eldar-Finkelman H (The role of glycogen synthase kinase-3 in insulin resistance and type 2 diabetes. Expert Opin Ther Targets 6:555-561.2002).

Klein PS, Melton DA (A molecular mechanism for the effect of lithium on development. Proc Natl Acad Sci U S A 93:8455-8459.1996).

Kondratova AA, Kondratov RV (The circadian clock and pathology of the ageing brain. Nat Rev Neurosci 13:325-335.2012).

Kudo T, Loh DH, Truong D, Wu Y, Colwell CS (Circadian dysfunction in a mouse model of Parkinson's disease. Exp Neurol 232:66-75.2011a).

Kudo T, Schroeder A, Loh DH, Kuljis D, Jordan MC, Roos KP, Colwell CS (Dysfunctions in circadian behavior and physiology in mouse models of Huntington's disease. Exp Neurol 228:80-90.2011b).

Kuhlman SJ, Silver R, Le Sauter J, Bult-Ito A, McMahon DG (Phase resetting light pulses induce Per1 and persistent spike activity in a subpopulation of biological clock neurons. J Neurosci 23:1441-1450.2003).

Kurabayashi N, Hirota T, Sakai M, Sanada K, Fukada Y (DYRK1A and glycogen synthase kinase 3beta, a dual-kinase mechanism directing proteasomal degradation of CRY2 for circadian timekeeping. Mol Cell Biol 30:1757-1768.2010).

Lal H, Zhou J, Ahmad F, Zaka R, Vagnozzi RJ, Decaul M, Woodgett J, Gao E, Force T (Glycogen synthase kinase-3alpha limits ischemic injury, cardiac rupture, post-myocardial infarction remodeling and death. Circulation 125:65-75.2012).

LeSauter J, Silver R (Lithium lengthens the period of circadian rhythms in lesioned hamsters bearing SCN grafts. Biol Psychiatry 34:75-83.1993).

Li J, Lu WQ, Beesley S, Loudon AS, Meng QJ (Lithium impacts on the amplitude and period of the molecular circadian clockwork. PLoS One 7:e33292.2012).

Martinek S, Inonog S, Manoukian AS, Young MW (A role for the segment polarity gene shaggy/GSK-3 in the Drosophila circadian clock. Cell 105:769-779.2001).

Mason R, Biello SM (A neurophysiological study of a lithium-sensitive phosphoinositide system in the hamster suprachiasmatic (SCN) biological clock in vitro. Neurosci Lett 144:135-138.1992).

McManus EJ, Sakamoto K, Armit LJ, Ronaldson L, Shpiro N, Marquez R, Alessi DR (Role that phosphorylation of GSK3 plays in insulin and Wnt signalling defined by knockin analysis. EMBO J 24:1571-1583.2005).

Meredith AL, Wiler SW, Miller BH, Takahashi JS, Fodor AA, Ruby NF, Aldrich RW (BK calcium-activated potassium channels regulate circadian behavioral rhythms and pacemaker output. Nat Neurosci 9:1041-1049.2006).

Nakamura TJ, Nakamura W, Yamazaki S, Kudo T, Cutler T, Colwell CS, Block GD (Age-related decline in circadian output. J Neurosci 31:10201-10205.2011).

Pendergast JS, Friday RC, Yamazaki S (Distinct functions of Period2 and Period3 in the mouse circadian system revealed by in vitro analysis. PLoS One 5:e8552.2010).

Pennartz CM, de Jeu MT, Bos NP, Schaap J, Geurtsen AM (Diurnal modulation of pacemaker potentials and calcium current in the mammalian circadian clock. Nature 416:286-290.2002).

Pitts GR, Ohta H, McMahon DG (Daily rhythmicity of large-conductance Ca2+ -activated K+ currents in suprachiasmatic nucleus neurons. Brain Res 1071:54-62.2006).

Polter A, Beurel E, Yang S, Garner R, Song L, Miller CA, Sweatt JD, McMahon L, Bartolucci AA, Li X, Jope RS (Deficiency in the inhibitory serine-

phosphorylation of glycogen synthase kinase-3 increases sensitivity to mood disturbances. Neuropsychopharmacology 35:1761-1774.2010).

Polter AM, Li X (Glycogen Synthase Kinase-3 is an Intermediate Modulator of Serotonin Neurotransmission. Front Mol Neurosci 4:31.2011).

Robles MS, Boyault C, Knutti D, Padmanabhan K, Weitz CJ (Identification of RACK1 and protein kinase Calpha as integral components of the mammalian circadian clock. Science 327:463-466.2010).

Sahar S, Zocchi L, Kinoshita C, Borrelli E, Sassone-Corsi P (Regulation of BMAL1 protein stability and circadian function by GSK3beta-mediated phosphorylation. PLoS One 5:e8561.2010).

Schwartz WJ, Gross RA, Morton MT (The suprachiasmatic nuclei contain a tetrodotoxin-resistant circadian pacemaker. Proc Natl Acad Sci U S A 84:1694-1698.1987).

Sokolowski B, Orchard S, Harvey M, Sridhar S, Sakai Y (Conserved BK channel-protein interactions reveal signals relevant to cell death and survival. PLoS One 6:e28532.2011).

Spengler ML, Kuropatwinski KK, Schumer M, Antoch MP (A serine cluster mediates BMAL1-dependent CLOCK phosphorylation and degradation. Cell Cycle 8:4138-4146.2009).

Takahashi JS, Hong HK, Ko CH, McDearmon EL (The genetics of mammalian circadian order and disorder: implications for physiology and disease. Nat Rev Genet 9:764-775.2008).

Tyagarajan SK, Ghosh H, Yevenes GE, Nikonenko I, Ebeling C, Schwerdel C, Sidler C, Zeilhofer HU, Gerrits B, Muller D, Fritschy JM (Regulation of GABAergic

synapse formation and plasticity by GSK3beta-dependent phosphorylation of gephyrin. Proc Natl Acad Sci U S A 108:379-384.2011).

Wang J, Yin L, Lazar MA (The orphan nuclear receptor Rev-erb alpha regulates circadian expression of plasminogen activator inhibitor type 1. J Biol Chem 281:33842-33848.2006).

Wei J, Liu W, Yan Z (Regulation of AMPA receptor trafficking and function by glycogen synthase kinase 3. J Biol Chem 285:26369-26376.2010).

Welsh DK, Takahashi JS, Kay SA (Suprachiasmatic nucleus: cell autonomy and network properties. Annu Rev Physiol 72:551-577.2010).

Woodgett JR (Molecular cloning and expression of glycogen synthase kinase-3/factor A. EMBO J 9:2431-2438.1990).

Yamada N, Shimoda K, Ohi K, Takahashi S, Takahashi K (Free-access to a running wheel shortens the period of free-running rhythm in blinded rats. Physiol Behav 42:87-91.1988).

Yang S, Van Dongen HP, Wang K, Berrettini W, Bucan M (Assessment of circadian function in fibroblasts of patients with bipolar disorder. Mol Psychiatry 14:143-155.2009).

Zeidner LC, Buescher JL, Phiel CJ (A novel interaction between Glycogen Synthase Kinase-3alpha (GSK-3alpha) and the scaffold protein Receptor for Activated C-Kinase 1 (RACK1) regulates the circadian clock. Int J Biochem Mol Biol 2:318-327.2011).

Table 1. Circadian analysis of wheel running behavior of WT and DKI mice on a mixed background.

	WT			*n*	DKI			*n*
LD								
Activity (rev/min)	12.0	±	0.9	16	2.4	±	0.9**	16
Light Activity (rev/day)	1235	±	968	16	152	±	158**	16
Dark Activity (rev/day)	16062	±	4443	16	3294	±	5026**	16
Total Activity (rev/day)	17297	±	4912	16	6443	±	5162**	16
% Lights on Activity (%)	6.8	±	4.8	16	8.7	±	6.4	16
		±				±		
DD		±				±		
Tau (h)	23.42	±	0.16	17	23.81	±	0.10**	15
Power	1363	±	343	17	524	±	62**	15
Activity (rev/min)	14.11	±	1.04	17	0.83	±	0.34**	16
Alpha Length (h)	12.38	±	0.73	17	14.44	±	0.48**	14
Fragmentation (bouts/day)	4.3	±	0.5	17	6.1	±	0.4*	16
Avg. Bout Length (min)	133	±	12.6	17	21.7	±	2.3**	16

**$p < 0.001$; *$p < 0.01$; Mann-Whitney U test

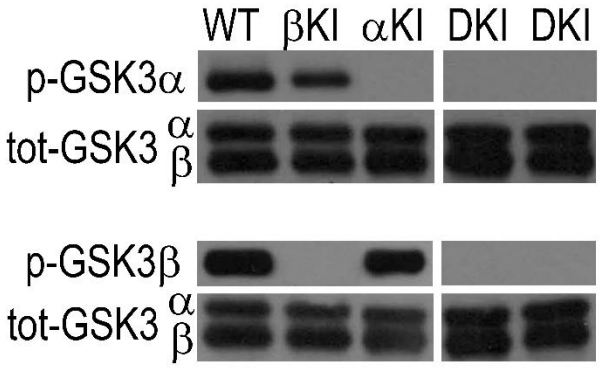

Figure 1. Representative immunoblots of p-GSK3α/β in SCN tissue of WT, α-KI, β-KI, and DKI mice. Immunostaining for p-GSK3α S21 (top) and p-GSK3β S9 (bottom) showing loss of inhibitory phosphorylation of GSK3α, GSK3β, or both in SCN of α-KI, β-KI, or DKI mice, respectively. Total GSK3α/β staining shows loading control for each blot.

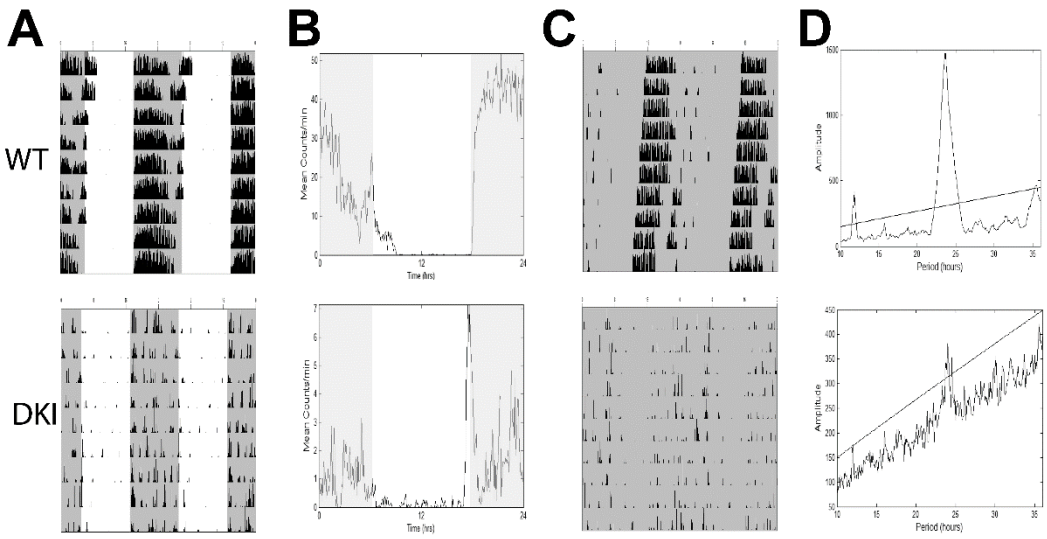

Figure 2. Representative wheel-running behavior for WT (top) and DKI (bottom) mice on a mixed background. (A) Double-plotted actograms show behavior in a 12:12 light cycle (LD). (B) Activity profile plots showing averaged LD activity based on actograms in A. (C) Double-plotted actograms show behavior starting 6 days after release into constant dark (DD). (D) Representative χ^2-periodogram plots showing free-running period and amplitude for behavior in C. Line indicates 0.001% significance level. Shaded areas indicate lights off.

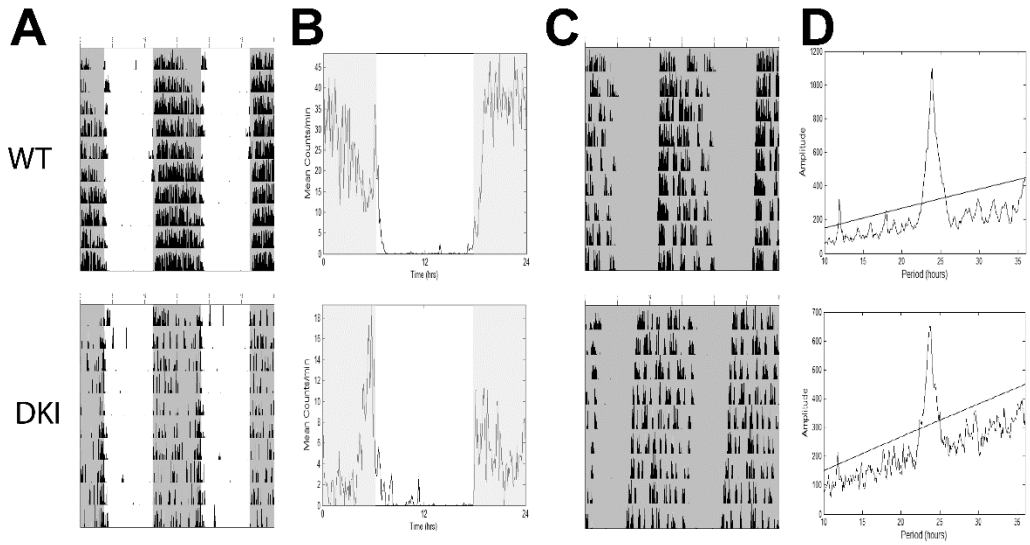

Figure 3. Representative wheel-running behavior for C57BL/6J WT (top) and DKI (bottom) mice. (A) Double-plotted actograms show entrained behavior in LD. (B) Activity profile plots show averaged LD activity based on behavior in A. (C) Double-plotted actograms show behavior starting 12 days after release into DD. (D) Representative χ^2-periodogram plots showing free-running period and amplitude for behavior in C. Line indicates 0.001% significance level. Shaded areas indicate lights off.

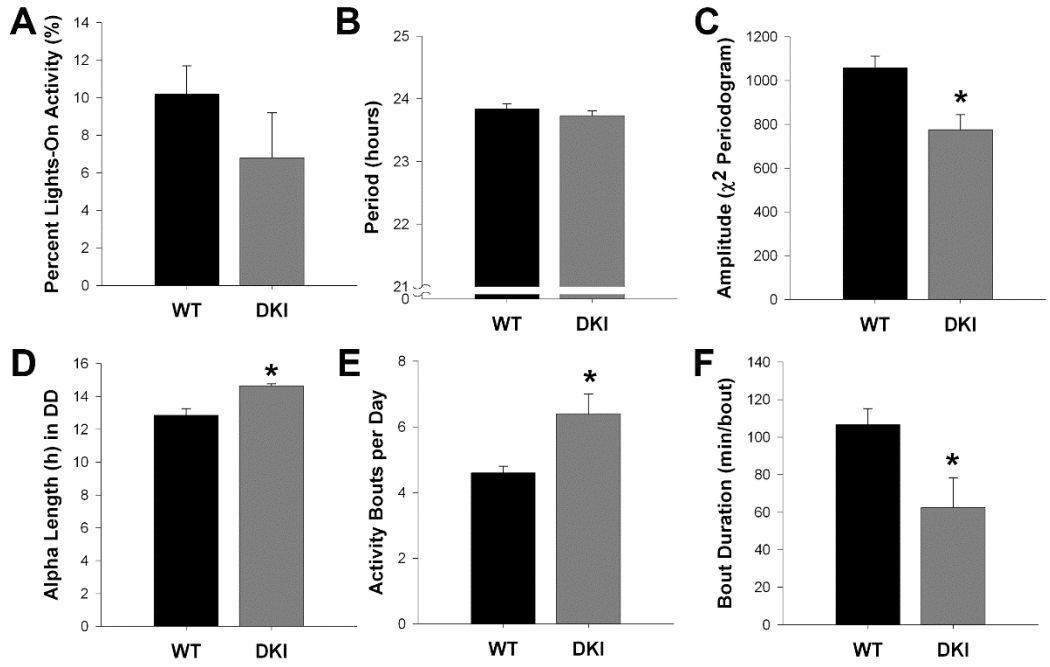

Figure 4. Summary of circadian behavioral parameters for C57BL/6J DKI mice. Bar graphs indicating the mean ± SEM of percent activity during lights on in LD (A), free-running period (B), χ^2-periodogram amplitude (C), alpha length (D), activity fragmentation (E), and bout duration (F) for C57BL/6J WT (n = 5) and DKI (n = 6) mice. *$p < 0.05$

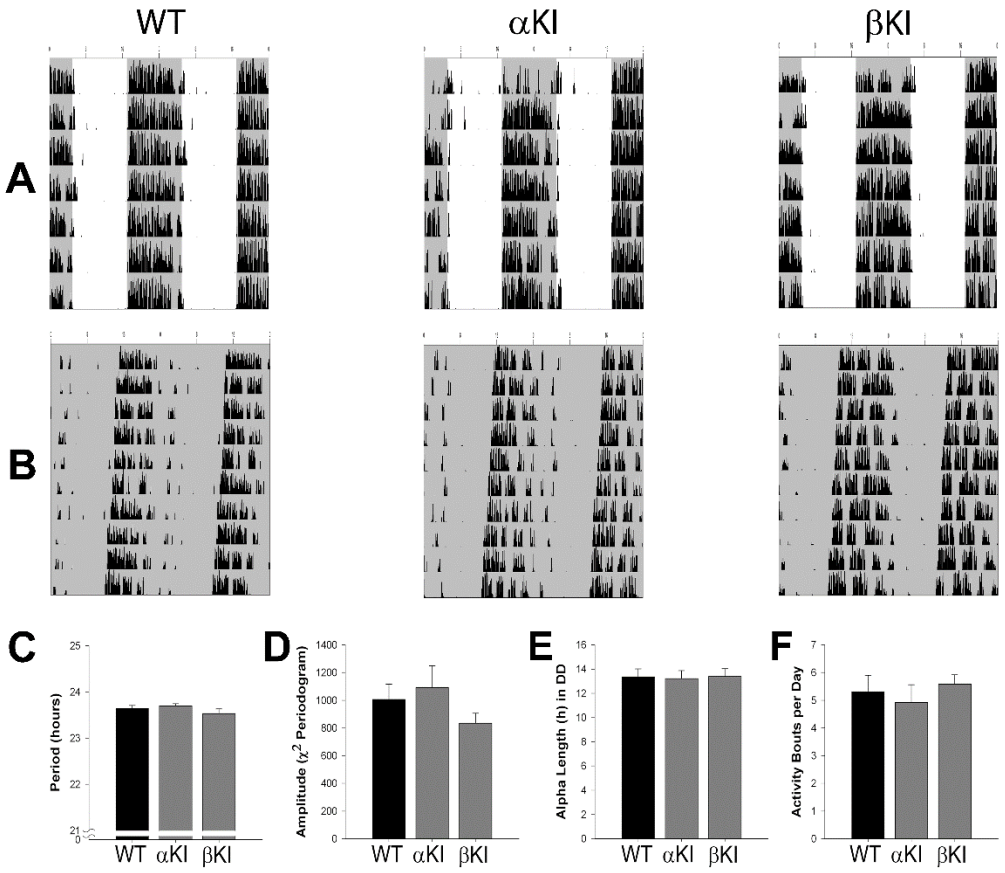

Figure 5. Summary of circadian locomotor activity for α-KI and β-KI mice. (A,B) Representative wheel-running behavior for WT (left), α-KI (middle), and β-KI (right) mice. Double-plotted actograms show locomotor activity in LD (A) and DD (B). Shaded areas indicate lights off. (C-F) Bar graphs indicating the mean ± SEM of free-running period (C), χ^2-periodogram amplitude (D), alpha length (E), and activity bouts per day (F) for WT (n = 10), α-KI (n = 5), and β-KI (n = 6) mice. One-way ANOVA; $p > 0.05$ for all graphs.

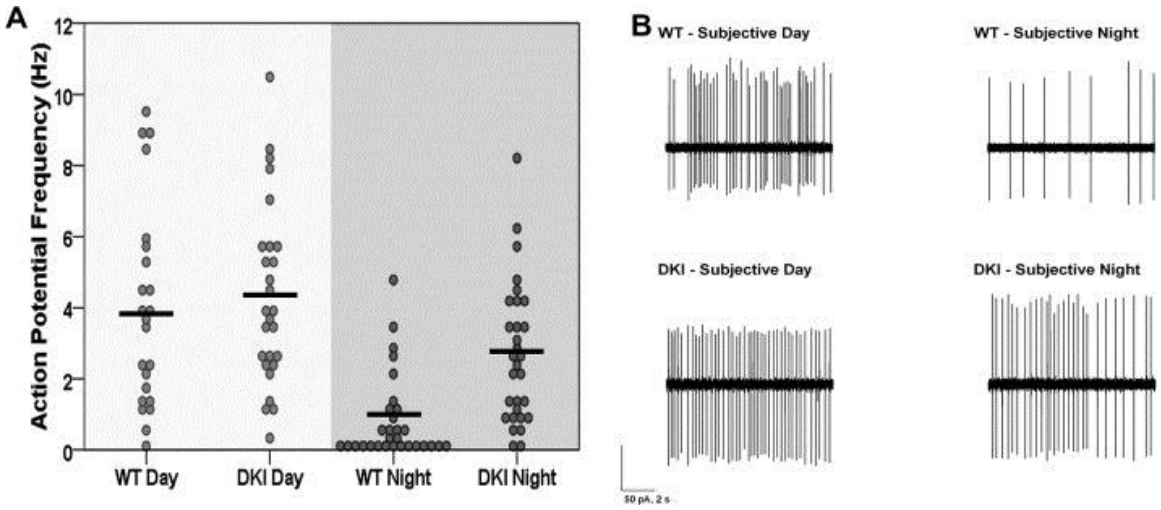

Figure 6. Neurophysiological activity of SCN neurons from C57 DKI mice. (A) Spontaneous action potential frequencies of SCN neurons during the subjective day (CT 6-8) and subjective night (CT 18-20) from WT and DKI mice housed in DD. Black bars indicate the means for each group. (B) Representative cell-attached loose-patch traces (10 s) from results quantified in A. *Significantly different from all other groups, $p < 0.005$, 2-3 slices per genotype per time point.

CHAPTER 3

GLYCOGEN SYNTHASE KINASE 3 REGULATES LIGHT SIGNALING IN THE SUPRACHIASMATIC NUCLEUS

by

JODI R. PAUL, ALEX S. McKEOWN, STACIE K. TOTSCH, TIM W. KRAFT, RITA M. COWELL, AND KAREN L. GAMBLE

In preparation for *European Journal of Neuroscience*

Format adapted for dissertation

Abstract

Glycogen synthase kinase 3 (GSK3) is a serine-threonine kinase that is an emerging regulator of mammalian circadian rhythms at the behavioral, molecular and neurophysiological levels. In the central circadian pacemaker, the suprachiasmatic nucleus (SCN), GSK3 exhibits a rhythm in inhibitory phosphorylation across the 24h day. We have recently shown that GSK3 is capable of influencing both the molecular clock and SCN neuronal activity rhythms. However, whether GSK3 regulates the response to environmental cues such as light is not yet known. The goal of the present study was to test the hypothesis that GSK3 activation mediates light-induced SCN excitability and photic entrainment. Immunofluorescence staining in the SCN of mice showed that late-night light exposure significantly increased GSK3 activity (decreased pGSK3β levels) 30-60 minutes after the light-pulse. Additionally, pharmacological inhibition of GSK3 blocked the typical light-induced excitability in SCN neurons; however, this effect was not associated with changes in resting membrane potential or input resistance. Behaviorally, mice with constitutively active GSK3 re-entrained to a 6-h phase advance in the light-dark cycle in significantly fewer days than WT control animals. Furthermore, the behavioral and SCN neuronal activity of GSK3-KI mice was phase-advanced compared to WT, in both normal and light-exposed conditions. Finally, GSK3-KI mice exhibited normal negative-masking behavior and electroretinographic responses to light, suggesting that the enhanced photic entrainment is not due to an overall increased sensitivity to light in these animals. Taken together, these results provide strong evidence that GSK3 activation contributes to light-induced phase-resetting at both the neurophysiological and behavioral levels.

Introduction

Entrainment is the process by which internal circadian rhythms are synchronized to the external environment. Although there are many environmental factors that can influence circadian rhythmicity (i.e. food availability, arousal), light is the major entraining signal to the master circadian pacemaker, the suprachiasmatic nucleus (SCN; (Czeisler, 1995; Golombek & Rosenstein, 2010)). Exposure to light at specific times of the night differentially shifts the phase of the molecular clock and behavioral activity rhythms (Golombek & Rosenstein, 2010). This process of phase-resetting in response to an acute light-pulse (LP) begins with glutamate release from the retinohypothalamic tract onto SCN neurons (Hannibal, 2002), resulting in an influx of Ca2+ through NMDA receptors and subsequent activation of multiple signal cascades. These cascades, which include activation of mitogen activated protein kinases (MAPKs) extracellular signal-related kinases 1 and 2 (ERK1/2; (Obrietan *et al.*, 1998; Butcher *et al.*, 2003)), lead to the rapid induction of gene expression, including *period1* (*Per1*; (Tischkau *et al.*, 2003)). In the late-night, this upregulation of *Per1* is followed by a persistent increase in SCN neuronal activity 3-5 hours later (Kuhlman *et al.*, 2003).

Although much work has examined the molecular events involved in the process of phase-resetting, very little is known about link connecting light-induced molecular events to neurophysiological excitability (Colwell, 2011). One candidate mediator is glycogen synthase kinase 3 (GSK3), a serine-threonine kinase that is an emerging regulator of mammalian circadian rhythms. Much of the previous research on the role of GSK3 in the circadian system has focused on its phosphorylation of multiple components of the core-molecular clock (Iitaka *et al.*, 2005; Kurabayashi *et al.*, 2010; Sahar *et al.*,

2010). However, we have recently reported that chronic GSK3 activation increases SCN neuronal activity, highlighting GSK3 as a regulator of neurophysiological rhythms as well (Paul *et al.*, 2012). Thus, GSK3 is in a unique position to provide the link between molecular rhythms and neuronal excitability. Additionally, research examining the role of GSK3 in the process of phase-resetting has been limited. Therefore, the goal of the present study was to test the hypothesis that GSK3 activation mediates light-induced SCN excitability and photic entrainment.

Material and methods

Animals

Three to 7 month old homozygous *Per1*::GFP (Kuhlman *et al.*, 2000), wild-type (WT) C57-BL6/J, and GSK3α/β$^{21A/21A/9A/9A}$ (GSK3-KI) mice (McManus *et al.*, 2005) on a C57-BL6/J background were group-housed in a 12:12 light/dark (LD) cycle (unless stated otherwise) with food and water *ad libitum* in accordance with UAB IACUC guidelines. Due to the increased variability in activity onset seen in female mice (Iwahana *et al*. 2008), only male mice were used for behavioral measures; however, both male and female animals were used for all other experiments. All animals were euthanized with cervical dislocation and rapid decapitation. Mice were sacrificed between Zeitgeber Time (ZT) 22-23 (where ZT 0 equals time of lights-on) for all experiments.

Behavior

Mice were housed in individual wheel cages, and wheel-running activity was recorded and analyzed using ClockLab software (Actimetrics, Wilmette, IL, USA). The

phase angle for each mouse was determined prior to shifting the light cycle by 6 h. Animals were considered to be entrained when the activity onset occurred within 20 min of the baseline phase angle. For the negative masking experiments, mice were maintained in LD, and exposed to 4-h LP of increasing intensity (~5-lux, dim red light; ~10-lux, dim white; and ~300-lux, bright white light) each night (ZT 14-18), with a 24-h period of normal LD in between. The amount of activity during the LP was compared to the activity at the same time on the previous night.

For acute LP experiments, we used a modified Aschoff type-II protocol (Jud *et al.*, 2005) in which mice in LD were released into constant dark (DD) for 10 days (LP-), re-entrained to LD for 14 days, released into DD again, and exposed to a 1-hour LP (~300 lux) at ZT 22 on the first day in DD (LP+). To eliminate the non-photic effects of wheel-running, the running-wheel was locked during the 1-hour LP and during the equivalent time in the LP- condition (ZT 22-23 on first day in DD). Regression lines were fit to the activity onsets on the last 5 days in LD and on days 4-10 in DD. The magnitude of the phase-shift was calculated as the difference between the activity onsets predicted by each fit line on the second day in DD.

Electrophysiology

WT and GSK3-KI mice, homozygous for *Per1*::GFP held in a 12:12 LD cycle were exposed to a 15-min LP (~500 lux) at ZT 22 and sacrificed immediately following. For no-light controls, animals were sacrificed and enucleated in the dark with the aid of night-vision goggles at ZT 22.25. Fresh coronal brain slices (200 um thickness) were prepared on a vibrating microtome (Campden 7000SMZ, World Precision Instruments,

Lafayette, IN, USA) while bathed in ice-cold oxygenated high-sucrose saline (in mM: 250 sucrose, 26 $NaHCO_3$, 1.25 Na_2HPO_4-$7H_2O$, 1.2 $MgSO_4$-$7H_2O$, 10 glucose, 2.5 $MgCl_2$, 3.5 KCl. Slices were allowed to rest for 20-min in a bath containing room-temperature, oxygenated solution of 50% high-sucrose saline and 50% normal saline (in mM: 130 NaCl, 20 $NaHCO_3$, 1 Na_2HPO_4-$7H_2O$, 1.3 $MgSO_4$-$7H_2O$, 10 glucose, 3.5 KCl, 2.5 $CaCl_2$). For recordings involving a pharmacological treatment, slices were transferred to heated bath of normal saline containing CHIR-99021 (CHIR; 1uM; Stemgent, Lexington, MS, USA) or vehicle (DMSO; 0.002%) for 1-hour (ZT 23-24). Slices were then transferred to a recording chamber and continuously perfused (2ml/min) with oxygenated, normal saline heated to 34 ± 0.5°C. Cells were visualized using an Axio Examiner microscope (Zeiss). Glass pipettes were pulled at a resistance of 3-5MΩ and filled with a filtered internal solution (in mM: (in mM: 135 K-gluconate, 10 KCl, 10 HEPES, 0.5 EGTA; pH 7.4). Electrophysiological signals were processed and controlled by a Multiclamp 700B amplifier and pClamp 10.02 software (Axon Instruments, Union City, CA, USA) in gap-free or current-clamp mode. Recordings were sampled at 20 kHz and filtered at 10 kHz. Spontaneous firing rate was measured as the average action potential frequency from a 2-min recording. Resting membrane potential (RMP) was determined as the half-width voltage between action potentials. All recordings were made between ZT 1-3 or ZT 0-3.

Immunohistochemisty (IHC)

Per1::GFP mice were exposed mice were exposed to a 15-min light pulse (~300 lux) at ZT 22, returned to darkness, sacrificed and enucleated 30-60 minutes later. Brains

were harvested and processed for IHC using rabbit anti-pGSK3β (1:1000; Cell Signaling, Danvers, MA, USA) and mouse anti-rabbit Alexafluor 488 (1:500; Invitrogen). Fluorescence intensity was measured in Image J software (NIH) by drawing a standard region of interest for the ventral, dorsal and whole SCN. The background intensity, taken from the anterior hypothalamus just outside the SCN was subtracted from all values.

Electroretinogram (ERG) Recordings

Following overnight dark adaptation, mice were anesthetized under dim red illumination with 100 mg/kg ketamine and 10 mg/kg xylazine. Under anesthesia, both eyes were treated with proparacaine HCl (0.5%) followed by a mixture of phenylephrine HCl (2.5%) and tropicamide (1%) for pupil dilation. A gold reference electrode was electrically connected to one eye and a platinum wire fiber-optic combination was connected to the other. Light stimuli were delivered directly onto the eye through the fiber-optic with a 100-W tungsten bulb light-source. Calibrated neutral density filters were used to control stimulus intensity, and the stimulus wavelength was 505 nm ± 15 nm (wide-band filter). Stimulus flashes (2ms) were controlled by a computer-driven Uniblitz shutter. Electrical responses were amplified (DC 300 Hz) and digitized at 2 KHz. Data analysis was performed using IGOR software (WaveMetrics).

Data Analysis

All statistics were calculated using SPSS 22 software. Data were analyzed with independent samples t-tests, two-way ANOVAs, two-way mixed-design ANOVAs, and linear-mixed model ANOVAS (using the Generalized Estimating Equations in SPSS).

Where indicated, post hoc tests were conducted using Tukey's HSD or Fisher's LSD for planned comparisons. Significance was ascribed at $P < 0.05$.

Results

Late-night light exposure induces GSK3β activation in SCN

In the early stages of photic-phase-shifting, signal cascades such as the MAPK (Obrietan *et al.*, 1998) or the mammalian target of rapamycin (mTOR) pathways (Cao *et al.*, 2008) are activated through kinase phosphorylation (e.g. induction of pERK1/2, p-p70 S6 kinase), initiating the molecular response to photic stimuli. To determine whether GSK3 was among one of the kinases involved in late-night phase-resetting, we exposed WT mice to a 15-min LP at ZT 22 and examined phosphorylation of GSK3β (pGSK3β) levels in the SCN of light-exposed and no-light controls at 30 and 60 min after LP onset. In control animals, pGSK3β levels were high throughout the whole SCN (Fig. 1A) as expected, according to previously published research (Iitaka *et al.*, 2005). Exposure to an acute LP significantly activated (dephosphorylated) GSK3β (two-way ANOVA, main effect of light, $F_{1,8} = 25.268$, $P = 0.001$; Fig. 1B) at both time points, reducing pGSK3β levels by more than 50% overall. Though the light-induced suppression of pGSK3β appeared to occur predominantly in the ventral (core) region of the SCN (two-way ANOVA, main effect of light, $F_{1,8} = 22.538$, $P < 0.001$; Fig. 1C), pGSK3β levels were significantly reduced by light in the dorsal region as well (two-way ANOVA, main effect of light, $F_{1,8} = 13.638$, $P < 0.01$; Fig. 1D).

GSK3 activation is necessary for light-induced SCN neuronal activity

Three to five hours following late-night light exposure, electrical activity is persistently elevated in the light-responsive neurons of the SCN which can be identified using the *Per1*::GFP reporter mouse model (Kuhlman). Recent work has demonstrated that GSK3 activation promotes neuronal excitability in both the SCN (Paul *et al.*, 2012) and hippocampus (Hsu *et al.*, 2015); therefore, we next sought to determine whether GSK3 activation was necessary for light-induced increase in SCN firing. To do this, we treated acute brain slices from light-exposed (LP+) or no light control (LP-) *Per1*::GFP mice with a small molecule GSK3 inhibitor, CHIR-99021 (CHIR; 1 μM) or vehicle (DMSO; 0.002%) for 1 hour (ZT 23-24) and performed fluorescence targeted loose-patch recordings on SCN neurons 3-5 hours after light exposure (ZT 1-3). As expected, light-exposure significantly increased the spontaneous firing rate (SFR) in vehicle-treated slices, with LP+ cells spiking more than 2.5 times faster than LP- cells, on average (two-way ANOVA, light X treatment interaction, $F_{1,165} = 7.849$, $P < 0.01$; Tukey's HSD *post hoc* test, $P < 0.001$; Fig. 2A, B). However, CHIR treatment significantly suppressed the SFR of LP+ neurons compared to vehicle treated LP+ cells ($P < 0.01$). Instead, the mean SFR of SCN CHIR treated LP+ neurons was essentially equal to that of the CHIR-treated LP- cells ($P = 0.997$). Interestingly, there was no difference between vehicle and CHIR treated LP- groups, suggesting that the effect of CHIR was specific to light-induced excitability ($P = 0.88$).

The increase in SCN activity following a late-night LP has previously been associated with a depolarized resting membrane potential and increased input resistance (Kuhlman *et al.*, 2003). To determine whether GSK3 inhibition blocked light-induced

excitability by acting on the membrane properties of the cell, we performed whole-cell current clamp recordings in LP+ slices treated with either CHIR or vehicle using the same paradigm as above. There were no significant differences in the resting membrane potential (independent samples t-test, $t(27) = 0.434$, $P = 0.668$; Fig. 2C) or input resistance ($t(25) = 1.066$, $P = 0.296$; Fig. 2D, E) between LP+ vehicle- or CHIR-treated cells.

Chronic activation of GSK3 enhances behavioral and neurophysiological response to light

We next sought to determine the role of GSK3 activation in regulating the effect of light on circadian rhythms at the behavioral level by comparing WT mice to mice with constitutive activation of GSK3 (*i.e.*, GSK3-KI mice) such that both α and β isoforms of GSK3 can no longer be phosphorylated and inactivated (McManus *et al.*, 2005; Paul *et al.*, 2012). To examine effect of chronic GSK3 activity on photic entrainment, we first measured rate of re-entainment of GSK3-KI and WT mice to a 6-hour advance in the light-cycle (Fig. 3A, B). When the light-cycle was advanced by 6 h, GSK3-KI animals entrained to the new LD cycle in significantly fewer days than WT mice (means ± SEM: GSK3-KI, 4.75 ± 0.41; WT, 7.4 ± 0.62 days; independent samples t-test, $t(20) = -3.677$, $P = 0.001$; Fig. 3).

To determine whether the enhanced photic entrainment of GSK3-KI mice in was due to increased sensitivity to light outside of the circadian system, we next examined negative masking behavior in GSK3-KI and WT mice. While maintained in LD, mice were exposed to a 4-hour pulse of dim red, dim white, or bright white light in the middle

of the night (ZT 14-18; Fig. 4A, B). Negative masking was measured as the percent of activity during the LP relative to amount activity during the same time on the previous day (Fig. 4B). When exposed to dim red light, the majority of WT mice (5/7) exhibited a slight increase in wheel-running activity, known as positive masking, whereas, in the GSK3-KI group, dim red light decreased activity in 4/7 animals; however, the percent of activity was not significantly different between groups. Furthermore, both genotypes exhibited similar levels of negative masking during the dim- and bright-white light pulses (two-way mixed design ANOVA, main effect of light intensity, $F_{2,11} = 79.007$, $P < 0.001$; Fig. 4B).

As an additional measure of non-circadian light processing, we investigated whether there were any gross retinal abnormalities in these mice. Specifically, we performed ERG analysis on GSK3-KI mice (n = 7; Fig. 4C) and WT controls (n = 6; Fig. 4D) and found that there were no significant differences between the two mouse lines in any of the parameters of dark-adapted retinal function that were tested (Fig. 4E). Light-adapted ERG, designed to isolate cone photoreceptor responses, also demonstrated similarity between WT and GSK3-KI mice (Fig. 4E). Likewise, there were no significant differences in the timing (time-to-peak, means ± SEM: WT, 124 ± 4; GSK3-KI, 116 ± 5 ms) or amplitude (means ± SEM: WT, 60.0 ± 14; GSK3-KI, 46.5 ± 5 μV) of the photopic negative response (PNR), which represents ganglion cell activity (Fig. 4F). Overall, the retinas of each mouse line do not appear to be functionally different. Taken together with the negative-masking behavior, these results suggest that the effect of GSK3 on photic entrainment is likely not due to altered retinal function.

We also tested the phase-shifting effects of an acute light-pulse in WT and GSK3-KI mice using a modified Aschoff type-II protocol (see methods). Briefly, we first measured the phase-angles of mice in two conditions: first, after release into DD with no light exposure (LP-; Fig. 5A, B) and second after re-entrainment and release into DD following a 60-min LP (LP+) at ZT 22 (Fig. 5C, D). As expected, exposure to a late-night LP caused a significant advance in both genotypes (mixed-design ANOVA, main effect of light, $F_{1,12} = 70.227$, $P < 0.001$; Fig. 5E). Surprisingly, the magnitude of the light-induced phase-shift was not different between genotypes (non-significant light x genotype interaction, $P = 0.692$). Instead, the activity onsets of GSK3-KI mice were significantly more advanced than WT mice in both LP- and LP+ conditions (main effect of genotype, $F_{1,12} = 5.360$, $P < 0.05$; Fig. 5E). Light exposure also significantly shortened the free-running period in DD similarly in both genotypes (mixed-design ANOVA, main effect of light, $F_{1,12} = 12.242$, $P < 0.005$; Fig. 5F).

To determine whether the chronic GSK3 activity affected the SCN neurophysiological response to light, we performed targeted loose-patch recordings in SCN slices from light-exposed (LP+) or no-light control (LP-), GSK3-KI or WT mice, using the same paradigm as in the previous recordings (Fig. 2). Because the behavior of GSK3-KI mice was phase-advanced compared to WT mice in both LP- and LP+ conditions, we examined the spontaneous SCN activity 2-5 hours after light-exposure (ZT 0-3). Overall, SCN firing was significantly increased in GSK3-KI and light-exposed slices (linear mixed-model ANOVA**;** main effect of light, $X^2(1) = 24.717$, $P < 0.001$; main effect of genotype, $X^2(1) = 9.568$, $P < 0.005$; Fig. 6A); however, as shown in Fig. 6B and 6C, timing of light-induced excitability differed between genotypes (three-way

interaction, $X^2(2) = 7.254$, $P < 0.05$). In WT slices, light exposure did not increase SCN firing until the second hour of recording (LP- WT vs LP+ WT: first hour, $P = 0.458$; second hour, $P < 0.05$), whereas in LP+ GSK3-KI slices, the SFR was significantly increased as early as ZT 0 (Fig. 6B). Furthermore, in the LP- groups, GSK3-KI cells were significantly more excited than WT neurons in the ZT 2-3 time window. These results suggest that, similar to the advanced behavioral phase-angle (Fig. 5), the early-morning increase in SCN excitability of GSK3-KI mice was advanced in both LP- and LP+ conditions.

Discussion

In the present study, we present strong evidence that GSK3 activation serves a critical role in photic entrainment and light-induced SCN excitability. Specifically, we found that: 1) acute late-night light exposure activates GSK3β in the SCN, 2) GSK3 activation is necessary for light-induced neuronal excitability, 3) mice with constitutively active GSK3 exhibit enhanced photic entrainment despite having normal non-circadian light processing, and 4) locomotor activity onset and the early morning rise in SCN neuronal activity of GSK3-KI animals is phase-advanced in both sham and LP-stimulated conditions

Our first result that GSK3 is activated by late-night light exposure is consistent with another recent report showing a light-induced decrease in the number of pGSK3β positive cells in rat SCN (Cervena *et al.*, 2015). However, in that study, the change in GSK3β phosphorylation was not observed until two hours after light exposure as opposed to the data presented here which suggests the change in GSK3 activity occurs more

rapidly, as early as 30 min post LP. These conflicting results are likely due to the numerous methodological differences, including animal species, LP timing and housing condition of the animals prior to experiment (DD vs. LD).

Unlike the transient activation of other light responsive kinases such as ERK1/2 (Butcher *et al.*, 2003; Cervena *et al.*, 2015) and other MAPKs (Nakaya *et al.*, 2003), which return to pre-LP levels within an hour after light exposure, GSK3β activation persists at least one hour after the LP has ended (Fig. 1). Glutamate-induced phase-advances in SCN firing rhythms are attenuated when MAPK inhibitors and glutamate are applied simultaneously (Tischkau *et al.*, 2000). In contrast, we discovered that inhibition of GSK3 as late as 1-2 hours after the light stimulus was sufficient to block the increase in SCN firing during early phase-resetting period. This result demonstrates a need for persistent GSK3 activation long after other light-responsive kinases have returned to baseline activity levels. Interestingly, exposure to non-photic stimuli have been shown to block light-induced phase-shifts, even with exposure separated by up to an hour in time (Lall & Biello, 2002). Thus, GSK3 activity could be an intriguing target of other entrainment pathways as well.

Our finding that GSK3 activation promotes light-induced phase-advances is supported by the results that mice expressing chronically active forms of GSK3 exhibit rapid re-entrainment to an advance in the light-cycle. Interestingly, the enhanced response to light demonstrated in GSK3-KI mice was specific to circadian behavior, as GSK3-KI mice responded no differently from WT controls in negative masking behavior or in ERG responses under multiple lighting conditions. Conflicting with our data showing normal ERG responses in GSK3-KI mice, previous work has shown a decrease

or increase in ERG b-wave amplitude in GSK3β-overexpressing or -haploinsuffient mice, respectively (Lavoie *et al.*, 2014). However, in the GSK3-KI mice used here, both isoforms of GSK3 are expressed at physiological levels suggesting that changes in the amount total GSK3 rather than levels of phosphorylation are necessary for changes in retinal function.

In addition to accelerating the rate of photic-entrainment, chronic activation of GSK3 also advanced the phase-angle of entrainment in wheel-running activity. This finding is consistent with past work showing that significant delays in the phase-angle of mice fed lithium, a known to GSK3 inhibitor (Iwahana *et al.*, 2004). Typically, the changes in the phase-angle of entrainment are associated with a change in the free-running period under constant conditions. Surprisingly, the FRP of GSK3-KI mice was no different than WT, despite exhibiting an advanced phase-angle. One intriguing explanation for the advanced behavioral rhythms is the elevated SCN neuronal activity also seen in the GSK3-KI animals. A recent study has demonstrated that optogenetic stimulation of SCN neurons alone is sufficient to shift both molecular and behavior rhythms, mimicking the effects of a light-pulse (Jones *et al.*, 2015). Future work in the GSK3-KI animals examining SCN activity throughout the entire circadian cycle could provide more insight into the behavioral phenotype seen in these animals (Paul *et al.*, 2012) as well as further elucidate the connection between neurophysiological and behavioral rhythms.

Taken together, the results of this study provide support for the hypothesis that GSK3 activity promotes light-induced SCN excitability. Previous work on GSK3 regulation of the circadian system has focused predominantly on daily rhythmicity;

however, the results presented here strongly suggest that GSK3 is a previously unexplored regulator of photic entrainment as well. GSK3 dysregulation has also been implicated in numerous disorders that have also been associated with chronic light exposure at night, such as depression (Bedrosian *et al.*, 2013), obesity (Fonken *et al.*, 2013; Fonken & Nelson, 2014), and cancer (Dauchy *et al.*, 2014). Therefore, better understanding the effects of light on GSK3 and its role in regulating SCN neurophysiology could provide new treatment strategies for these disorders in the future.

References

Bedrosian, T.A., Weil, Z.M. & Nelson, R.J. (2013) Chronic dim light at night provokes reversible depression-like phenotype: possible role for TNF. *Mol Psychiatry*, **18**, 930-936.

Butcher, G.Q., Lee, B. & Obrietan, K. (2003) Temporal regulation of light-induced extracellular signal-regulated kinase activation in the suprachiasmatic nucleus. *J Neurophysiol*, **90**, 3854-3863.

Cao, R., Lee, B., Cho, H.Y., Saklayen, S. & Obrietan, K. (2008) Photic regulation of the mTOR signaling pathway in the suprachiasmatic circadian clock. *Mol Cell Neurosci*, **38**, 312-324.

Cervena, K., Pacesova, D., Spisska, V. & Bendova, Z. (2015) Delayed Effect of the Light Pulse on Phosphorylated ERK1/2 and GSK3beta Kinases in the Ventrolateral Suprachiasmatic Nucleus of Rat. *J Mol Neurosci*, **56**, 371-376.

Colwell, C.S. (2011) Linking neural activity and molecular oscillations in the SCN. *Nat Rev Neurosci*, **12**, 553-569.

Czeisler, C.A. (1995) The effect of light on the human circadian pacemaker. *Ciba Found Symp*, **183**, 254-290; discussion 290-302.

Dauchy, R.T., Xiang, S., Mao, L., Brimer, S., Wren, M.A., Yuan, L., Anbalagan, M., Hauch, A., Frasch, T., Rowan, B.G., Blask, D.E. & Hill, S.M. (2014) Circadian

and melatonin disruption by exposure to light at night drives intrinsic resistance to tamoxifen therapy in breast cancer. *Cancer Res*, **74**, 4099-4110.

Fonken, L.K., Aubrecht, T.G., Melendez-Fernandez, O.H., Weil, Z.M. & Nelson, R.J. (2013) Dim light at night disrupts molecular circadian rhythms and increases body weight. *J Biol Rhythms*, **28**, 262-271.

Fonken, L.K. & Nelson, R.J. (2014) The effects of light at night on circadian clocks and metabolism. *Endocr Rev*, **35**, 648-670.

Golombek, D.A. & Rosenstein, R.E. (2010) Physiology of circadian entrainment. *Physiol Rev*, **90**, 1063-1102.

Hannibal, J. (2002) Neurotransmitters of the retino-hypothalamic tract. *Cell Tissue Res*, **309**, 73-88.

Hsu, W.C., Nenov, M.N., Shavkunov, A., Panova, N., Zhan, M. & Laezza, F. (2015) Identifying a kinase network regulating FGF14:Nav1.6 complex assembly using split-luciferase complementation. *PLoS One*, **10**, e0117246.

Iitaka, C., Miyazaki, K., Akaike, T. & Ishida, N. (2005) A role for glycogen synthase kinase-3beta in the mammalian circadian clock. *J Biol Chem*, **280**, 29397-29402.

Iwahana, E., Akiyama, M., Miyakawa, K., Uchida, A., Kasahara, J., Fukunaga, K., Hamada, T. & Shibata, S. (2004) Effect of lithium on the circadian rhythms of locomotor activity and glycogen synthase kinase-3 protein expression in the mouse suprachiasmatic nuclei. *Eur J Neurosci*, **19**, 2281-2287.

Iwahana, E., Karatsoreos, I., Shibata, S. & Silver, R. (2008) Gonadectomy reveals sex differences in circadian rhythms and suprachiasmatic nucleus androgen receptors in mice. *Horm Behav*, **53**, 422-430.

Jones, J.R., Tackenberg, M.C. & McMahon, D.G. (2015) Manipulating circadian clock neuron firing rate resets molecular circadian rhythms and behavior. *Nat Neurosci*, **18**, 373-375.

Jud, C., Schmutz, I., Hampp, G., Oster, H. & Albrecht, U. (2005) A guideline for analyzing circadian wheel-running behavior in rodents under different lighting conditions. *Biol Proced Online*, **7**, 101-116.

Kuhlman, S.J., Quintero, J.E. & McMahon, D.G. (2000) GFP fluorescence reports Period 1 circadian gene regulation in the mammalian biological clock. *Neuroreport*, **11**, 1479-1482.

Kuhlman, S.J., Silver, R., Le Sauter, J., Bult-Ito, A. & McMahon, D.G. (2003) Phase resetting light pulses induce Per1 and persistent spike activity in a subpopulation of biological clock neurons. *J Neurosci*, **23**, 1441-1450.

Kurabayashi, N., Hirota, T., Sakai, M., Sanada, K. & Fukada, Y. (2010) DYRK1A and glycogen synthase kinase 3beta, a dual-kinase mechanism directing proteasomal degradation of CRY2 for circadian timekeeping. *Mol Cell Biol*, **30**, 1757-1768.

Lall, G.S. & Biello, S.M. (2002) Attenuation of phase shifts to light by activity or neuropeptide Y: a time course study. *Brain Res*, **957**, 109-116.

Lavoie, J., Hebert, M. & Beaulieu, J.M. (2014) Glycogen synthase kinase-3 overexpression replicates electroretinogram anomalies of offspring at high genetic risk for schizophrenia and bipolar disorder. *Biol Psychiatry*, **76**, 93-100.

McManus, E.J., Sakamoto, K., Armit, L.J., Ronaldson, L., Shpiro, N., Marquez, R. & Alessi, D.R. (2005) Role that phosphorylation of GSK3 plays in insulin and Wnt signalling defined by knockin analysis. *EMBO J*, **24**, 1571-1583.

Nakaya, M., Sanada, K. & Fukada, Y. (2003) Spatial and temporal regulation of mitogen-activated protein kinase phosphorylation in the mouse suprachiasmatic nucleus. *Biochem Biophys Res Commun*, **305**, 494-501.

Obrietan, K., Impey, S. & Storm, D.R. (1998) Light and circadian rhythmicity regulate MAP kinase activation in the suprachiasmatic nuclei. *Nat Neurosci*, **1**, 693-700.

Paul, J.R., Johnson, R.L., Jope, R.S. & Gamble, K.L. (2012) Disruption of circadian rhythmicity and suprachiasmatic action potential frequency in a mouse model with constitutive activation of glycogen synthase kinase 3. *Neuroscience*, **226**, 1-9.

Sahar, S., Zocchi, L., Kinoshita, C., Borrelli, E. & Sassone-Corsi, P. (2010) Regulation of BMAL1 protein stability and circadian function by GSK3beta-mediated phosphorylation. *PLoS One*, **5**, e8561.

Tischkau, S.A., Gallman, E.A., Buchanan, G.F. & Gillette, M.U. (2000) Differential cAMP gating of glutamatergic signaling regulates long-term state changes in the suprachiasmatic circadian clock. *J Neurosci*, **20**, 7830-7837.

Tischkau, S.A., Mitchell, J.W., Tyan, S.H., Buchanan, G.F. & Gillette, M.U. (2003) Ca2+/cAMP response element-binding protein (CREB)-dependent activation of Per1 is required for light-induced signaling in the suprachiasmatic nucleus circadian clock. *J Biol Chem*, **278**, 718-723.

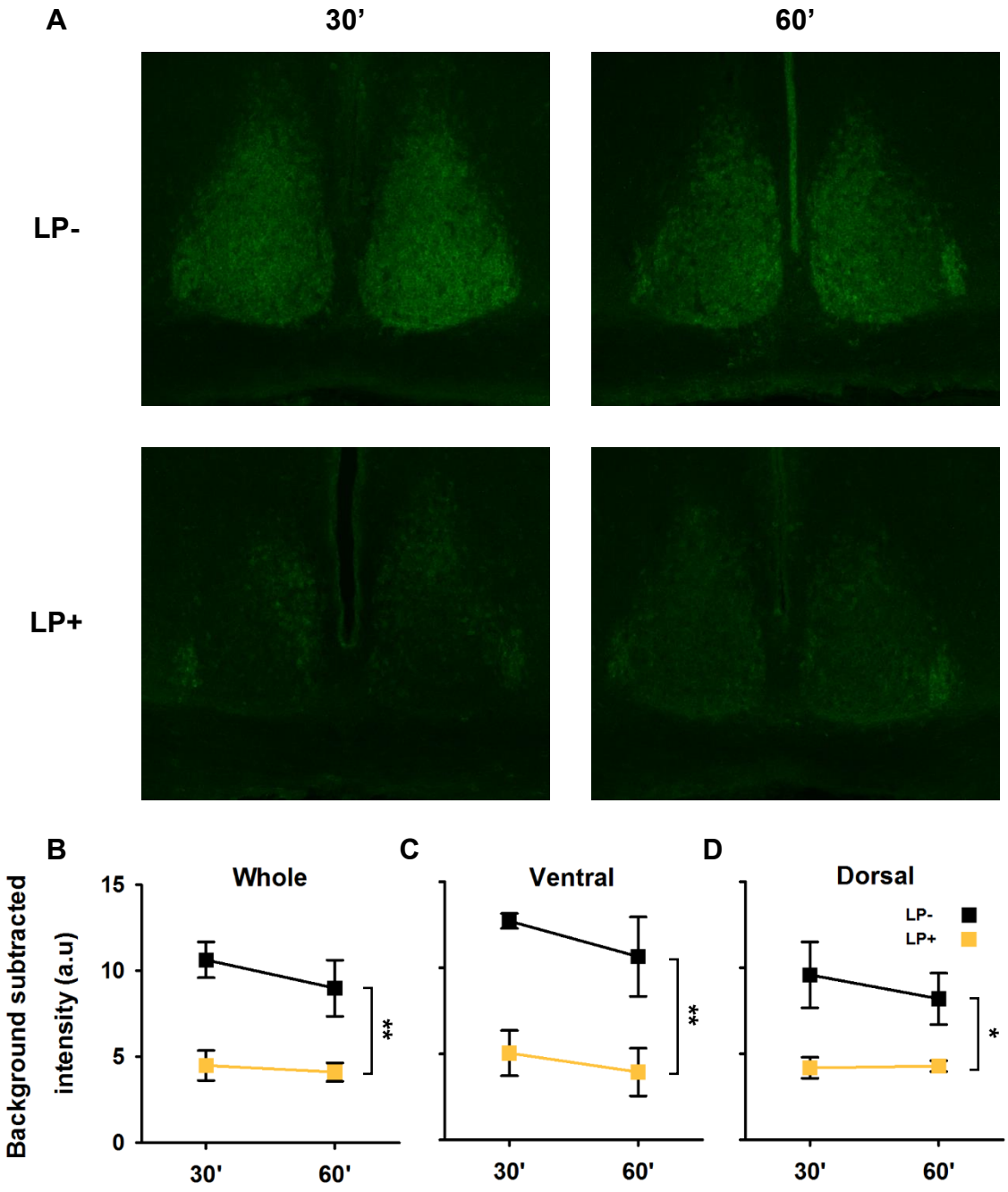

Figure 1. Acute light-pulse at ZT22 reduces GSK3β phosphorylation in SCN. Representative images of anti-pGSK3β staining (A) and quantification of background subtracted fluorescence intensity for whole (B), ventral (C) and dorsal (D) regions of SCN sections from mice 30- or 60-minutes after exposure to a 15-minute light pulse (LP+, yellow) or no light controls (LP-, black) taken at the same time. N = 3 sections per group per time point. Main effect of light *$P < 0.01$, **$P < 0.005$.

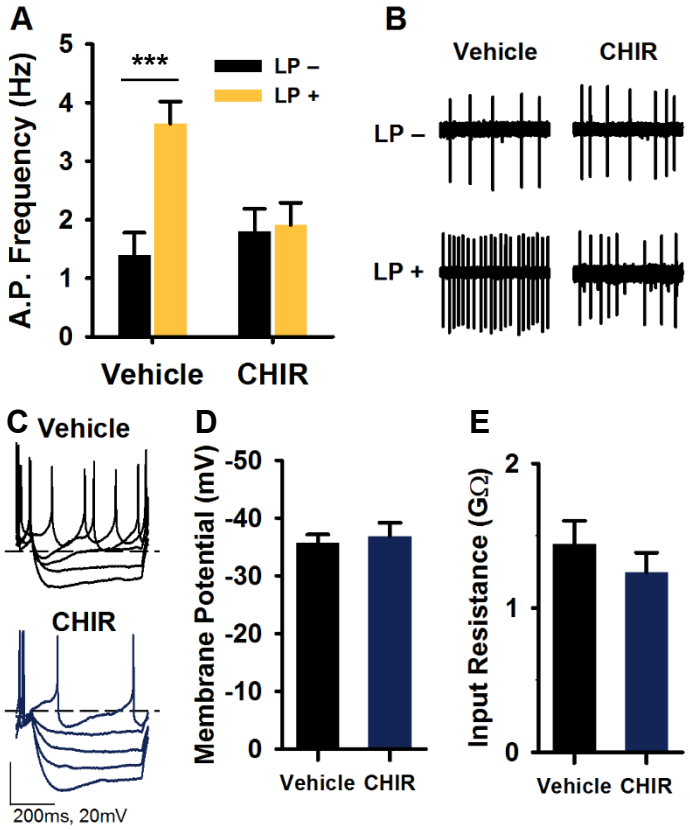

Figure 2. GSK3 inhibition blocks light-induced increase in SCN neuronal activity. (A) Spontaneous action potential frequencies (means ± SEM) of SCN neurons treated with vehicle (DMSO, 0.002%) or CHIR (1 µM) for 1 hour (ZT 23-24) following exposure to 15-min light-pulse (LP+) or no light (LP-) at ZT 22. Recordings were made 3-5 hours after onset of photic stimulus (ZT 1-3). (B) Representative cell-attached loose-patch traces (5 s) from each group in (A). ***P < 0.001, n = 41-43 cells, 3-4 slices per group. (C-D) Means ± SEM of resting membrane potential (C) and input resistance (D) from LP+ SCN neurons treated with vehicle or CHIR (as in A). (E) Representative current clamp recordings from cells quantified in (C-D). n = 13-15 cells, 2-3 slices per group.

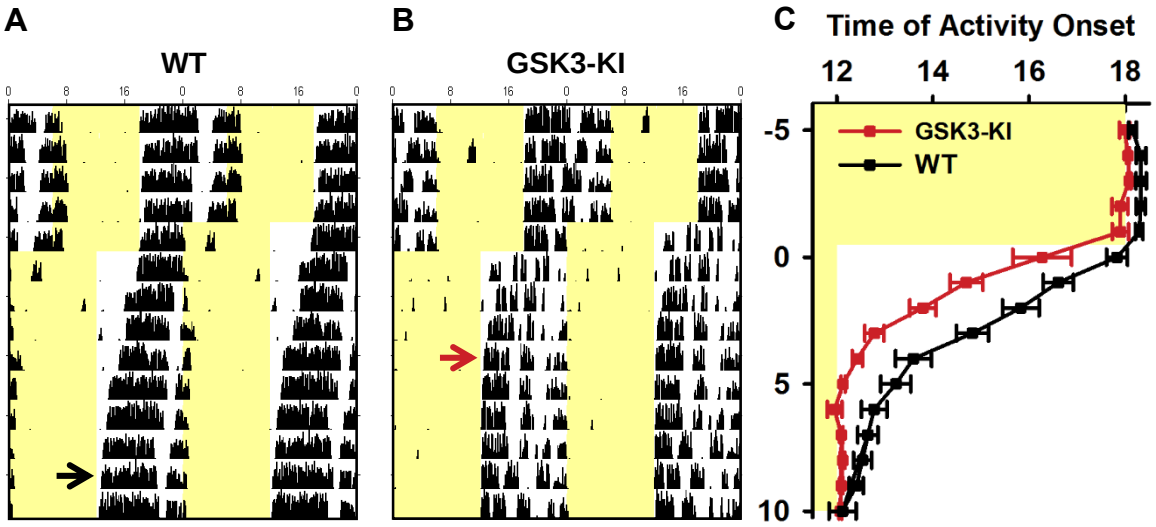

Figure 3. Chronic GSK3 activation enhances re-entrainment to advance in light-cycle. (A-B) Representative double-plotted actograms of wheel-running behavior from WT (A) and GSK3-KI (B) mice undergoing a 6-hour advance in the LD cycle. Arrows indicated the first day each animal is considered re-entrained to the new LD cycle. (C) Daily activity onset (mean ± SEM) for days before and after advance in the LD cycle (day 0). Grey bars mark the times of lights-off. n = 10-12 animals per genotype.

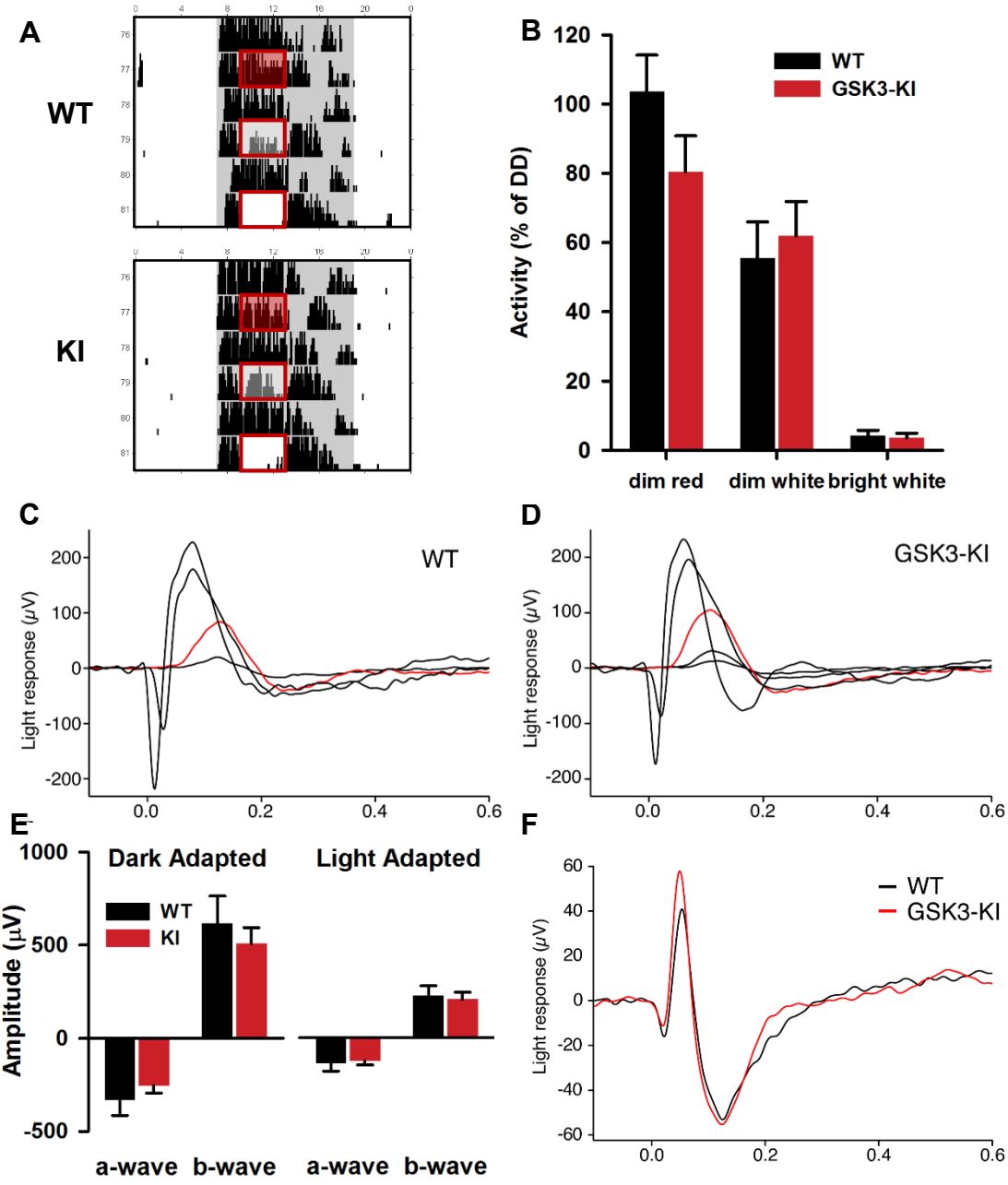

Figure 4. Chronic GSK3 activation does not alter negative masking behavior or ERG responses to light. (A) Representative single-plotted actograms from WT and GSK3-KI mice exposed to increasing intensities of light for 4 hours during the dark phase (shown in box). Gray marks the time of lights off. (B) Means ± SEM of the percent of activity during LP relative to activity on the previous day. (C-D) Representative ERG recordings from WT (C) and GSK3-KI (D) mice elicited by increasingly intense 2 ms

flashes of light that delivered 2.2, 30, 5100, and 23,550 photons/μm^2 to the cornea. Red trace is the b-wave elicited by flash intensity of 30 photons/μm^2. (E) Means ± SEM of dark adapted and light adapted ERG amplitudes elicited by 2 ms flash of light at highest intensity in (C-D). (F) The photopic negative response was elicited by averaging a series of 10 brief flashes (5100 photons/μm^2) that were delivered on a steady background (4500 photons/$\mu m^2 sec^1$). The maximum amplitude and time-to-peak of the trough that follows the response represents the values of the PNR reported.

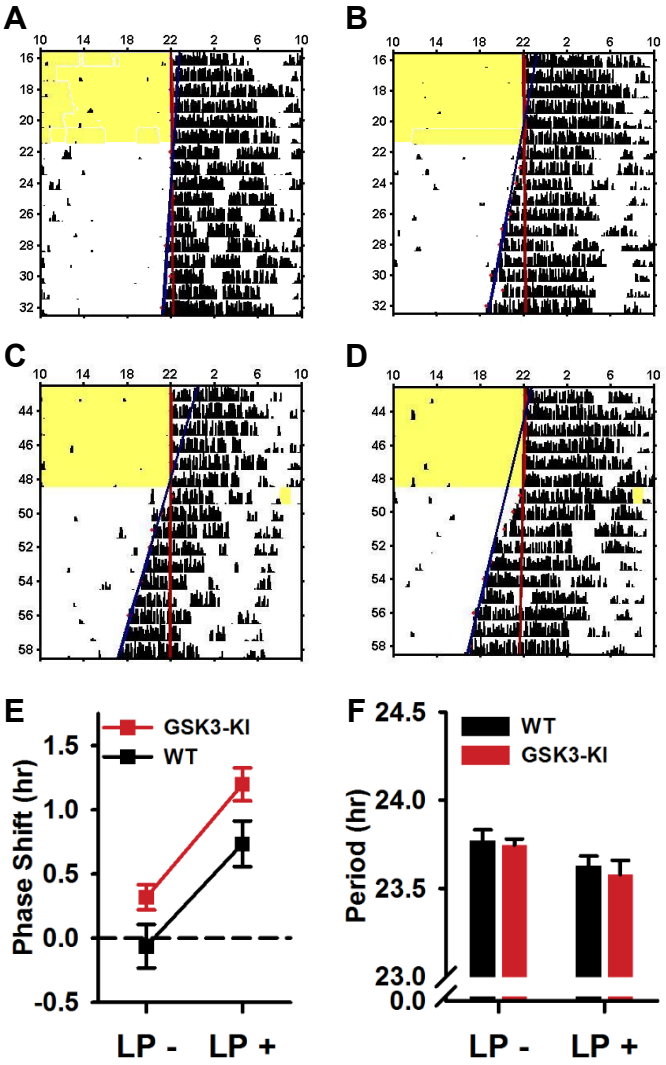

Figure 5. Phase-angle of entrainment is advanced in GSK3-KI mice and following acute LP in late-night. (A-D) Representative single-plotted actograms of WT (A, C) and GSK3-KI (B, D) mice exposed to a 1-hr LP with accompanying wheel-clip (C-D; LP+) or wheel-clip alone (A-B; LP-) at ZT 22 on first day in DD. A line was fit to the activity onsets for the last 5 days in LD and days 3-9 in DD. The difference of these fit lines on day 1 in DD was defined as the phase shift. (E-F) Means ± SEM of phase-shift magnitude (E) and free-running period in DD (F) for animals represented in A-B. Main effect of light ($P < 0.001$) and genotype ($P < 0.05$), n = 7 mice per genotype.

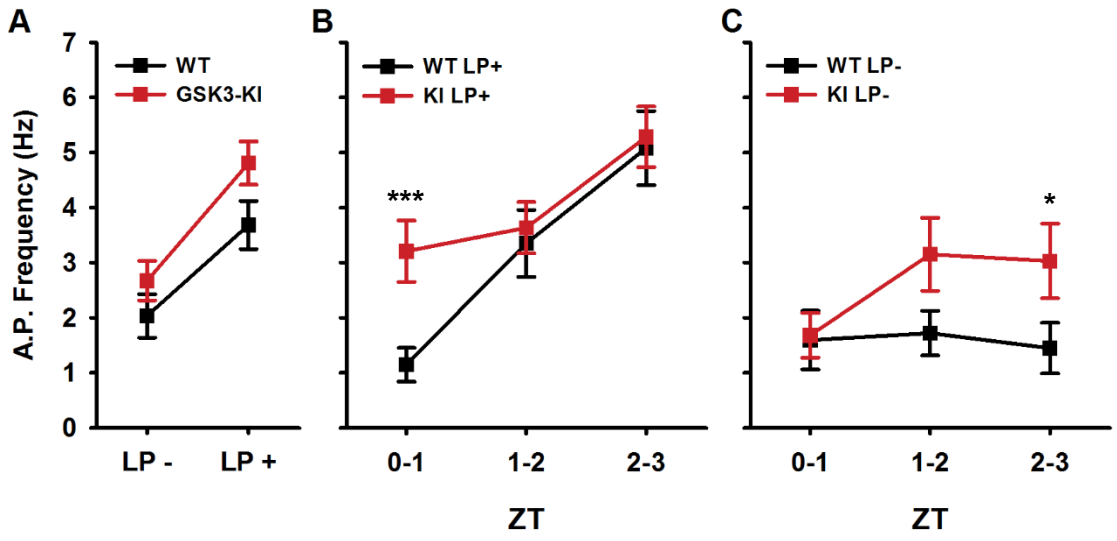

Figure 6. Light-induced increase in SCN excitability occurs earlier in GSK3-KI mice. (A) Spontaneous AP frequencies (means ± SEM) of SCN neurons from WT or GSK3-KI mice following exposure to a 15-min light-pulse (LP+) or no light (LP-) at ZT 22. Recordings were made 2-5 hours after onset of photic stimulus (ZT 0-3). Main effect of light, $P < 0.001$; main effect of genotype, $P < 0.005$; n = 61, 92 cells, 3-6 slices per group. (B-C) Graph (means ± SEM) of data from (A) divided into 1-hr bins depicting WT and GSK3-KI SFR from LP+ (B) or LP- (C) groups. ***$P = 0.001$, *$P < 0.05$; Fisher's LSD post hoc test.

CHAPTER 4

GSK3 REGULATION OF PERSISTENT NA^+ CURRENT ENCODES DAILY RHYTHMS OF EXCITABILITY

by

JODI R. PAUL, DANIEL DeWOSKIN, DANIEL B. FORGER, AND KAREN L. GAMBLE

Submitted to *PLOS Biology*

Format adapted for dissertation

Abstract

How neurons encode intracellular biochemical signaling cascades into electrical signals is not fully understood. Neurons in the central circadian (daily) clock in mammals provide a model system to investigate electrical encoding of biochemical timing signals. Using a combined modeling/experimental approach, we show how the activation of glycogen synthase kinase 3 (GSK3) contributes to neuronal excitability through regulation of the persistent sodium current (I_{NaP}). I_{NaP} exhibits a day/night difference in peak magnitude and is regulated by GSK3. Using mathematical modeling, we predict and confirm that GSK3 activation of I_{NaP} affects the action potential after-hyperpolarization, which increases the spontaneous firing rate without affecting the resting membrane potential. Together, these results demonstrate a crucial link between the molecular circadian clock and electrical activity, providing examples of kinase regulation of electrical activity and the propagation of intracellular signals in neuronal networks.

Introduction

Much information processing in the brain occurs through electrical signaling, where the opening and closing of ion channels controls the properly timed firing of action potentials. At the same time, biochemical networks within neurons separately regulate transcription, translation, and post-translational modifications to determine cell fate, time cellular events, and control cell size. How neurons integrate information between the two levels has remained a key open problem in neuroscience.

An important model system for studying this phenomenon is the neuronal network within the suprachiasmatic nuclei (SCN) of the hypothalamus, which forms the

central circadian (24-h) pacemaker [1]. Within the neurons of the SCN, an intracellular clock generates daily rhythms through regulation of transcription factors, kinases, and other signaling molecules [2]. Timing information is relayed to the rest of the body through a variety of electrical behaviors and signals produced by SCN neurons [3]. Understanding how cellular timekeeping and electrical activity are integrated is an essential ongoing question in the field. Since many of the molecular and electrical components of the clock are well characterized, the SCN is a perfect system for investigating the greater question in neuroscience of how intracellular biochemical information is electrically encoded.

One potential link between cellular biochemistry and electrical activity is glycogen synthase kinase 3 (GSK3). GSK3 activation enhances the spontaneous firing rate [4], is regulated in a circadian manner [5, 6], and modulates molecular timekeeping within SCN neurons [5], providing a potential link between the molecular and electrical activities of the SCN. Here, we test the hypothesis that GSK3 regulates specific ionic currents that affect the spontaneous firing of action potentials. As GSK3 is implicated in many other intracellular processes [7-10] (e.g., inflammatory pathways, neurotrophic signaling, Wnt and mTOR cascades), GSK3 could provide a universal link between the biochemical state of the cell and its electrical activity.

It has been previously reported that several specific ionic currents are activated in a circadian manner [3], and thus, may provide a primary mechanism for controlling circadian variation in electrical activity. The presumed mechanism of circadian regulation of many currents, however, is through transcriptional regulation of their channels, which is energetically inefficient. Another challenge to this hypothesis is that experimental and

computational studies implicate sodium currents as the most important regulators of firing rate in SCN neurons [11, 12], but no evidence to support a day-night difference in these currents has been presented to date. Here we propose another mechanism for the regulation of the electrical activity of a neuron by molecular signaling through GSK3. Using a combination of mathematical modeling and experimental work, we show that GSK3 efficiently regulates the firing rate of the cell by modulation of a persistent sodium current without causing the significant depolarization that could signal back to the molecular circadian clock.

Results

Inhibition of GSK3 suppresses neuronal excitability in a time-of-day dependent manner

We initially determined whether acute regulation of GSK3 changes the electrical activity of SCN neurons during the day and night. Compared to vehicle, inhibition of GSK3 with a pharmacological inhibitor (CHIR99021; 1 μM) significantly decreased the spontaneous firing rate (SFR) of SCN neurons from hypothalamic slices in a phase-specific manner ($p = 0.018$; Fig 1A and 1B). GSK3 inhibition significantly suppressed SFR during the day between Zeitgeber Time (ZT) 4 and 8 ($p < 0.001$). Conversely, at night (ZT 14-18), both treatment groups were similarly quiescent ($p = 0.608$). The observed day-time suppression was replicated with another GSK3 inhibitor (SB415286; 1 μM), which significantly decreased SFR by 66% compared to vehicle (mean ± SEM, vehicle: 5.05 ± 0.44; SB415286, 1.71 ± 0.28; n = 34-38 cells/group). These results suggest that inhibition of GSK3 suppresses SCN neuronal excitability during the day.

The firing rate of neurons can be regulated by numerous mechanisms, including depolarization of the membrane [13]. We conducted whole-cell current clamp recordings to determine whether CHIR-induced suppression of excitability was due to membrane hyperpolarization. Consistent with recent reports [14, 15], day-phase SCN neurons exhibited a wide range of resting membrane potentials (RMP) which was not affected by GSK3 inhibition ($p = 0.133$; Fig 1C). There was also no significant difference in input resistance (Fig S1A and S1B), suggesting that the decreased excitability in CHIR-treated neurons was not due to an increase in the potassium leak conductance [16].

As seen in the vehicle-treated controls during the midday (Fig 1C), SCN neurons are capable of exhibiting multiple phenotypes in spontaneous electrical activity [17] and can be classified as silent, spiking, having depolarized low-amplitude membrane oscillations, or exhibiting depolarization block. In spontaneously spiking neurons, action potentials are separated (or generated) by smooth depolarizing ramps to threshold (Fig 1E). In contrast, when GSK3 was inhibited, cells within this same voltage range exhibited no spontaneous activity (Fig 1D). Interestingly, a subset of cells continued to exhibit calcium-driven low amplitude membrane potential oscillations in the presence of CHIR (similar to tetrodoxin in [12, 18]), and the frequency of these oscillations was not different from vehicle-treated cells (Fig S1C), suggesting that GSK3 inhibition may modulate SCN excitability through suppression of a TTX-sensitive, voltage-gated sodium current. Because the persistent sodium current has been shown to provide at least part of the excitatory drive to action potential (AP) threshold [12], which appeared to be diminished in CHIR-treated cells, we next considered the effect of GSK3 activation on the persistent sodium current.

GSK3 inhibition suppresses a persistent sodium current specifically during the day

Recent work has implicated GSK3 in regulating the expression of $Na_v1.6$ channels [19, 20], which are thought to be one of the major sources of a slowly-inactivating, or persistent, sodium current or I_{NaP} [21], Although small in magnitude, I_{NaP} typically contributes to excitation of repetitively firing neurons by augmenting small depolarizations during the interspike interval [12]. In SCN cells, I_{NaP} is proposed to provide the excitatory drive toward threshold [12], and silencing I_{NaP} suppresses action potential firing in SCN cells [22]. Therefore, we examined the effect of GSK3 inhibition on I_{NaP} by measuring the current response to a slow (59 mV/s), depolarizing voltage ramp from -100 mV to 10 mV [23] before and after treatment with the selective persistent sodium channel blocker riluzole (20 μM, 3-min). The voltage ramp elicited an inward current in vehicle-treated cells at the range of I_{NaP} activation, starting at -52.4 ± 1.1 mV and peaking at -26.8 ± 0.7 mV (means ± SEM; n = 20 cells). During the day, the magnitude of peak I_{NaP} was significantly reduced in CHIR-treated cells compared to vehicle-treated controls at baseline ($p = 0.042$; Fig 2A and 2B). Riluzole significantly suppressed the amount of inward current ($p < 0.001$) and eliminated the difference between CHIR- and vehicle-treated cells (Fig 2C). However, at night, CHIR did not suppress baseline I_{NaP} compared to vehicle-treated controls (Fig 2D, 2E and 2F). These results suggest that GSK3 inhibition decreases I_{NaP} in day-phased SCN neurons and that this current is driven at least in part by GSK3 activation. Because circadian regulation of GSK3 inactivation increases throughout the night [5] when SCN cells are mostly

quiescent, GSK3 regulation of I_{NaP} provides a previously unexplored mechanism underlying the daily rhythms in SCN excitability.

I_{NaP} is regulated by time-of-day and activation of GSK3

Complementary to the present results that GSK3 inhibition suppressed SCN activity during the day but not the night, we have recently reported that chronic GSK3 activation increases neuronal firing at night, but not the day [4]. To determine if chronic GSK3 activation enhances I_{NaP} in SCN neurons, we measured I_{NaP} currents from wild-type mice and transgenic mice with constitutive GSK3 activation (*i.e.*, GSK3-KI mice) due to serine-alanine substitutions at the two inhibitory phosphorylation sites in subunits GSK3α and GSK3β (S21 and S9, respectively) [24]. Although previous reports have suggested that I_{NaP} does not exhibit a day/night difference in the SCN based on gene expression [3, 25]; until now, no study has examined I_{NaP} isolated current at both times of the day.

We found that WT neurons exhibited a significant increase in I_{NaP} during the day compared to the night ($p = 0.02$; Fig 3A). Further, I_{NaP} was enhanced in GSK3-KI cells compared to WT cells ($p = 0.008$; Fig 3B and 3C). Surprisingly, the effect of chronic GSK3 activation was independent of time of day as both genotypes exhibited a day-night different in I_{NaP} magnitude ($p = 0.01$; Fig 3B, 3C and 3D). Follow-up recordings from WT and GSK3-KI cells at night in the presence of $CdCl_2$ (0.1mM) and TEA (10mM) yielded similar results (Fig S2), suggesting that enhanced inward current was not driven by calcium or potassium currents and could be due to shuttling or sequestration of constitutively active GSK.

Mathematical model predicts GSK3 effect on I_{NaP} through modulation of channel conductance

To investigate how GSK3 affects neuronal excitability through I_{NaP}, we incorporated the I_{NaP} current into a conductance-based single cell model of SCN electrophysiology that simulates electrical activity with millisecond resolution based on sodium, potassium, calcium (L-type and non L-type), calcium-activated potassium, and leak (Na-leak and K-leak) currents[17]. We modified the published model with the addition of I_{NaP} with dynamics fit using the voltage ramp data (Fig 2 and 3) as described in the Methods section. We found that the dynamics of I_{NaP} are consistent with a conductance-based model of the form $I_{NaP} = -g_{NaP}(V-E_{Na})p$, with the activating gating variable p ranging between 0 and 1. Currents for all experimental conditions could be fit to this form by varying the maximal conductance g_{NaP} (Fig S3: g_{NaP} values are GSK3-KI, day: 2.27; GSK3-KI, night: 2.13; WT, day: 2.09; WT, night: 1.59; CHIR, day: 1.97; CHIR, night: 1.46). This finding suggests that the action of GSK3 on I_{NaP} is primarily through changing the maximal conductance of I_{NaP} channels rather than the channel kinetics.

We validated the model after the addition of the I_{NaP} current by performing voltage ramp simulations mimicking the analogous experiments presented in Figures 2 and 3 (Fig 4). Simulated voltage ramps with and without I_{NaP} matched the magnitudes of the inward currents seen experimentally in each condition: with simulated application of CHIR (Fig 4A), wild-type (Fig 4B), and with simulated constitutively active GSK3 (Fig 4C), where each condition is reproduced simply by tuning the maximal conductance of the I_{NaP} current (g_{NaP}).

I_{NaP} mediates GSK3-induced excitability at night

Since the effects of I_{NaP} have been shown to be different in isolated cells or in a network, we used this ionic single cell model in a previously validated SCN neuronal network model [17, 26]. This model also used a validated model of the intracellular timekeeping system within individual cells. Using the model, we tuned the strength of I_{NaP} to mimic the transition from low to normal to high GSK3 activity (e.g. CHIR to WT to GSK3-KI) and then examined the resulting changes in neuronal excitability. A total of 1024 GABAergic and VIP-coupled SCN neurons were studied, and the WT cells exhibited a variety of firing activities with circadian variation. As g_{NaP} is increased to the level of GSK3-KI mice, the model predicted that many of the cells which were normally quiescent at night became spontaneously active. Voltage for a sample quiescent WT neuron at night varied little from the RMP (Fig 5A), whereas the identical simulated neuron with g_{NaP} increased to GSK3-KI levels fired action potentials spontaneously (Fig 5B). Furthermore, approximately half of cells in the WT network were quiescent at night, while in the GSK3-KI network, the majority of neurons were spiking (Fig 5C). Since all parameters other than g_{NaP} were identical between the simulations, the change in activity must have been due to the persistent sodium current.

To test this model prediction, we examined the spontaneous firing rate of WT and GSK3-KI SCN neurons following application of riluzole (10 μM) and compared it to vehicle controls. Consistent with our previous work, vehicle-treated GSK3-KI cells had a significantly increased spontaneous firing rate compared to WT neurons ($p < 0.001$; Fig 5D and 5E). This hyper-excitability was rescued in riluzole-treated GSK3-KI cells ($p <$

0.001), which did not differ from either WT group. Since the majority of SCN neurons are relatively quiescent during the night, we also quantified the number of spiking versus non-spiking cells from WT and GSK3-KI mice in riluzole- and vehicle-treated conditions and found significant differences between groups ($p < 0.001$; Fig 5F). While ~40% of WT neurons were silent, almost all of the GSK3-KI neurons were spiking ($p < 0.001$), as predicted by the model. Moreover, the ratio of spiking to non-spiking cells was restored to WT levels upon riluzole treatment, while riluzole had no effect on WT neurons at night ($p = 0.5$; Fig 5F). Taken together, these results suggest that active GSK3 promotes neuronal excitability in an I_{NaP}-dependent manner.

GSK3 promotes excitability through control of AHP but not RMP

We next investigated how I_{NaP} affects intrinsic excitability. Often increases in excitability are due to depolarization of the RMP; however, the model unexpectedly predicted that increasing I_{NaP} in firing neurons causes an increase in firing rate with minimal change to the RMP of the cells (Fig 6A and 6B). This model prediction is consistent with our experimental results that GSK3 inhibition suppresses SCN activity without affecting RMP (Fig 1).

Further analysis of our model simulations revealed that the increased excitation through I_{NaP} is instead caused by suppression of the AP after-hyperpolarization (AHP). In both spiking and initially silent WT neurons at night, increasing the magnitude of I_{NaP} by increasing g_{NaP} from CHIR to GSK3-KI levels caused the minimum voltage attained after an action potential to become more depolarized without changing the RMP (Fig 6A and 6B). Thus the magnitude of the AHP diminished, allowing cells to fire more rapidly (Fig

6A and 6B). According to the model, the degree of after-hyperpolarization following an action potential depends on the balance of I_{NaP} (positive-inward) and I_{KCa} (positive-outward) currents. By plotting each of the currents that contribute to changes in membrane voltage, it is apparent that most of the currents involved in generating the action potential shut off rapidly (Fig 6C)**.** Only I_{NaP} and I_{KCa} persist through the interspike interval, setting the AHP magnitude and the depolarizing ramp back toward threshold. Increasing I_{NaP} or decreasing I_{KCa} causes a decrease in the AHP magnitude and consequently speeds up the firing rate. Conversely, decreasing I_{NaP} or increasing I_{KCa} increases the AHP magnitude and slows firing (Fig 6D).

To test the prediction that increasing I_{NaP} decreases AHP without affecting RMP experimentally, we performed whole-cell current clamp recordings in WT and GSK3-KI neurons during the day and night (Fig 7A and 7B). As predicted by the model, there was no correlation between peak I_{NaP} and RMP ($r = -0.094$, $p = 0.463$; Fig S4). Both genotypes exhibited a day/night difference in RMP ($p = 0.008$), and there was no difference in RMP between genotypes for the majority of neurons (two-way ANOVA with depolarization block cells excluded; $p = 0.433$; Fig 7C). However, for the subset of neurons in depolarization block, constitutive activation of GSK3 resulted in a more depolarized RMP (Two-way ANOVA with all cells included; $p = 0.016$; Fig 7C). This effect was predicted by the model as well since the voltage-gated sodium channels responsible for I_{NaP} are held open at the higher voltages seen in depolarization block-type neurons, leading to an increase in RMP (Fig 7D). Additionally, analysis of the action potential waveforms of the spontaneously active cells from the same recordings revealed a significant decrease in the AHP in the GSK3-KI neurons ($p = 0.012$), particularly

during the night, such that the day-night difference in AHP is diminished in GSK3-KI neurons (Fig 8A and 8B). Moreover, consistent with the model prediction, both the AHP amplitude and the SFR of all spontaneously spiking cells were significantly negatively correlated with I_{NaP} peak current, such that the larger the I_{NaP} magnitude, the smaller the after-hyperpolarization ($r = -0.732$, $p < 0.001$; Fig 8C) and faster the SFR ($r = -0.550$, $p = 0.001$; Fig 8D).

Discussion

Here, we present evidence that the rhythmically phosphorylated kinase GSK3 [5] promotes neuronal excitability through regulation of I_{NaP}. In particular, we find that: 1) GSK3 activity regulates I_{NaP}, 2) I_{NaP} exhibits a day/night difference in peak magnitude that is regulated by GSK3, and 3) I_{NaP} promotes firing and decreases AP after-hyperpolarization without affecting RMP. Our experiments were conducted in the SCN, the site of the central circadian pacemaker. As molecular circadian timekeeping can be found in many parts of the brain [27], this mechanism could be widely used in the brain to control many systems. Of particular interest are the regions of the brain that regulate mood, as impaired molecular circadian timekeeping has been implicated in mood disorders [28]. Given that GSK3 phosphorylation and I_{NaP} are altered by mood stabilizing drugs such as lithium [29] and riluzole [30], respectively, this work may provide a potential basis for the chronotherapeutic control of mood.

Despite the known importance of I_{NaP} as a pacemaker potential in many types of spontaneously active neurons [31-34], including the SCN [12, 22, 23], I_{NaP} has been largely overlooked as a potential contributor to the circadian modulation of rhythmic

firing [3, 22, 35]. However, the present study is the first to show that I_{NaP} is greater in magnitude during the day (~5 pA) than at night. This difference in I_{NaP} magnitude is sufficient to have a notable impact on excitability of compact, high R_{input} neurons such as those in the SCN. Prior work has shown that blockade of I_{NaP} with riluzole acutely silences spontaneous firing [22] and chronically dampens the circadian amplitude of SFR rhythms of individual SCN neurons [35]. Conversely, our results demonstrate that high, day-like I_{NaP} levels seen in GSK3-KI neurons at night are sufficient to induce spiking in neurons that would normally be silent (Fig 6) as well as increase the SFR of already spiking neurons (Fig 7A).

By combining modeling and experimental methods, we present an intriguing approach for how the molecular circadian clock controls electrical activity. Unlike Na^+ leak currents which were recently shown to promote excitability of clock neurons by membrane depolarization [36], our data show a mechanism for how I_{NaP} regulates the firing rate of action potentials without affecting the RMP of neurons that are hyperpolarized or spiking. We also show that the balance between I_{NaP} and I_{KCa} controls both the depolarizing ramp toward the action potential threshold and, surprisingly, the magnitude of the after-hyperpolarization following an action potential. This balance could be crucial to action potential frequency as a previous modeling/experimental study proposes that changes in RMP can phase shift the circadian clock [26]. Thus, the mechanism we propose can faithfully reflect the state of the circadian clock in firing rate, without disrupting molecular circadian timekeeping itself.

Our work also shows how changes in I_{NaP} permeate throughout the SCN network. Since the SCN is coupled via mainly inhibitory GABA, increasing the firing rate causes

more inhibitory post-synaptic currents, which could slow firing. However, inhibitory post-synaptic currents can both increase and decrease firing in SCN neurons [26], so the effects of inhibitory GABA are not always intuitive. Nevertheless, our modeling and experimental data show an increase in firing rate throughout the network, and in particular, a change in the electrical state of neurons that produces an increase in the proportion of neurons that are firing. Together, this work highlights GSK3 as a mechanism for modulating not just firing of a single cell, but also global network properties.

Further clarification of the details of GSK3 regulation is an interesting question for future study. Despite much work, the actual mechanism of circadian regulation of GSK3 activity remains unknown. Interestingly, the suppression of I_{NaP} by pharmacological GSK3 inhibition was restricted to the day, when GSK3 activity is high, whereas the effect of GSK3 activation was not phase-specific. That is, GSK3-KI had enhanced, but unexpectedly rhythmic I_{NaP}. We cannot rule out a compensatory mechanism or developmental effects as explanations of this result, although it should be noted that no gross developmental differences have been previously reported in this animal model [24]. Alternatively, this finding could point toward another mechanism, in addition to phosphorylation, by which GSK3 function is regulated within the SCN (i.e. sequestration, localization, or priming kinases) [37]. GSK3 likely directly phosphorylates individual persistent sodium channels by a mechanism that also remains to be found. Intriguingly, aging-induced circadian decline is associated with disrupted SCN firing rate and AHP in the absence of altered PER2 expression [38, 39], leading to the proposal that SCN neuronal activity may be the "weak link" in the circadian system [3]. Given that p-

GSK3 levels are decreased in the SCN of aged rodents, GSK3 control of I_{NaP} may be one source of age-related circadian disruption. While more work is necessary to explore this concept as well as the biophysical mechanism by which GSK3 activates I_{NaP}, this work suggests a promising new motif in which a kinase can directly regulate electrical activity acutely and without transcriptional cost. Because of its efficiency, this is a motif likely to be found in other brain regions as well.

Methods

Animals

Homozygous *Per1*::GFP [40], wild-type (WT) C57-BL6/J, and GSK3$\alpha/\beta^{21A/21A/9A/9A}$ (GSK3-KI) mice (2-5 months old; male and female) backcrossed for at least 10 generations to C57BL/6 mice, in which regulatory serine-alanine substitution on both isoforms of GSK3 rendered GSK3 de-phosphorylated and constitutively active [24] were group-housed (2-5 animals per cage) in a 12:12 light/dark (LD) cycle with *ad libitum* access to food and water and handled in accordance with the University of Alabama at Birmingham (UAB) Institutional Animal Care and Use Committee (IACUC) and National Institutes of Health (NIH) guidelines. Mice were euthanized with cervical dislocation and rapid decapitation.

Electrophysiology

Sample sizes were based on previous work with similar effect sizes and significant differences between groups, given the same methodologies for both loose patch and whole cell electrophysiology [41-43]. Fresh brain slices were prepared from

mice sacrificed between ZT 2-3 or ZT 11-12 for day and night recordings, respectively using previously published methods (as in [4]). All recordings were made between ZT 4-8 or ZT 14-18. For GSK3 inhibitor experiments, the chamber was perfused with extracellular solution containing 1μM CHIR-99021 (Stemgent, San Diego, CA) or vehicle (0.002% DMSO) starting at ZT 3.5 or ZT 13.5, and targeted recordings were made from SCN cells between ZT 4-8 or 14-18. For riluzole loose-patch recordings, bath-application of vehicle (0.01% DMSO) or 10μM Riluzole began at ZT 13 and recordings were made from ZT 14-18. Electrodes with a pipette resistance of ~4-6 MΩ were filled with filtered, K^+-gluconate solution (as in [4]). Firing-rate was measured as the average of a 120-sec record. Comparisons of genotypes did not allow randomization to WT/GSK3-KI groups (but see congenic strain background above). In addition, no specific methods were used to randomize mice to experimental groups or to blind investigators to treatment; however treatment, time-of-day, and genotype measurements were always interleaved.

Whole-cell electrophysiology

Slices were prepared using the same methods and solutions described previously [4]. Riluzole-sensitive current was measured using a slow depolarizing voltage ramp (-100mV to +10mV, 59mV/s) before and after 3 min Riluzole (20μM) application[22]. At least 5-10 sweeps of the voltage ramp protocol were averaged for each cell, and baseline subtracted by fitting the linear portion between -85mV and -65mV to zero[22]. Peak sodium current was determined as the minimum point of a 4th-7th order polynomial fit applied to the baseline subtracted curve between -55mV to -10mV. For current clamp

recordings, cells were recorded in gap-free current clamp mode. Resting membrane potential (RMP) was determined as the average voltage half-way between two action potentials. Cells were classified by neurophysiological phenotypes based on RMP and spontaneous event amplitude. Using a k-means cluster analysis, each neuron was grouped into one of four categories while blind to experimental group. Based on the results, SCN neurons were classified as either (1) silent, (2) spiking, (3) having depolarized electrical states with low amplitude membrane oscillations (DLAMO), or (4) exhibiting depolarization block[17]. For cells classified as spiking, the AP after-hyperpolarization was measured using the template search function in Clampfit 10 (Axon Instruments) to determine the average anti-peak amplitude for each cell. In all whole-cell experiments, recordings were made within 5 minutes of breaking into the cell. Cells with greater than -50pA of leak recorded in the seal test, with excessive break through spikes in voltage-ramp protocol (indicative of poor voltage control), or which did not exhibit a rebound spike after terminating a hyperpolarizing current injection were excluded from the analysis.

Data analysis

Data were analyzed with independent samples t-tests, two-way ANOVAs, linear mixed model two-way ANOVA, Pearson's correlation, three-way loglinear analysis and chi-squared tests with SPSS 21.0 (IBM Statistics). In the event that assumptions of normality and homogenous variances were not met (tested by Shapiro-Wilks and Levene's tests, respectively), a nonparametric Kruskal-Wallis or the Scheirer, Ray, and

Hare extension of the Kruskal Wallis was used instead. Significance was ascribed at $p < 0.05$.

Model fitting of I_{NaP}

The voltage dependence of I_{NaP} was determined using the current response to a 59 mV/s depolarizing voltage ramp, from -100 mV to 10 mV. Current values were fit for voltages between -65 mV and -20 mV, since cellular voltages are usually in this range. For fitting, the transient sodium current in the model was ignored since the effects of this current were seen in some experimental recordings, but not all, and never contributed to the inward current in the same voltage range as I_{NaP}. The least current was seen in night phase cells after treatment with riluzole. This was taken as the baseline, and subtracted away from current response curves for day and night phase cells in three experimental conditions: wildtype, after treatment with the GSK3 blocker CHIR, and in slices from GSK3-KI animals. The dynamics of the I_{NaP} current were consistent with a conductance-based model of the form $I_{NaP} = -g_{NaP}(V-E_{Na})p$, with the activating gating variable p ranging between 0 and 1. Fitting the currents, we found that p should satisfy the standard Hodgkin-Huxley style gating variable equation

$$\frac{dp}{dt} = \frac{p_\infty(V) - p}{\tau_p}$$

with

$$p_\infty(V) = \frac{1}{\left(1 + \exp\left(-\frac{V+25}{7.4}\right)\right)^{1.5}}$$

and $\tau_p = 100$. Currents for all experimental conditions could be fit to this form by varying g_{NaP} (Figure S3: g_{NaP} values are GSK3-KI day 2.27, GSK3-KI night 2.13, WT day 2.09, WT night 1.59, CHIR day 1.97, CHIR night 1.46,).

This current was included into a detailed multiscale ordinary differential equation model of the SCN [26] containing both a molecular clock model, describing the transcriptional/translational feedback loops at the heart of circadian timekeeping, as well as detailed cellular electrophysiology with millisecond resolution. The SCN electrophysiology model (adapted from [17] included circadian variation in two conductances (g_{KCa} and $g_{K\text{-}leak}$). We additionally incorporate GSK3 control of the I_{NaP} amplitude through the function S = 21.0*(gto-1.66), where gto is the molecular clock variable corresponding to GSK3 activity [44, 45]. The maximal I_{NaP} conductance is then given by:

WT: g_{NaP} = 1.59+0.5/(1.0+exp(-S))

CHIR: g_{NaP} = 1.46+0.51/(1.0+exp(-S))

GSK3-KI: g_{NaP} = 2.13+0.14/(1.0+exp(-S))

according to the values for day and night in each experimental condition, as in Figure S3. This reproduces the day-night difference in I_{NaP} amplitude described above. To compensate for the addition of this current, we reduce the circadian drive of g_{KCa} and $g_{K\text{-}leak}$ to 60% of its original value (R = 6.81*clk*(G-0.25)). Additionally, the magnitude of the GABA current was reduced (g_{GABA}=0.1). All other parameters were as in [26]. With these small modifications, the model reproduces the circadian variation in electrical activity seen experimentally and the many electrical states seen within the normal SCN 24-hour cycle (Figure 5c and data not shown; [15, 17].

Code availability

The code for our single cell model of the electrical activity of SCN neurons with I_{NaP} will be deposited on ModelDB. From this code, the single cell and network behavior can be generated. Details of our model network simulations can be found in [26].

References

1. Welsh DK, Takahashi JS, Kay SA. Suprachiasmatic nucleus: cell autonomy and network properties. Annu Rev Physiol. 2010;72:551-77. Epub 2010/02/13. doi: 10.1146/annurev-physiol-021909-135919. PubMed PMID: 20148688.

2. Partch CL, Green CB, Takahashi JS. Molecular architecture of the mammalian circadian clock. Trends in cell biology. 2014;24(2):90-9. doi: 10.1016/j.tcb.2013.07.002. PubMed PMID: 23916625; PubMed Central PMCID: PMC3946763.

3. Colwell CS. Linking neural activity and molecular oscillations in the SCN. Nat Rev Neurosci. 2011;12(10):553-69. Epub 2011/09/03. doi: nrn3086 [pii]

10.1038/nrn3086. PubMed PMID: 21886186.

4. Paul JR, Johnson RL, Jope RS, Gamble KL. Disruption of circadian rhythmicity and suprachiasmatic action potential frequency in a mouse model with constitutive activation of glycogen synthase kinase 3. Neuroscience. 2012;226:1-9. Epub 2012/09/19. doi: S0306-4522(12)00881-0 [pii]

10.1016/j.neuroscience.2012.08.047. PubMed PMID: 22986169; PubMed Central PMCID: PMC3490018.

5. Besing RC, Paul JR, Hablitz LM, Rogers CO, Johnson RL, Young ME, et al. Circadian Rhythmicity of Active GSK3 Isoforms Modulates Molecular Clock Gene

Rhythms in the Suprachiasmatic Nucleus. J Biol Rhythms. 2015. doi: 10.1177/0748730415573167. PubMed PMID: 25724980.

6. Iitaka C, Miyazaki K, Akaike T, Ishida N. A role for glycogen synthase kinase-3beta in the mammalian circadian clock. J Biol Chem. 2005;280(33):29397-402. Epub 2005/06/24. doi: M503526200 [pii]

10.1074/jbc.M503526200. PubMed PMID: 15972822.

7. Hur EM, Zhou FQ. GSK3 signalling in neural development. Nat Rev Neurosci. 2010;11(8):539-51. Epub 2010/07/22. doi: nrn2870 [pii]

10.1038/nrn2870. PubMed PMID: 20648061.

8. Li X, Jope RS. Is glycogen synthase kinase-3 a central modulator in mood regulation? Neuropsychopharmacology. 2010;35(11):2143-54. Epub 2010/07/30. doi: npp2010105 [pii]

10.1038/npp.2010.105. PubMed PMID: 20668436; PubMed Central PMCID: PMC3055312.

9. Taelman VF, Dobrowolski R, Plouhinec JL, Fuentealba LC, Vorwald PP, Gumper I, et al. Wnt signaling requires sequestration of glycogen synthase kinase 3 inside multivesicular endosomes. Cell. 2010;143(7):1136-48. Epub 2010/12/25. doi: S0092-8674(10)01356-5 [pii]

10.1016/j.cell.2010.11.034. PubMed PMID: 21183076; PubMed Central PMCID: PMC3022472.

10. Beurel E, Michalek SM, Jope RS. Innate and adaptive immune responses regulated by glycogen synthase kinase-3 (GSK3). Trends in immunology. 2010;31(1):24-31. doi: 10.1016/j.it.2009.09.007. PubMed PMID: 19836308; PubMed Central PMCID: PMC2818223.

11. Sim CK, Forger DB. Modeling the electrophysiology of suprachiasmatic nucleus neurons. J Biol Rhythms. 2007;22(5):445-53. doi: 10.1177/0748730407306041. PubMed PMID: 17876065.

12. Jackson AC, Yao GL, Bean BP. Mechanism of spontaneous firing in dorsomedial suprachiasmatic nucleus neurons. J Neurosci. 2004;24(37):7985-98. doi: 10.1523/JNEUROSCI.2146-04.2004. PubMed PMID: 15371499.

13. Kuhlman SJ, McMahon DG. Encoding the ins and outs of circadian pacemaking. J Biol Rhythms. 2006;21(6):470-81. PubMed PMID: 17107937.

14. Wang TA, Yu YV, Govindaiah G, Ye X, Artinian L, Coleman TP, et al. Circadian rhythm of redox state regulates excitability in suprachiasmatic nucleus neurons. Science. 2012;337(6096):839-42. Epub 2012/08/04. doi: science.1222826 [pii]

10.1126/science.1222826. PubMed PMID: 22859819; PubMed Central PMCID: PMC3490628.

15. Belle MD, Diekman CO, Forger DB, Piggins HD. Daily electrical silencing in the mammalian circadian clock. Science. 2009;326(5950):281-4. Epub 2009/10/10. doi: 326/5950/281 [pii]

10.1126/science.1169657. PubMed PMID: 19815775.

16. Kuhlman SJ, McMahon DG. Rhythmic regulation of membrane potential and potassium current persists in SCN neurons in the absence of environmental input. EurJNeurosci. 2004;20(4):1113-7. PubMed PMID: 431.

17. Diekman CO, Belle MD, Irwin RP, Allen CN, Piggins HD, Forger DB. Causes and consequences of hyperexcitation in central clock neurons. PLoS Comput Biol. 2013;9(8):e1003196. doi: 10.1371/journal.pcbi.1003196. PubMed PMID: 23990770; PubMed Central PMCID: PMC3749949.

18. Pennartz CM, de Jeu MT, Bos NP, Schaap J, Geurtsen AM. Diurnal modulation of pacemaker potentials and calcium current in the mammalian circadian clock. Nature. 2002;416(6878):286-90. PubMed PMID: 11875398.

19. Shavkunov AS, Wildburger NC, Nenov MN, James TF, Buzhdygan TP, Panova-Elektronova NI, et al. The fibroblast growth factor 14.voltage-gated sodium channel complex is a new target of glycogen synthase kinase 3 (GSK3). J Biol Chem. 2013;288(27):19370-85. doi: 10.1074/jbc.M112.445924. PubMed PMID: 23640885; PubMed Central PMCID: PMC3707642.

20. Tapia M, Del Puerto A, Puime A, Sanchez-Ponce D, Fronzaroli-Molinieres L, Pallas-Bazarra N, et al. GSK3 and beta-catenin determines functional expression of sodium channels at the axon initial segment. Cellular and molecular life sciences : CMLS. 2013;70(1):105-20. doi: 10.1007/s00018-012-1059-5. PubMed PMID: 22763697.

21. Enomoto A, Han JM, Hsiao CF, Chandler SH. Sodium currents in mesencephalic trigeminal neurons from Nav1.6 null mice. J Neurophysiol. 2007;98(2):710-9. Epub 2007/05/25. doi: 00292.2007 [pii]

10.1152/jn.00292.2007. PubMed PMID: 17522178.

22. Kononenko NI, Shao LR, Dudek FE. Riluzole-sensitive slowly inactivating sodium current in rat suprachiasmatic nucleus neurons. J Neurophysiol. 2004;91(2):710-8. PubMed PMID: 14573554.

23. Pennartz CM, Bierlaagh MA, Geurtsen AM. Cellular mechanisms underlying spontaneous firing in rat suprachiasmatic nucleus: involvement of a slowly inactivating component of sodium current. J Neurophysiol. 1997;78(4):1811-25. PubMed PMID: 9325350.

24. McManus EJ, Sakamoto K, Armit LJ, Ronaldson L, Shpiro N, Marquez R, et al. Role that phosphorylation of GSK3 plays in insulin and Wnt signalling defined by knockin analysis. EMBO J. 2005;24(8):1571-83. Epub 2005/03/26. doi: 7600633 [pii]

10.1038/sj.emboj.7600633. PubMed PMID: 15791206; PubMed Central PMCID: PMC1142569.

25. Panda S, Antoch MP, Miller BH, Su AI, Schook AB, Straume M, et al. Coordinated transcription of key pathways in the mouse by the circadian clock. Cell. 2002;109(3):307-20. PubMed PMID: 12015981.

26. DeWoskin D, Myung J, Belle MD, Piggins HD, Takumi T, Forger DB. Distinct roles for GABA across multiple timescales in mammalian circadian timekeeping. Proc Natl Acad Sci U S A. 2015. Epub in press.

27. Dibner C, Schibler U, Albrecht U. The mammalian circadian timing system: organization and coordination of central and peripheral clocks. Annu Rev Physiol. 2010;72:517-49. Epub 2010/02/13. doi: 10.1146/annurev-physiol-021909-135821. PubMed PMID: 20148687.

28. McClung CA. How might circadian rhythms control mood? Let me count the ways. Biol Psychiatry. 2013;74(4):242-9. doi: 10.1016/j.biopsych.2013.02.019. PubMed PMID: 23558300; PubMed Central PMCID: PMC3725187.

29. Can A, Schulze TG, Gould TD. Molecular actions and clinical pharmacogenetics of lithium therapy. Pharmacol Biochem Behav. 2014;123:3-16. doi: 10.1016/j.pbb.2014.02.004. PubMed PMID: 24534415; PubMed Central PMCID: PMC4220538.

30. Lapidus KA, Soleimani L, Murrough JW. Novel glutamatergic drugs for the treatment of mood disorders. Neuropsychiatr Dis Treat. 2013;9:1101-12. doi: 10.2147/NDT.S36689. PubMed PMID: 23976856; PubMed Central PMCID: PMC3747027.

31. Carter BC, Giessel AJ, Sabatini BL, Bean BP. Transient sodium current at subthreshold voltages: activation by EPSP waveforms. Neuron. 2012;75(6):1081-93. doi: 10.1016/j.neuron.2012.08.033. PubMed PMID: 22998875; PubMed Central PMCID: PMC3460524.

32. Yamada-Hanff J, Bean BP. Persistent sodium current drives conditional pacemaking in CA1 pyramidal neurons under muscarinic stimulation. J Neurosci. 2013;33(38):15011-21. doi: 10.1523/JNEUROSCI.0577-13.2013. PubMed PMID: 24048831; PubMed Central PMCID: PMC3776055.

33. Do MT, Bean BP. Sodium currents in subthalamic nucleus neurons from Nav1.6-null mice. J Neurophysiol. 2004;92(2):726-33. doi: 10.1152/jn.00186.2004. PubMed PMID: 15056687.

34. Do MT, Bean BP. Subthreshold sodium currents and pacemaking of subthalamic neurons: modulation by slow inactivation. Neuron. 2003;39(1):109-20. PubMed PMID: 12848936.

35. Kononenko NI, Honma S, Dudek FE, Honma K. On the role of calcium and potassium currents in circadian modulation of firing rate in rat suprachiasmatic nucleus neurons: multielectrode dish analysis. Neurosci Res. 2008;62(1):51-7. Epub 2008/07/08. doi: S0168-0102(08)00175-2 [pii]

10.1016/j.neures.2008.06.001. PubMed PMID: 18602427.

36. Flourakis M, Kula-Eversole E, Hutchison AL, Han TH, Aranda K, Moose DL, et al. A Conserved Bicycle Model for Circadian Clock Control of Membrane Excitability. Cell. 2015;162(4):836-48. doi: 10.1016/j.cell.2015.07.036. PubMed PMID: 26276633; PubMed Central PMCID: PMCPMC4537776.

37. Beurel E, Grieco SF, Jope RS. Glycogen synthase kinase-3 (GSK3): regulation, actions, and diseases. Pharmacol Ther. 2015;148:114-31. doi: 10.1016/j.pharmthera.2014.11.016. PubMed PMID: 25435019; PubMed Central PMCID: PMC4340754.

38. Farajnia S, Michel S, Deboer T, vanderLeest HT, Houben T, Rohling JH, et al. Evidence for neuronal desynchrony in the aged suprachiasmatic nucleus clock. J Neurosci. 2012;32(17):5891-9. doi: 10.1523/JNEUROSCI.0469-12.2012. PubMed PMID: 22539850.

39. Nakamura TJ, Nakamura W, Yamazaki S, Kudo T, Cutler T, Colwell CS, et al. Age-related decline in circadian output. J Neurosci. 2011;31(28):10201-5. doi: 10.1523/JNEUROSCI.0451-11.2011. PubMed PMID: 21752996; PubMed Central PMCID: PMC3155746.

40. LeSauter J, Yan L, Vishnubhotla B, Quintero JE, Kuhlman SJ, McMahon DG, et al. A short half-life GFP mouse model for analysis of suprachiasmatic nucleus organization. Brain Res. 2003;964(2):279-87. PubMed PMID: 455.

41. Besing RC, Hablitz LM, Paul JR, Johnson RL, Prosser RA, Gamble KL. Neuropeptide Y-induced phase shifts of PER2::LUC rhythms are mediated by long-term suppression of neuronal excitability in a phase-specific manner. Chronobiol Int. 2012;29(2):91-102. Epub 2012/02/14. doi: 10.3109/07420528.2011.649382. PubMed PMID: 22324550.

42. Hablitz LM, Molzof HE, Paul JR, Johnson RL, Gamble KL. Suprachiasmatic nucleus function and circadian entrainment are modulated by G protein-coupled inwardly rectifying (GIRK) channels. J Physiol. 2014;592(Pt 22):5079-92. doi: 10.1113/jphysiol.2014.282079. PubMed PMID: 25217379; PubMed Central PMCID: PMC4259544.

43. Gamble KL, Kudo T, Colwell CS, McMahon DG. Gastrin-Releasing Peptide Modulates Fast Delayed Rectifier Potassium Current in Per1-Expressing SCN Neurons. J Biol Rhythms. 2011;26(2):99-106. Epub 2011/04/02. doi: 26/2/99 [pii]

10.1177/0748730410396678. PubMed PMID: 21454290.

44. Kim JK, Forger DB, Marconi M, Wood D, Doran A, Wager T, et al. Modeling and validating chronic pharmacological manipulation of circadian rhythms. CPT: pharmacometrics & systems pharmacology. 2013;2:e57. doi: 10.1038/psp.2013.34. PubMed PMID: 23863866; PubMed Central PMCID: PMC3734602.

45. Kim JK, Forger DB. A mechanism for robust circadian timekeeping via stoichiometric balance. Molecular systems biology. 2012;8:630. doi:

10.1038/msb.2012.62. PubMed PMID: 23212247; PubMed Central PMCID: PMC3542529.

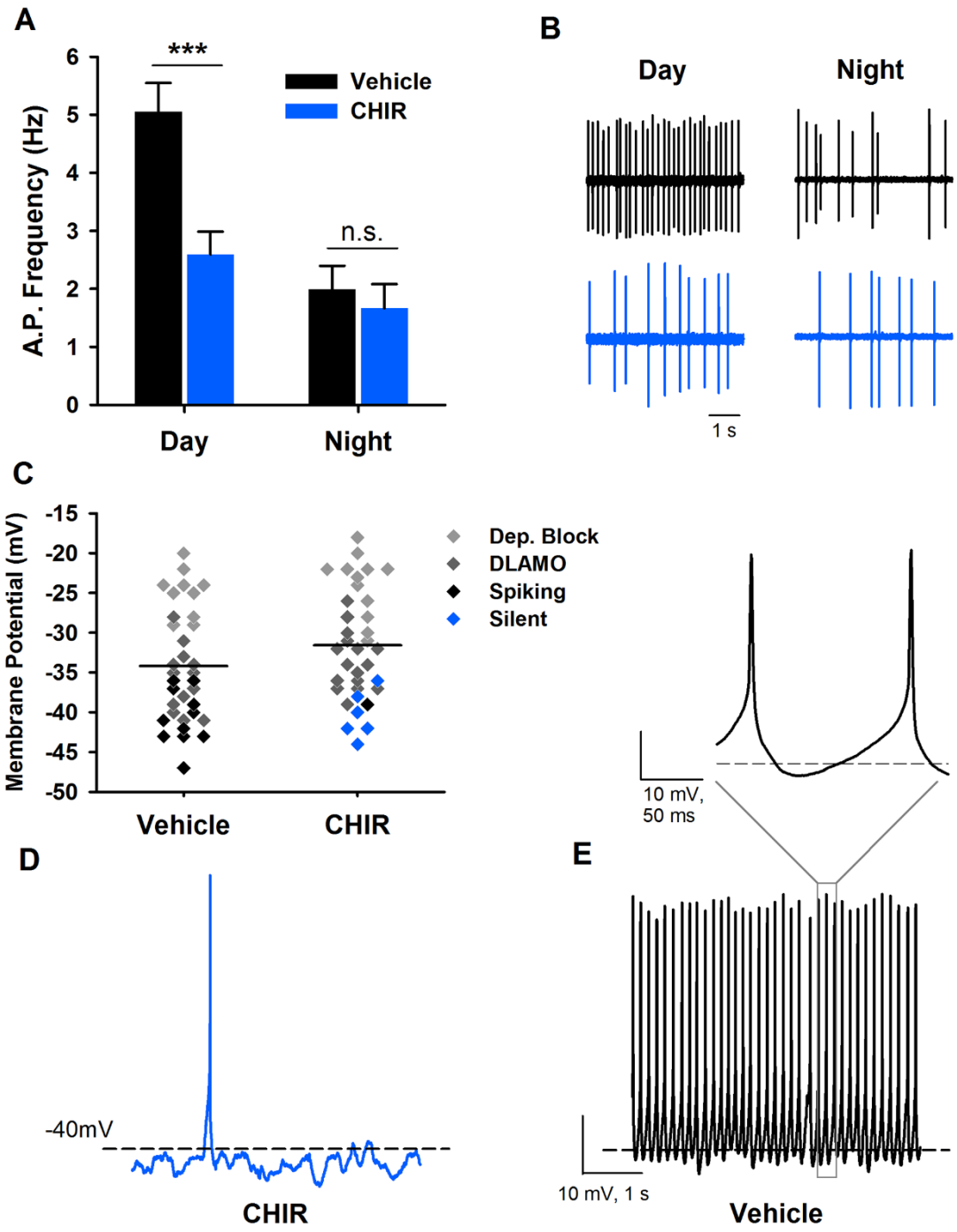

Figure 1. GSK3 inhibition suppresses excitability.
(A) Spontaneous action potential frequencies (mean ± SEM) from 2-min loose-patch recordings of neurons treated with vehicle (0.002% DMSO) or CHIR-99021 (CHIR, 1µM) during the day (ZT 4-8) or early-night (ZT 14-18). CHIR significantly suppressed SCN

activity during the day (***$p < 0.001$) but not the night (n.s. $p = 0.608$). Two-way ANOVA; treatment X time interaction, $F_{(1,146)} = 5.772$, $p = 0.018$. From left to right, n = 38 cells, 4 slices; 41 cells, 4 slices; 38 cells, 3 slices; 33 cells, 3 slices.
(B) Representative cell-attached loose-patch traces (10 s) from each group.
(C) Dot plot of resting membrane potential for individual SCN neurons treated with vehicle or CHIR during the mid-day (ZT 4-8). Line indicates mean for each group. There was no difference in RMP between groups. Independent samples t-test; $t_{(67)} = -1.521$, $p = 0.133$; n = 34-35 cells, 5-6 slices per group.
(D-E) Representative current clamp traces (5 s) of SCN neurons from each group in (C). Inset shows depolarizing ramp between action potentials in control cells.

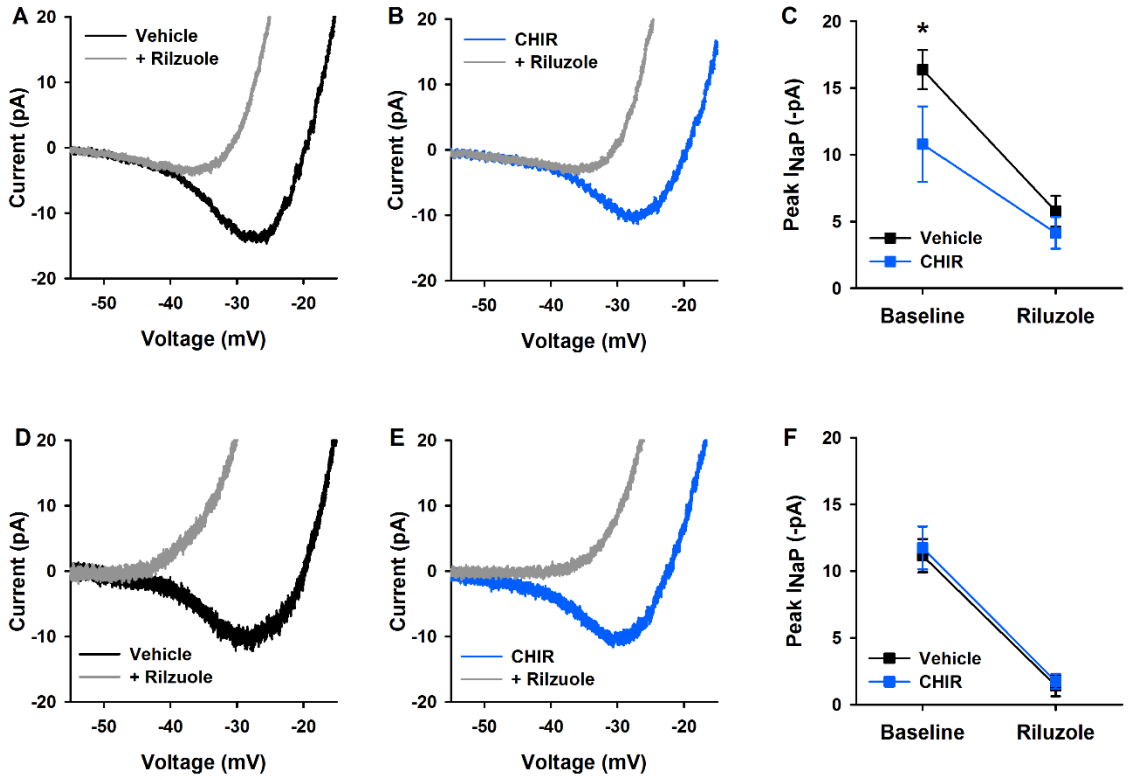

Figure 2. GSK3 inhibition suppresses I_{NaP} during the day but not the night.
(A-B**,** D-E) Average normalized response to slow depolarizing voltage ramp (-100 to +10 mV; 59 mV/s) from SCN cells treated with (A, D) vehicle (DMSO, 0.002%) or (B, E) GSK3 inhibitor (CHIR, 1μM) at baseline and after 3-min treatment with persistent sodium current blocker, riluzole (20 μM).
(C, F) Peak inward current (mean ± SEM) at baseline and after riluzole treatment. Recordings made between ZT 4-8 (A-C) or ZT 14-18 (D-F). During the day (C) CHIR-treated cells had significantly reduced inward current at baseline (*p = 0.042) that was lost after blockade of I_{NaP} with riluzole (p = 0.350). Two-way, mixed-design ANOVA; Treatment X Riluzole interaction, $F_{(1,31)}$ = 5.455, p = 0.026; n = 13-20 cells, 4 slices per group. At night (F) peak inward current did not differ between CHIR- and vehicle-treated cells at baseline or after treatment with riluzole (non-significant main effect of CHIR, $F_{(1,33)}$ = 0.150, p = 0.748; n = 13-22 cells, 4 slices per group).

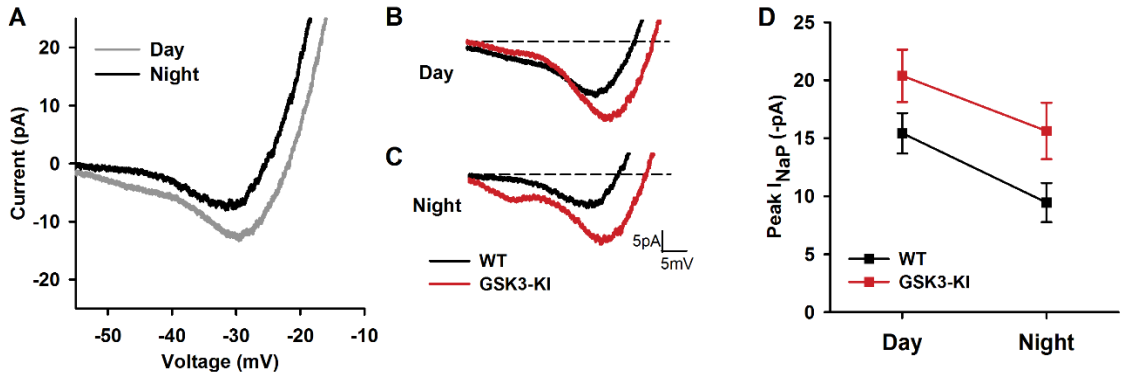

Figure 3. I_{NaP} enhanced during the day and by chronic GSK3 activation.
(A) Average normalized response to slow depolarizing voltage ramp (-100 to +10 mV; 59 mV/s) from SCN cells from WT during the mid-day or early-night.
(B-C) Average normalized responses to voltage ramp from WT or GSK3-KI SCN cells during the day (B) or night (C).
(D) Means ± SEM of peak inward current from cells in (A-C). Two-way ANOVA; main effect of time, $F_{(1,80)} = 7.009$, $p = 0.01$; main effect of genotype, $F_{(1,80)} = 7.506$, $p = 0.008$. For all panels: WT day, n = 28 cells, 5 slices; WT night, n = 22 cells, 3 slices; GSK3-KI day, n = 18 cells, 4 slices; GSK3-KI night, n = 16 cells, 3 slices.

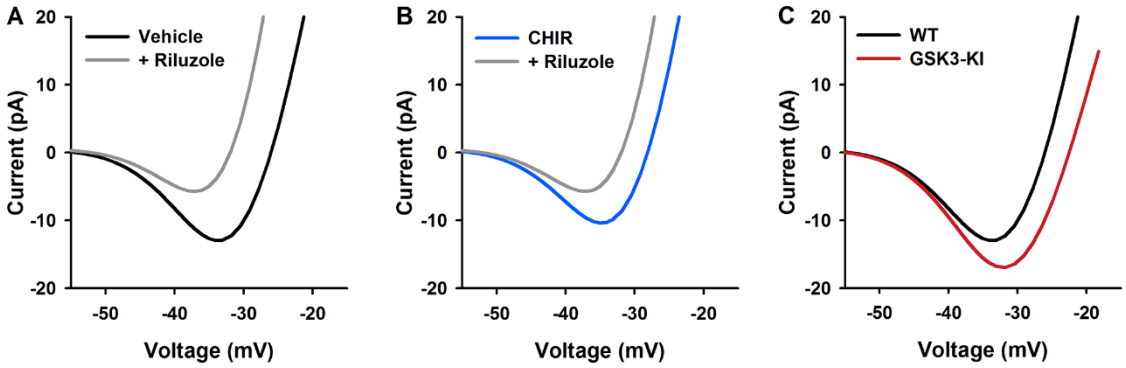

Figure 4. Modeling of voltage-ramp experiments.
(A) Simulations of the voltage-ramp protocol in WT model cells with and without riluzole (R=3.1, vehicle: g_{NaP}=2.08, riluzole: g_{NaP}=0). Our model matched the data collected in Fig 2A and shows the effects of the persistent sodium current in the model.
(B) Simulations of the voltage-ramp protocol under CHIR with and without riluzole (R=3.1, vehicle: g_{NaP}=1.46, riluzole: g_{NaP}=0). This matches Fig 2B and shows the effect of inhibiting GSK3 in our model.
(C) Simulations of the voltage-ramp protocol in the GSK3-KI compared to WT (R=3.1, WT: g_{NaP}=2.08, GSK3-KI: g_{NaP}=2.85). This matches the data in Fig 3B, and shows how the overactive kinase increases the persistent sodium current.

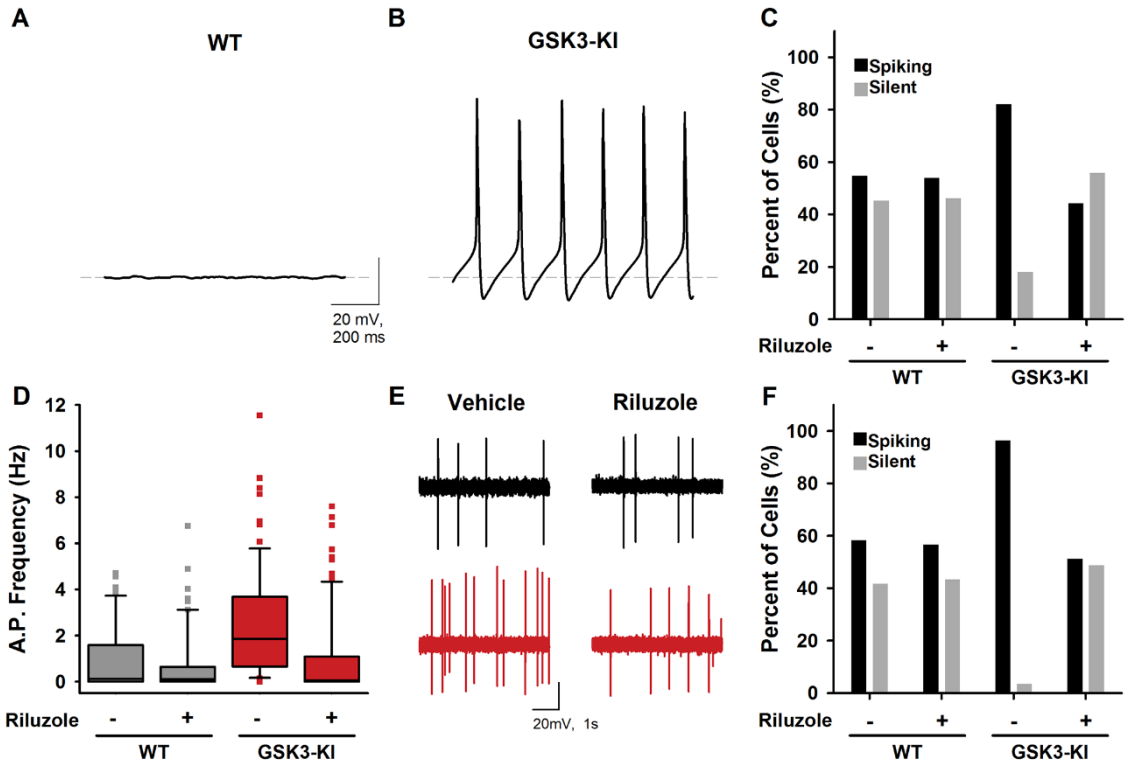

Figure 5. Riluzole blocks GSK3-induced excitability.
(A-B) Representative model recordings (1 s) from nighttime cell with I_{NaP} at WT (A) or GSK3-KI (B) level shows that increasing I_{NaP} alone is sufficient to induce spontaneous activity in a silent cell. Gray line indicates RMP (-63.4 mV).
(C) Percentage of silent versus spiking neurons seen in SCN network model at night with WT or GSK3-KI levels of I_{NaP} before and after I_{NaP} blockade with riluzole.
(D) Box plot of early-night spontaneous action potential frequencies of SCN neurons from WT or GSK3-KI mice treated with vehicle (DMSO, 0.01%) or riluzole (10 µM), showing 10^{th} and 90^{th} percentiles (whiskers), 25^{th} and 75^{th} percentiles (box borders), median (center line), and outliers (symbols). Scheirer-Ray-Hare Kruskal-Wallis test, main effect of genotype, $H_{(1)} = 7.009$, $p < 0.001$; main effect of treatment, $H_{(1)} = 8.089$, $p < 0.001$, and interaction, $H_{(1)} = 4.834$, $p < 0.001$, post hoc asymptotic significance, $p < 0.001$.
(E) Representative cell-attached loose-patch traces (5 s) from each group.
(F) Quantification of silent versus non-silent cells for each group in (D-E). Three-way loglinear analysis, three-way interaction, $X^2_{(1)} = 25.852$, $p < 0.001$. Follow-up chi-squared tests revealed that GSK3-KI cells were significantly more likely to be spiking than WT vehicle-treated cells ($X^2_{(1)} = 32.428$, $p < 0.001$). Blocking I_{NaP} with riluzole increased the proportion of silent cells in GSK3-KI slices ($X^2_{(1)} = 44.735$, $p < 0.001$) up to that of WT levels ($X^2_{(1)} = 0.430$, $p = 0.313$), whereas riluzole had no effect on the proportion of silent cells in WT slices ($X^2_{(1)} = 0.034$, $p = 0.5$). For panels (D, F): WT and WT + riluzole, n = 60 cells, 2 slices; GSK3-KI, n = 84 cells, 3 slices; GSK3-KI + riluzole, n = 86 cells, 3 slices.

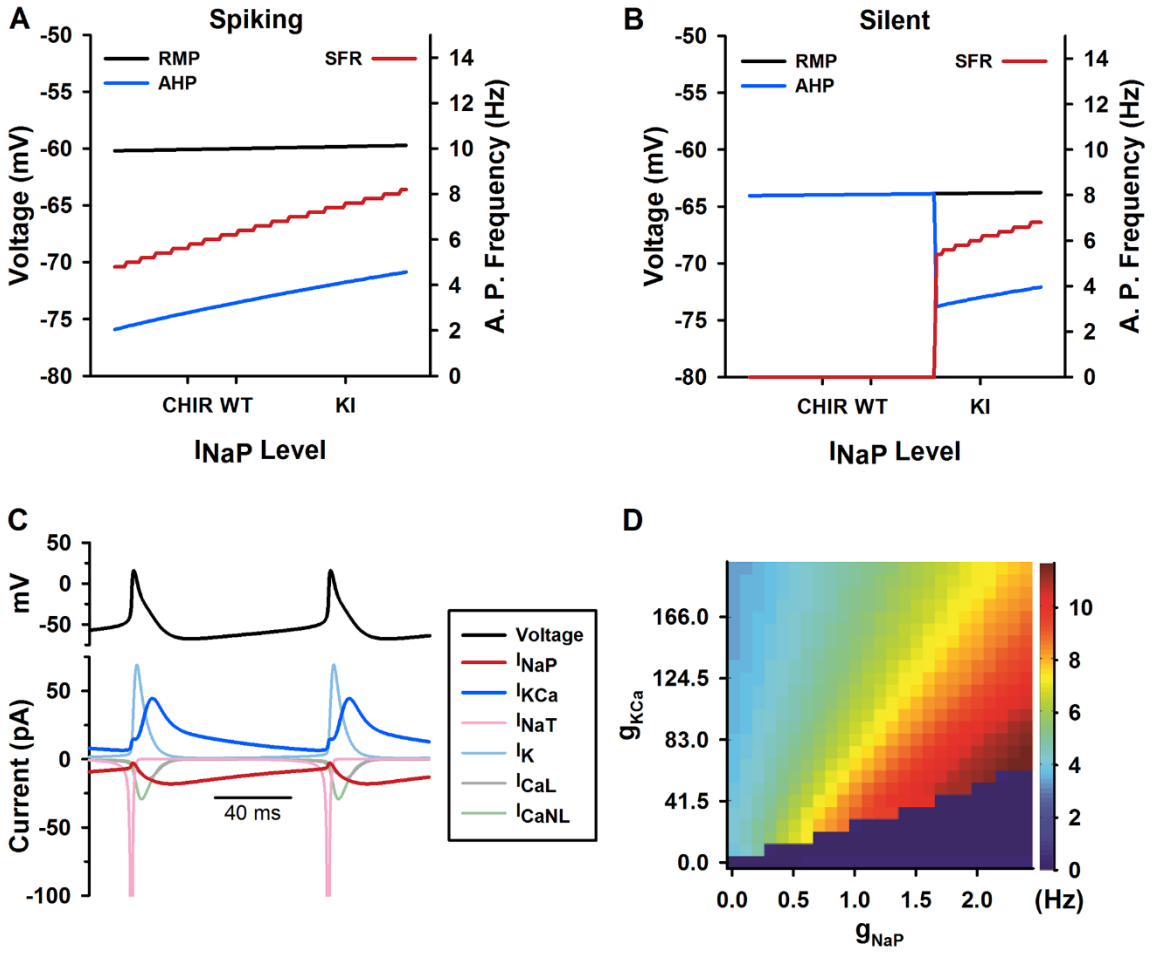

Figure 6. Model predicts I_{NaP} promotes excitability through AHP but not RMP.
(A-B) Model prediction of resting membrane potential (RMP), minimum voltage attained after an action potential (AHP), and spontaneous firing rate (SFR) at different levels of I_{NaP} for a WT-spiking (A) or WT-silent (B) SCN neuron at night. The WT-silent neuron begins to fire when I_{NaP} is increased to GSK3-KI levels. When either neuron fires, increasing I_{NaP} increases the SFR without changing the RMP by decreasing the magnitude of the AHP.
(C) Various currents associated with a typical SCN action potential. During the AHP and ramp back to threshold, all currents other than I_{NaP} and I_{KCa} have inactivated.
(D) Heat map showing the contributions of g_{NaP} and g_{KCa} toward setting the SFR (in Hz) of SCN neurons.

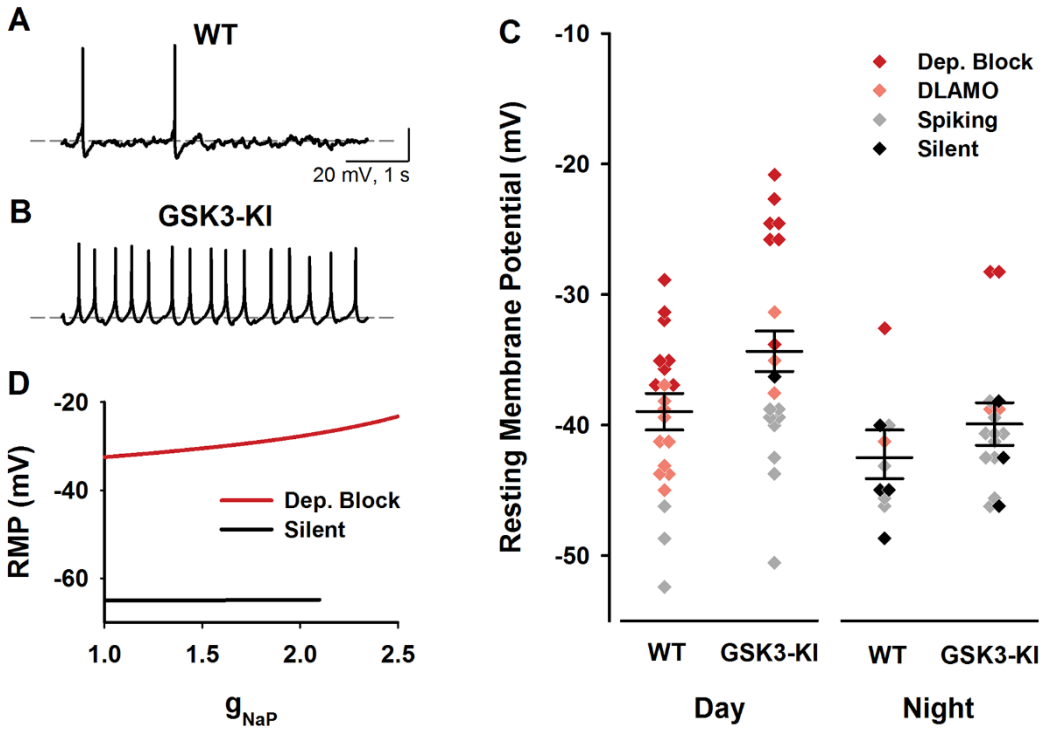

Figure 7. GSK3 activity promotes nighttime excitability without affecting RMP.
(A-B) Representative whole-cell current clamp recordings (5 s) from WT (A) and GSK3-KI (B) SCN neurons in early-night. Dashed gray line indicates -40 mV.
(C) Dot plot of resting membrane potential for individual WT or GSK3-KI SCN neurons recorded from during the day or early-night. Lines indicate mean ± SEM for each group. Cells were significantly more depolarized during the day and in GSK3-KI slices. Two-way ANOVA; main effect of time, $F_{(1,64)} = 7.474$, $p = 0.008$; main effect of genotype, $F_{(1,64)} = 6.099$, $p = 0.016$. From left-to-right, n = 21 cells, 4 slices; 19 cells, 3 slices; 11 cells, 3 slices; 17 cells, 3 slices. The effect of genotype on RMP was driven by groups of cells in depolarized block (non-significant main effect of genotype when depolarized block cells were excluded from analysis; $F_{(1,54)} = 0.623$, $p = 0.433$).
(D) Model prediction of effect of I_{NaP} conductance (g_{NaP}) on RMP shows that increasing g_{NaP} causes a cell in depolarization block to further depolarize but has no effect on the RMP of a hyperpolarized, silent cell.

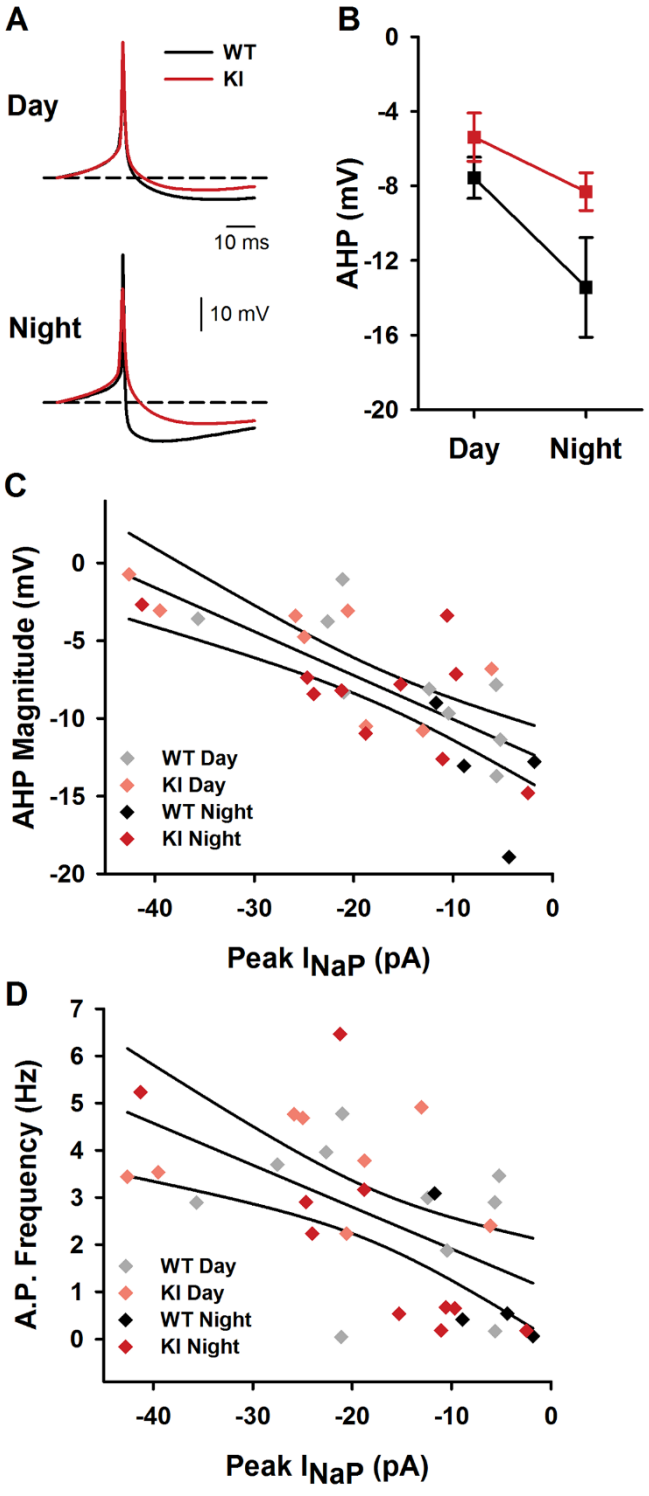

Figure 8. GSK3 decreases the AHP magnitude through I_{NaP}.
(A) Average action potential waveforms from spontaneously active SCN neurons from WT or GSK3-KI mice recorded in mid-day or early-night. For visualization, all waveforms were adjusted to same baseline (-40 mV, dashed line) before averaging.

(B) Mean ± SEM of AHP magnitude (difference from RMP) from cells represented in (A). AHP amplitude was significantly decreased during the day and in GSK3-KI cells. Two-way ANOVA; main effect of time, $F_{(1,30)} = 10.266$, $p = 0.003$; main effect of genotype, $F_{(1,30)} = 7.085$, $p = 0.012$. For panels (A-B): WT day and GSK3-KI night, n = 11 cells, 3 slices; WT night, n = 4 cells, 3 slices; GSK3-KI day, n = 8 cells, 3 slices.
(C) Amplitude of AHP and peak I_{NaP} of spiking cells from all groups are significantly correlated. Pearson correlation, $R = -0.732$, $p < 0.001$. Lines represent linear fit and 95% confidence intervals of all cells in plot.
(D) Spontaneous AP frequency and peak I_{NaP} of spiking cells from all groups are significantly correlated. Pearson correlation, $R = -0.550$, $p = 0.001$. Lines represent linear fit and 95% confidence intervals for all cells in plot. For panels (C-D): WT day, n = 9 cells; WT night, n = 4 cells; GSK3-KI day, n = 8 cells; GSK3-KI night, n = 10 cells.

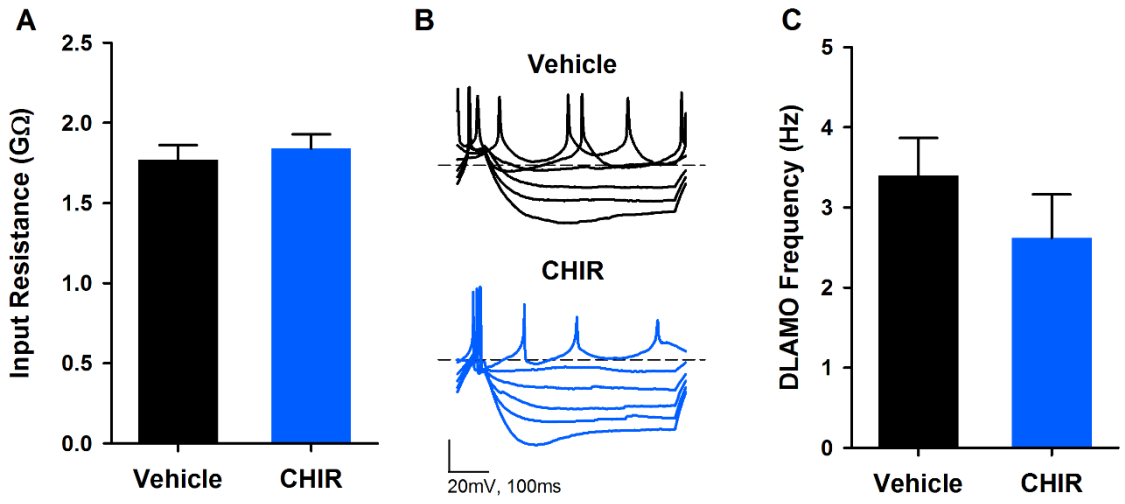

Figure S1. GSK3 inhibition does not alter input resistance or DLAMO frequency.
(A) Bar graph (mean ± SEM) for input resistance of vehicle and CHIR treated SCN cells recorded during the day (independent samples t-test; $t_{(64)} = -0.562$, $p = 0.576$; n = 31-35 cells, 3-4 slices per group).
(B) Representative current clamp traces from vehicle and CHIR treated SCN cells which were injected with progressive steps of hyperpolarizing current (5 pA steps from -25 pA to 0 pA).
(C) Bar graph (mean ± SEM) for oscillation frequency of vehicle and CHIR treated SCN cells exhibiting DLAMO's (independent samples t-test; $t_{(27)} = 1.061$, $p = 0.298$; n = 13-16 cells, 3-4 slices per group).

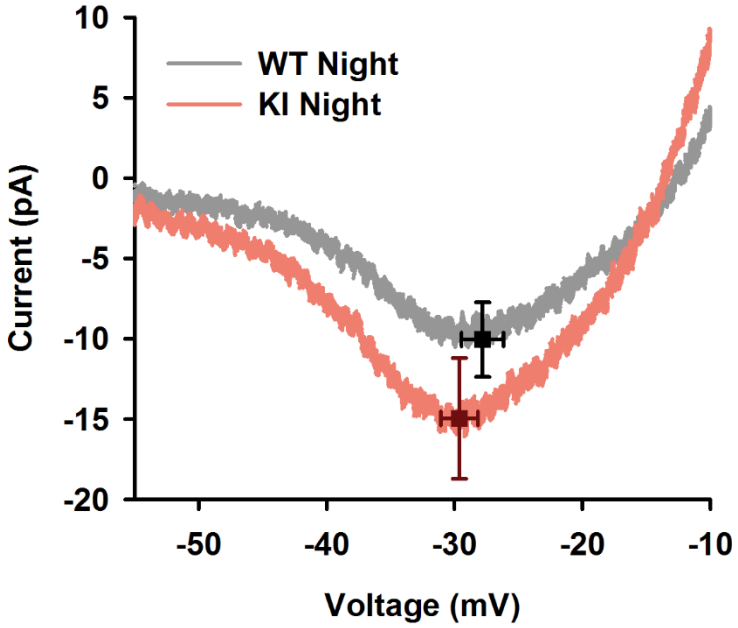

Figure S2. Calcium and potassium channel blockers do not alter enhanced inward current in GSK3-KI mice.
Average normalized response to slow depolarizing voltage ramp (-100 to +10 mV; 59mV/s) of SCN cells from WT or GSK3-KI during the early-night in the presence of TEA (10mM) and $CdCl_2$ (0.1mM). Peak I_{NaP} (means ± SEM shown as black and red symbols) in these conditions were similar to those measured in normal saline (see Fig 3C). n = 5-7 cells, 2 slices per group.

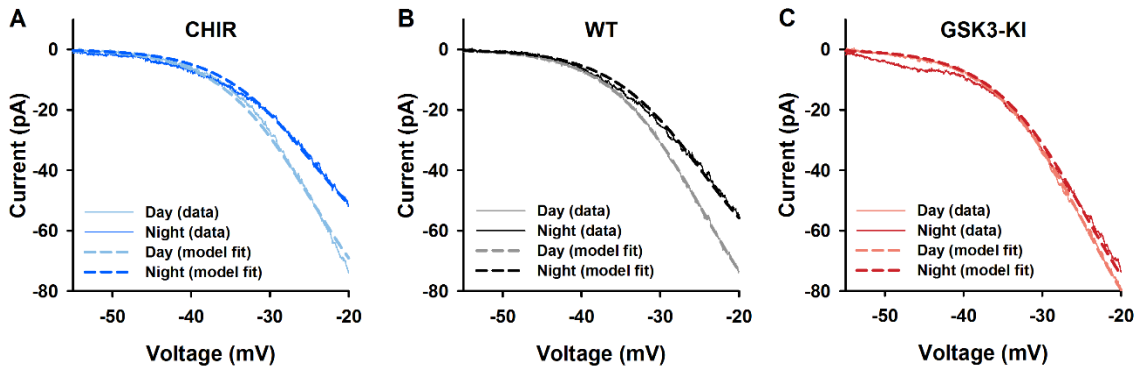

Figure S3. Computational model fits experimental data of the circadian change in peak I_{NaP}. Voltage ramps used to fit our model of I_{NaP}. Data (solid lines), and model predictions (dashed) are compared in the CHIR (A), WT (B) and GSK3-KI (C) conditions. Day and night curves were fit to determine the circadian change in peak current.

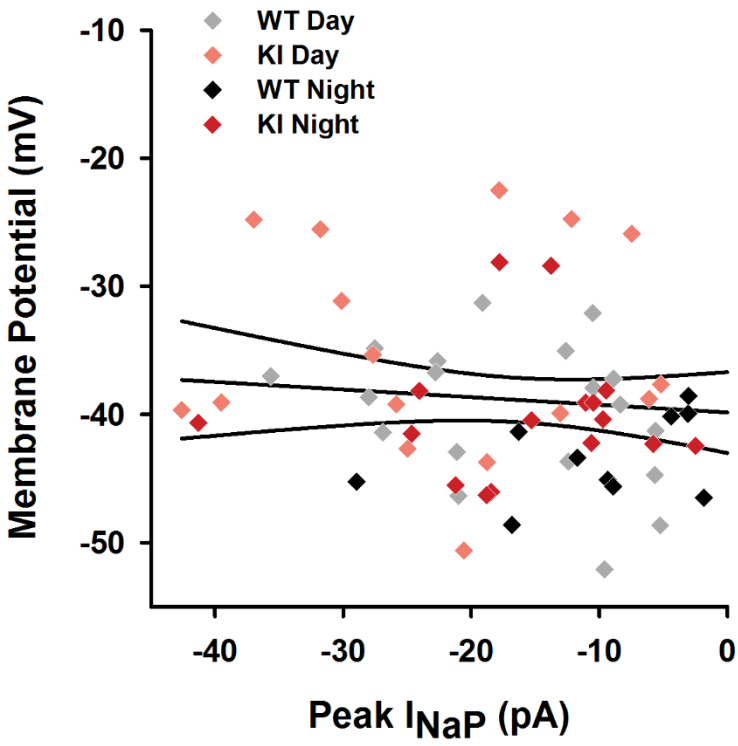

Figure S4. RMP is not correlated with peak I_{NaP} in SCN neurons from WT and GSK3-KI mice.
Pearson correlation, R = -0.094, p = 0.463. Lines represent linear fit and 95% confidence intervals for all cells in plot. WT day, n = 19 cells, 4 slices; WT night, n = 10 cells, 3 slices; GSK3-KI day, n = 18 cells, 3 slices; GSK3-KI night, n = 16 cells, 3 slices.

CHAPTER 5

SUMMARY AND CONCLUSIONS

In the mammalian circadian system, the generation of endogenous rhythms and synchronization of those rhythms to the external environment takes place within the suprachiasmatic nucleus (SCN). This information is then relayed to the rest of the body through patterns of SCN neuronal activity, yet the mechanism connecting the molecular clock to membrane excitability remains unclear. To begin to fill this gap, this dissertation tested the hypothesis that GSK3 activity regulates circadian behavior and photic entrainment through promotion of SCN neuronal excitability and then identified the persistent sodium current (I_{NaP}) as an ionic component through which GSK3 influences SCN physiology.

Increasing evidence has shown that GSK3 expresses daily changes in phosphorylation (inactivation) levels in the SCN (Iwahana et al., 2004, Iitaka et al., 2005, Iwahana et al., 2007, Besing et al., 2015), but the importance of these changes in circadian rhythmicity have not been studied until now. Chapter 2 explored the role of GSK3 activity rhythms in general circadian rhythmicity of the organism by examining wheel-running behavior and SCN neuronal activity in mice expressing constitutively active forms of GSK3 (GSK3-KI; (McManus et al., 2005)). Chronic GSK3 activation resulted in dampened and fragmented behavioral rhythms and prolonged activity phase (shortened rest period). Importantly, constitutive activation of GSK3α or GSK3β alone

was not sufficient to disrupt behavioral rhythms, suggesting redundancy in the functions of the two isoforms in the circadian system. Along with this behavioral disruption, the day/night difference in SCN neuronal activity was also dampened in GSK3-KI animals, driven by high, day-like activity seen during the subjective night. Taken together the results of Chapter 2 demonstrate the importance of GSK3 activity rhythms in regulating SCN output signaling.

Aside from controlling endogenously driven behavioral rhythms, changes in SCN excitability have been associated with phase-resetting in response to external stimuli (Kuhlman et al., 2003). Therefore, Chapter 3 examined the role of GSK3 activation in the process of photic entrainment and light-driven increases in SCN activity. Exposure to a phase-advancing light pulse (LP) in the late-night dramatically decreased the pGSK3β levels (increased GSK3 activity) in SCN neurons, lasting up to one hour after LP onset. Additionally, pharmacological inhibition of GSK3 in the 1-2 hour period following a LP, completely blocked the typical increase in SCN action potential firing seen during the early-phase resetting period (3-5 hours post LP) but surprisingly did not affect RMP or R_{input}. Behaviorally, chronic activation of GSK3 accelerated the rate of re-entrainment to an advance in the light cycle and advanced the phase-angle of entrainment in both normal and LP exposed conditions. Similarly, the early-morning rise in SCN neuronal activity started earlier in GSK3-KI than in WT slices irrespective of light-exposure.

The fourth chapter identified I_{NaP} as a specific ion current through which GSK3 controls excitability in SCN neurons. An unexpected finding was that the persistent sodium current exhibited a previously overlooked day/night difference in peak current magnitude. Specifically, I_{NaP} was higher during the day, when GSK3 activity (Besing et

al., 2015) and SCN excitability (Inouye and Kawamura, 1979) are elevated. Furthermore, GSK3 inhibition reduced the I_{NaP} and spontaneous firing rate of SCN cells only during the day, bringing I_{NaP} down to "night"-like levels. Conversely, chronic activation of GSK3 increased I_{NaP} at both times of day. Finally, blocking I_{NaP} with riluzole completely rescued the night-time hyper-excitability of GSK3-KI neurons, and restored the ratio of silent/spiking cells to WT levels.

GSK3 in the circadian system: remaining questions

Rhythmic regulation of GSK3: other mechanisms?

The data presented here have highlighted the limitations of genetic models compared to pharmacological manipulations. The effect of pharmacological inhibition of GSK3 was predictably specific to experimental conditions in which GSK3 activity was expected to be high (*i.e.* during the day or after a phase-shifting LP). Conversely, chronic GSK3 activation, as in the GSK3-KI model, rather consistently caused the same effect in all conditions (*i.e.* day and night, with and without LP). The lack of phase-specific effect in the GSK3-KI animals raises an interesting question of whether GSK3 activity in the SCN is being regulated through another mechanism in addition to phosphorylation.

Though circadian phosphorylation of GSK3 at the inhibitory phosphosites S21 and S9 (for α and β) has been demonstrated in multiple tissues, including the SCN (Iwahana et al., 2004, Iitaka et al., 2005, Besing et al., 2015), more work is needed to determine how this phosphorylation cycle is being controlled by the clock. Additionally, there are multiple other mechanisms by which GSK3 activity is regulated that have yet to be explored. For example, phosphorylation of GSK3α/β on tyrosine-279/216 (Y279/216),

typically through auto-phosphorylation (Cole et al., 2004), increases GSK3 activity (Hughes et al., 1993). GSK3 can also be regulated through cellular localization or sequestration (Taelman et al., 2010). Finally, GSK3 requires many of its substrates to first be phosphorylated by another "priming" kinase before it can act on its target (Woodgett and Cohen, 1984, Cohen and Frame, 2001). Interestingly, two of the possible priming kinases for GSK3, CK1 and MAPKs, are both integrally involved in the circadian molecular clockwork (Gallego and Virshup, 2007, Goldsmith and Bell-Pedersen, 2013). Moreover, MAPK exhibits circadian and light-induced changes in activity within the SCN (Obrietan et al., 1998), which may account for some of the rhythms and light-induced changes that remain in GSK3-KI mice.

Is GSK3 involved in nonphotic entrainment?

Although light is the strongest zeitgeber in the mammalian circadian system, nonphotic cues also act as entraining signals in the SCN and often work in opposition to light. For example, access to a novel running wheel proceeding light exposure attenuates the magnitude of light-induced phase-shifts in hamsters (Mistlberger and Antle, 1998). This same effect can be replicated with microinjections of neuropeptide Y (NPY) into the SCN region (Huhman and Albers, 1994) and systemic injections of serotonin (5-HT) receptor 1A agonist 8-OH-DPAT (Rea et al., 1994). Interestingly, when serotonergic input from the median raphe nucleus to the SCN is ablated, animals exhibit accelerated entrainment to shifts in the light cycle as well as enhanced phase-shifts to an acute LP (Pickard and Rea, 1997), similar to GSK3-KI mice (Chapter 3). Activation of 5-HT_{1A} receptors has been shown to inhibit GSK3 activity through increased phosphorylation in

numerous brain areas outside the SCN (Li et al., 2004, Polter et al., 2012). Moreover, the light-opposing effects of 5-HT in drosophila appear to be dependent on inhibition of the GSK3 homolog, SGG (Yuan et al., 2005). Thus, phosphorylation of GSK3 in SCN neurons may provide convergence point for both photic and nonphotic pathways, allowing for the integration of multiple entrainment signals before relaying that information to the peripheral clocks.

Health implications

GSK3: the "weak link" in the aging circadian system

The decline in sleep and circadian rhythms associated with aging have been well documented across species. In humans, age has been associated with increased sleep fragmentation at night, high frequency of napping during the day, and progressively advanced phase-angle (Dijk and Duffy, 1999). Aging in mice has been associated with largely the same phenotype, with older animals showing lower activity levels, reduced circadian amplitude, and more frequency, but shorter duration, bouts of activity per day (fragmentation; (Nakamura et al., 2011, Farajnia et al., 2012)). These changes are remarkably similar to the circadian phenotype seen in adult GSK3-KI mice (Chapter 2). Moreover, aged mice also exhibit changes in SCN neuronal activity similar to those seen in GSK3-KI mice. *In vivo* multi-unit activity (MUA) recordings in the SCN of freely-moving mice, as well as *in vitro* MUA SCN recordings, both showed that rhythms of SCN firing, with trough levels of activity higher in old animals at night (Nakamura et al., 2011, Farajnia et al., 2012). Furthermore, current-clamp recordings from SCN neurons have shown a loss of the nighttime increase in action potential after-hyperpolarization

(AHP) amplitude in old animals (Farajnia et al., 2015). Given that pGSK3 levels have been shown to decrease with age throughout the brain (Peng et al., 2013), including the SCN (Iwahana et al., 2007), dysregulation of GSK3 activity might be an underlying cause of the circadian disruption associated with age.

Surprisingly, the aging-related decline in behavioral and SCN neurophysiological rhythms are not associated with changes in the molecular clock, as robust PER2 rhythms persist in SCN from aged mice (Nakamura et al., 2011, Sellix et al., 2012). This suggests that the decline in circadian system is down-stream of the molecular clock, and through changes in the electrophysiological properties of the cell that would not feed back onto the clock. Many of the previous mechanisms of regulating SCN excitability have focused on changes in the RMP, but modeling and experimental evidence suggests that changes in RMP would also impact the molecular clock (Diekman et al., 2013). However, GSK3 regulation of I_{NaP} provides a new mechanism by which SCN neuronal excitability can be altered without changing RMP. Therefore, further work exploring the changes in I_{NaP} in SCN neurons with age could provide new insight into underlying cause of circadian disruption in seen in normal aging.

Abnormal aging: Alzheimer's disease

Aside from changes seen in normal aging, circadian disruption has also been associated with numerous neurodegenerative disorders, including Huntington's and Parkinson's disease (Kudo et al., 2011b, Kudo et al., 2011c). One disorder that is of particular relevance to this dissertation because of the intersection of GSK3, circadian disruption, and aberrant neuronal excitability is Alzheimer's disease (AD). AD is a

progressive neurodegenerative form of dementia associated with elevated levels of the amyloid β (Aβ) peptide and the formation of pathological Aβ plaques and neurofibrillary tangles (Selkoe, 1999). Recent work has shown that the level of circulating Aβ, which is also found in the cerebrospinal fluid (CSF) of healthy individuals, is tightly coupled to sleep/wake cycles, with Aβ levels increasing throughout the activity phase of humans and rodents (Kang et al., 2009). Furthermore, prolonged sleep deprivation has been found to potentiate Aβ plaque formation in the multiple mouse models of AD (Kang et al., 2009). Interestingly, GSK3 activation (low pGSK3) is elevated in the brains of transgenic AD mice (Peng et al., 2013), and acute application of Aβ to hippocampal neurons *in vitro* decreases pGSK3 levels within 20 minutes (Scala et al., 2015). Additionally, Aβ-induced excitability in CA1 neurons can be rescued with pharmacological inhibitors of GSK3 (Scala et al., 2015) or I_{NaP} (Ren et al., 2014). Therefore, GSK3 regulation of neuronal excitability through I_{NaP} could have broad implications outside the circadian system as well.

Conclusions

Until now, the vast majority of research on GSK3's role in circadian rhythmicity has focused on its regulation of the molecular clock while neglecting its influence on membrane excitability. The studies presented here provide novel insight into GSK3's control over SCN neuronal activity, and highlight I_{NaP} as the first (of potentially many) specific ionic component that is regulated by GSK3 in the SCN. Aberrant GSK3 activity has been observed in animal models of numerous disorders, such as, depression (Polter et al., 2010), mania (Prickaerts et al., 2006), Fragile-X syndrome (Min et al., 2009,

Yuskaitis et al., 2010), and neurodegenerative diseases (Terwel et al., 2008, Duka et al., 2009, Armentero et al., 2011), which commonly show symptoms of circadian disruption in humans (Barnard and Nolan, 2008, Kronk et al., 2010). Therefore, further understanding GSK3's role in regulation of circadian output and photic entrainment could provide insight into the proper timing of treatments that inhibit GSK3 or the use of light therapy in conjunction with GSK3 inhibiting agents to restore proper rhythms in GSK3 activity.

GENERAL REFERENCES

Abrahamson EE, Moore RY (2001) Suprachiasmatic nucleus in the mouse: retinal innervation, intrinsic organization and efferent projections. Brain Res 916:172-191.

Albus H, Bonnefont X, Chaves I, Yasui A, Doczy J, van der Horst GT, Meijer JH (2002) Cryptochrome-deficient mice lack circadian electrical activity in the suprachiasmatic nuclei. Curr Biol 12:1130-1133.

Armentero MT, Sinforiani E, Ghezzi C, Bazzini E, Levandis G, Ambrosi G, Zangaglia R, Pacchetti C, Cereda C, Cova E, Basso E, Celi D, Martignoni E, Nappi G, Blandini F (2011) Peripheral expression of key regulatory kinases in Alzheimer's disease and Parkinson's disease. Neurobiol Aging 32:2142-2151.

Barnard AR, Nolan PM (2008) When clocks go bad: neurobehavioural consequences of disrupted circadian timing. PLoS Genet 4:e1000040.

Besing RC, Paul JR, Hablitz LM, Rogers CO, Johnson RL, Young ME, Gamble KL (2015) Circadian rhythmicity of active GSK3 isoforms modulates molecular clock gene rhythms in the suprachiasmatic nucleus. J Biol Rhythms 30:155-160.

Cohen P, Frame S (2001) The renaissance of GSK3. Nat Rev Mol Cell Biol 2:769-776.

Cole A, Frame S, Cohen P (2004) Further evidence that the tyrosine phosphorylation of glycogen synthase kinase-3 (GSK3) in mammalian cells is an autophosphorylation event. Biochem J 377:249-255.

Colwell CS (2011) Linking neural activity and molecular oscillations in the SCN. Nat Rev Neurosci 12:553-569.

Czeisler CA (1995) The effect of light on the human circadian pacemaker. Ciba Found Symp 183:254-290; discussion 290-302.

Daan S, Pittendrigh C (1976) A functional analysis of circadian pacemakers in nocturnal rodents: II. The variability of phase response curves. J Comp Physiol A 106:253-266.

Dibner C, Schibler U, Albrecht U (2010) The mammalian circadian timing system: organization and coordination of central and peripheral clocks. Annu Rev Physiol 72:517-549.

Diekman CO, Belle MD, Irwin RP, Allen CN, Piggins HD, Forger DB (2013) Causes and consequences of hyperexcitation in central clock neurons. PLoS Comput Biol 9:e1003196.

Dijk DJ, Duffy JF (1999) Circadian regulation of human sleep and age-related changes in its timing, consolidation and EEG characteristics. Ann Med 31:130-140.

Duka T, Duka V, Joyce JN, Sidhu A (2009) Alpha-Synuclein contributes to GSK-3beta-catalyzed Tau phosphorylation in Parkinson's disease models. FASEB J 23:2820-2830.

Durgan DJ, Pulinilkunnil T, Villegas-Montoya C, Garvey ME, Frangogiannis NG, Michael LH, Chow CW, Dyck JR, Young ME (2010) Short communication: ischemia/reperfusion tolerance is time-of-day-dependent: mediation by the cardiomyocyte circadian clock. Circ Res 106:546-550.

Eastman CI, Mistlberger RE, Rechtschaffen A (1984) Suprachiasmatic nuclei lesions eliminate circadian temperature and sleep rhythms in the rat. Physiol Behav 32:357-368.

Farajnia S, Meijer JH, Michel S (2015) Age-related changes in large-conductance calcium-activated potassium channels in mammalian circadian clock neurons. Neurobiol Aging 36:2176-2183.

Farajnia S, Michel S, Deboer T, vanderLeest HT, Houben T, Rohling JH, Ramkisoensing A, Yasenkov R, Meijer JH (2012) Evidence for neuronal desynchrony in the aged suprachiasmatic nucleus clock. J Neurosci 32:5891-5899.

Gallego M, Virshup DM (2007) Post-translational modifications regulate the ticking of the circadian clock. Nat Rev Mol Cell Biol 8:139-148.

Goldsmith CS, Bell-Pedersen D (2013) Diverse roles for MAPK signaling in circadian clocks. Adv Genet 84:1-39.

Golombek DA, Ralph MR (1995) Circadian responses to light: the calmodulin connection. Neurosci Lett 192:101-104.

Golombek DA, Rosenstein RE (2010) Physiology of circadian entrainment. Physiol Rev 90:1063-1102.

Green DJ, Gillette R (1982) Circadian rhythm of firing rate recorded from single cells in the rat suprachiasmatic brain slice. Brain Res 245:198-200.

Hannibal J (2002) Neurotransmitters of the retino-hypothalamic tract. Cell Tissue Res 309:73-88.

Herzog ED, Takahashi JS, Block GD (1998) Clock controls circadian period in isolated suprachiasmatic nucleus neurons. Nat Neurosci 1:708-713.

Hughes K, Nikolakaki E, Plyte SE, Totty NF, Woodgett JR (1993) Modulation of the glycogen synthase kinase-3 family by tyrosine phosphorylation. EMBO J 12:803-808.

Huhman KL, Albers HE (1994) Neuropeptide Y microinjected into the suprachiasmatic region phase shifts circadian rhythms in constant darkness. Peptides 15:1475-1478.

Hur EM, Zhou FQ (2010) GSK3 signalling in neural development. Nat Rev Neurosci 11:539-551.

Iitaka C, Miyazaki K, Akaike T, Ishida N (2005) A role for glycogen synthase kinase-3beta in the mammalian circadian clock. J Biol Chem 280:29397-29402.

Inouye ST, Kawamura H (1979) Persistence of circadian rhythmicity in a mammalian hypothalamic "island" containing the suprachiasmatic nucleus. Proc Natl Acad Sci U S A 76:5962-5966.

Itri JN, Michel S, Vansteensel MJ, Meijer JH, Colwell CS (2005) Fast delayed rectifier potassium current is required for circadian neural activity. Nat Neurosci 8:650-656.

Iwahana E, Akiyama M, Miyakawa K, Uchida A, Kasahara J, Fukunaga K, Hamada T, Shibata S (2004) Effect of lithium on the circadian rhythms of locomotor activity and glycogen synthase kinase-3 protein expression in the mouse suprachiasmatic nuclei. Eur J Neurosci 19:2281-2287.

Iwahana E, Hamada T, Uchida A, Shibata S (2007) Differential effect of lithium on the circadian oscillator in young and old hamsters. Biochem Biophys Res Commun 354:752-756.

Jackson AC, Yao GL, Bean BP (2004) Mechanism of spontaneous firing in dorsomedial suprachiasmatic nucleus neurons. J Neurosci 24:7985-7998.

Kang JE, Lim MM, Bateman RJ, Lee JJ, Smyth LP, Cirrito JR, Fujiki N, Nishino S, Holtzman DM (2009) Amyloid-beta dynamics are regulated by orexin and the sleep-wake cycle. Science 326:1005-1007.

Kinoshita C, Miyazaki K, Ishida N (2012) Chronic stress affects PERIOD2 expression through glycogen synthase kinase-3beta phosphorylation in the central clock. Neuroreport 23:98-102.

Kononenko NI, Shao LR, Dudek FE (2004) Riluzole-sensitive slowly inactivating sodium current in rat suprachiasmatic nucleus neurons. J Neurophysiol 91:710-718.

Kronk R, Bishop EE, Raspa M, Bickel JO, Mandel DA, Bailey DB, Jr. (2010) Prevalence, nature, and correlates of sleep problems among children with fragile X syndrome based on a large scale parent survey. Sleep 33:679-687.

Kudo T, Loh DH, Kuljis D, Constance C, Colwell CS (2011a) Fast delayed rectifier potassium current: critical for input and output of the circadian system. J Neurosci 31:2746-2755.

Kudo T, Loh DH, Truong D, Wu Y, Colwell CS (2011b) Circadian dysfunction in a mouse model of Parkinson's disease. Exp Neurol 232:66-75.

Kudo T, Schroeder A, Loh DH, Kuljis D, Jordan MC, Roos KP, Colwell CS (2011c) Dysfunctions in circadian behavior and physiology in mouse models of Huntington's disease. Exp Neurol 228:80-90.

Kuhlman SJ, McMahon DG (2004) Rhythmic regulation of membrane potential and potassium current persists in SCN neurons in the absence of environmental input. Eur J Neurosci 20:1113-1117.

Kuhlman SJ, McMahon DG (2006) Encoding the ins and outs of circadian pacemaking. J Biol Rhythms 21:470-481.

Kuhlman SJ, Silver R, Le Sauter J, Bult-Ito A, McMahon DG (2003) Phase resetting light pulses induce Per1 and persistent spike activity in a subpopulation of biological clock neurons. J Neurosci 23:1441-1450.

Lavoie J, Hebert M, Beaulieu JM (2013) Glycogen synthase kinase-3beta haploinsufficiency lengthens the circadian locomotor activity period in mice. Behav Brain Res 253:262-265.

Leak RK, Card JP, Moore RY (1999) Suprachiasmatic pacemaker organization analyzed by viral transynaptic transport. Brain Res 819:23-32.

Li X, Zhu W, Roh MS, Friedman AB, Rosborough K, Jope RS (2004) In vivo regulation of glycogen synthase kinase-3beta (GSK3beta) by serotonergic activity in mouse brain. Neuropsychopharmacology 29:1426-1431.

Liu AC, Tran HG, Zhang EE, Priest AA, Welsh DK, Kay SA (2008) Redundant function of REV-ERBalpha and beta and non-essential role for Bmal1 cycling in transcriptional regulation of intracellular circadian rhythms. PLoS Genet 4:e1000023.

Liu C, Weaver DR, Strogatz SH, Reppert SM (1997) Cellular construction of a circadian clock: period determination in the suprachiasmatic nuclei. Cell 91:855-860.

Llinas RR (1988) The intrinsic electrophysiological properties of mammalian neurons: insights into central nervous system function. Science 242:1654-1664.

Martinek S, Inonog S, Manoukian AS, Young MW (2001) A role for the segment polarity gene shaggy/GSK-3 in the Drosophila circadian clock. Cell 105:769-779.

Mason R, Biello SM (1992) A neurophysiological study of a lithium-sensitive phosphoinositide system in the hamster suprachiasmatic (SCN) biological clock in vitro. Neurosci Lett 144:135-138.

McManus EJ, Sakamoto K, Armit LJ, Ronaldson L, Shpiro N, Marquez R, Alessi DR (2005) Role that phosphorylation of GSK3 plays in insulin and Wnt signalling defined by knockin analysis. EMBO J 24:1571-1583.

Meijer L, Flajolet M, Greengard P (2004) Pharmacological inhibitors of glycogen synthase kinase 3. Trends Pharmacol Sci 25:471-480.

Meredith AL, Wiler SW, Miller BH, Takahashi JS, Fodor AA, Ruby NF, Aldrich RW (2006) BK calcium-activated potassium channels regulate circadian behavioral rhythms and pacemaker output. Nat Neurosci 9:1041-1049.

Min WW, Yuskaitis CJ, Yan Q, Sikorski C, Chen S, Jope RS, Bauchwitz RP (2009) Elevated glycogen synthase kinase-3 activity in Fragile X mice: key metabolic regulator with evidence for treatment potential. Neuropharmacology 56:463-472.

Mistlberger RE, Antle MC (1998) Behavioral inhibition of light-induced circadian phase resetting is phase and serotonin dependent. Brain Res 786:31-38.

Montgomery JR, Whitt JP, Wright BN, Lai MH, Meredith AL (2013) Mis-expression of the BK K(+) channel disrupts suprachiasmatic nucleus circuit rhythmicity and alters clock-controlled behavior. Am J Physiol Cell Physiol 304:C299-311.

Nakamura TJ, Nakamura W, Yamazaki S, Kudo T, Cutler T, Colwell CS, Block GD (2011) Age-related decline in circadian output. J Neurosci 31:10201-10205.

Obrietan K, Impey S, Storm DR (1998) Light and circadian rhythmicity regulate MAP kinase activation in the suprachiasmatic nuclei. Nat Neurosci 1:693-700.

Ouyang Y, Andersson CR, Kondo T, Golden SS, Johnson CH (1998) Resonating circadian clocks enhance fitness in cyanobacteria. Proc Natl Acad Sci U S A 95:8660-8664.

Panda S, Antoch MP, Miller BH, Su AI, Schook AB, Straume M, Schultz PG, Kay SA, Takahashi JS, Hogenesch JB (2002) Coordinated transcription of key pathways in the mouse by the circadian clock. Cell 109:307-320.

Peng CX, Hu J, Liu D, Hong XP, Wu YY, Zhu LQ, Wang JZ (2013) Disease-modified glycogen synthase kinase-3beta intervention by melatonin arrests the pathology and memory deficits in an Alzheimer's animal model. Neurobiol Aging 34:1555-1563.

Pennartz CM, Bierlaagh MA, Geurtsen AM (1997) Cellular mechanisms underlying spontaneous firing in rat suprachiasmatic nucleus: involvement of a slowly inactivating component of sodium current. J Neurophysiol 78:1811-1825.

Pennartz CM, de Jeu MT, Bos NP, Schaap J, Geurtsen AM (2002) Diurnal modulation of pacemaker potentials and calcium current in the mammalian circadian clock. Nature 416:286-290.

Phan TX, Chan GC, Sindreu CB, Eckel-Mahan KL, Storm DR (2011) The diurnal oscillation of MAP (mitogen-activated protein) kinase and adenylyl cyclase

activities in the hippocampus depends on the suprachiasmatic nucleus. J Neurosci 31:10640-10647.

Pickard GE, Rea MA (1997) Serotonergic innervation of the hypothalamic suprachiasmatic nucleus and photic regulation of circadian rhythms. Biol Cell 89:513-523.

Pittendrigh C, Daan S (1976) A functional analysis of circadian pacemakers in nocturnal rodents: I. The stability and lability of spontaneous frequency. J Comp Physiol A 106:223-252.

Pizzio GA, Hainich EC, Ferreyra GA, Coso OA, Golombek DA (2003) Circadian and photic regulation of ERK, JNK and p38 in the hamster SCN. Neuroreport 14:1417-1419.

Polter A, Beurel E, Yang S, Garner R, Song L, Miller CA, Sweatt JD, McMahon L, Bartolucci AA, Li X, Jope RS (2010) Deficiency in the inhibitory serine-phosphorylation of glycogen synthase kinase-3 increases sensitivity to mood disturbances. Neuropsychopharmacology 35:1761-1774.

Polter AM, Yang S, Jope RS, Li X (2012) Functional significance of glycogen synthase kinase-3 regulation by serotonin. Cell Signal 24:265-271.

Preitner N, Damiola F, Lopez-Molina L, Zakany J, Duboule D, Albrecht U, Schibler U (2002) The orphan nuclear receptor REV-ERBalpha controls circadian transcription within the positive limb of the mammalian circadian oscillator. Cell 110:251-260.

Prickaerts J, Moechars D, Cryns K, Lenaerts I, van Craenendonck H, Goris I, Daneels G, Bouwknecht JA, Steckler T (2006) Transgenic mice overexpressing glycogen

synthase kinase 3beta: a putative model of hyperactivity and mania. J Neurosci 26:9022-9029.

Ralph MR, Foster RG, Davis FC, Menaker M (1990) Transplanted suprachiasmatic nucleus determines circadian period. Science 247:975-978.

Rea MA, Glass JD, Colwell CS (1994) Serotonin modulates photic responses in the hamster suprachiasmatic nuclei. J Neurosci 14:3635-3642.

Ren SC, Chen PZ, Jiang HH, Mi Z, Xu F, Hu B, Zhang J, Zhu ZR (2014) Persistent sodium currents contribute to Abeta1-42-induced hyperexcitation of hippocampal CA1 pyramidal neurons. Neurosci Lett 580:62-67.

Reppert SM, Weaver DR (2002) Coordination of circadian timing in mammals. Nature 418:935-941.

Scala F, Fusco S, Ripoli C, Piacentini R, Li Puma DD, Spinelli M, Laezza F, Grassi C, D'Ascenzo M (2015) Intraneuronal Abeta accumulation induces hippocampal neuron hyperexcitability through A-type K(+) current inhibition mediated by activation of caspases and GSK-3. Neurobiol Aging 36:886-900.

Schwartz WJ, Gross RA, Morton MT (1987) The suprachiasmatic nuclei contain a tetrodotoxin-resistant circadian pacemaker. Proc Natl Acad Sci U S A 84:1694-1698.

Selkoe DJ (1999) Translating cell biology into therapeutic advances in Alzheimer's disease. Nature 399:A23-31.

Sellix MT, Evans JA, Leise TL, Castanon-Cervantes O, Hill DD, DeLisser P, Block GD, Menaker M, Davidson AJ (2012) Aging differentially affects the re-entrainment

response of central and peripheral circadian oscillators. J Neurosci 32:16193-16202.

Stafstrom CE (2007) Persistent sodium current and its role in epilepsy. Epilepsy Curr 7:15-22.

Stephan FK, Zucker I (1972) Circadian rhythms in drinking behavior and locomotor activity of rats are eliminated by hypothalamic lesions. Proc Natl Acad Sci U S A 69:1583-1586.

Taelman VF, Dobrowolski R, Plouhinec JL, Fuentealba LC, Vorwald PP, Gumper I, Sabatini DD, De Robertis EM (2010) Wnt signaling requires sequestration of glycogen synthase kinase 3 inside multivesicular endosomes. Cell 143:1136-1148.

Takahashi JS, Hong HK, Ko CH, McDearmon EL (2008) The genetics of mammalian circadian order and disorder: implications for physiology and disease. Nat Rev Genet 9:764-775.

Tapia M, Del Puerto A, Puime A, Sanchez-Ponce D, Fronzaroli-Molinieres L, Pallas-Bazarra N, Carlier E, Giraud P, Debanne D, Wandosell F, Garrido JJ (2013) GSK3 and beta-catenin determines functional expression of sodium channels at the axon initial segment. Cell Mol Life Sci 70:105-120.

Terwel D, Muyllaert D, Dewachter I, Borghgraef P, Croes S, Devijver H, Van Leuven F (2008) Amyloid activates GSK-3beta to aggravate neuronal tauopathy in bigenic mice. Am J Pathol 172:786-798.

Tischkau SA, Mitchell JW, Tyan SH, Buchanan GF, Gillette MU (2003) Ca2+/cAMP response element-binding protein (CREB)-dependent activation of Per1 is

required for light-induced signaling in the suprachiasmatic nucleus circadian clock. J Biol Chem 278:718-723.

Travnickova-Bendova Z, Cermakian N, Reppert SM, Sassone-Corsi P (2002) Bimodal regulation of mPeriod promoters by CREB-dependent signaling and CLOCK/BMAL1 activity. Proc Natl Acad Sci U S A 99:7728-7733.

Ueda HR, Hayashi S, Chen W, Sano M, Machida M, Shigeyoshi Y, Iino M, Hashimoto S (2005) System-level identification of transcriptional circuits underlying mammalian circadian clocks. Nat Genet 37:187-192.

von Gall C, Duffield GE, Hastings MH, Kopp MD, Dehghani F, Korf HW, Stehle JH (1998) CREB in the mouse SCN: a molecular interface coding the phase-adjusting stimuli light, glutamate, PACAP, and melatonin for clockwork access. J Neurosci 18:10389-10397.

Welsh DK, Takahashi JS, Kay SA (2010) Suprachiasmatic nucleus: cell autonomy and network properties. Annu Rev Physiol 72:551-577.

Wildburger NC, Laezza F (2012) Control of neuronal ion channel function by glycogen synthase kinase-3: new prospective for an old kinase. Front Mol Neurosci 5:80.

Wollnik F, Turek FW (1989) SCN lesions abolish ultradian and circadian components of activity rhythms in LEW/Ztm rats. Am J Physiol 256:R1027-1039.

Woodgett JR (1990) Molecular cloning and expression of glycogen synthase kinase-3/factor A. EMBO J 9:2431-2438.

Woodgett JR, Cohen P (1984) Multisite phosphorylation of glycogen synthase. Molecular basis for the substrate specificity of glycogen synthase kinase-3 and casein kinase-II (glycogen synthase kinase-5). Biochim Biophys Acta 788:339-347.

Yamazaki S, Kerbeshian MC, Hocker CG, Block GD, Menaker M (1998) Rhythmic properties of the hamster suprachiasmatic nucleus in vivo. J Neurosci 18:10709-10723.

Yamazaki S, Numano R, Abe M, Hida A, Takahashi R, Ueda M, Block GD, Sakaki Y, Menaker M, Tei H (2000) Resetting central and peripheral circadian oscillators in transgenic rats. Science 288:682-685.

Yoo SH, Yamazaki S, Lowrey PL, Shimomura K, Ko CH, Buhr ED, Siepka SM, Hong HK, Oh WJ, Yoo OJ, Menaker M, Takahashi JS (2004) PERIOD2::LUCIFERASE real-time reporting of circadian dynamics reveals persistent circadian oscillations in mouse peripheral tissues. Proc Natl Acad Sci U S A 101:5339-5346.

Yuan Q, Lin F, Zheng X, Sehgal A (2005) Serotonin modulates circadian entrainment in Drosophila. Neuron 47:115-127.

Yuskaitis CJ, Mines MA, King MK, Sweatt JD, Miller CA, Jope RS (2010) Lithium ameliorates altered glycogen synthase kinase-3 and behavior in a mouse model of fragile X syndrome. Biochem Pharmacol 79:632-646.

APPENDIX A

INSTITUTIONAL ANIMAL CARE AND USE COMMITTEE APPROVAL

THE UNIVERSITY OF ALABAMA AT BIRMINGHAM
Institutional Animal Care and Use Committee (IACUC)

MEMORANDUM

DATE: 24-Aug-2015

TO: Gamble, Karen Lynnette

FROM: Robert A. Kesterson, Ph.D., Chair

Institutional Animal Care and Use Committee (IACUC)

SUBJECT: **NOTICE OF APPROVAL**

The following application was approved by the University of Alabama at Birmingham Institutional Animal Care and Use Committee (IACUC) on 24-Aug-2015.

Protocol PI: Gamble, Karen Lynnette

Title: Circadian Dysfunction and GSK3 in Neurodegenerative Disease

Sponsor: National Institute of Neurological Disorders and Stroke/NIH/DHHS

Animal Project Number (APN): IACUC-09708

This institution has an Animal Welfare Assurance on file with the Office of Laboratory Animal Welfare (OLAW), is registered as a Research Facility with the USDA, and is accredited by the Association for Assessment and Accreditation of Laboratory Animal Care International (AAALAC).

Institutional Animal Care and Use Committee (IACUC) | Mailing Address:
CH19 Suite 403 | CH19 Suite 403
933 19th Street South | 1530 3rd Ave S
(205) 934-7692 | Birmingham, AL 35294-0019
FAX (205) 934-1188 |